The GEOLOGICAL BULLETIN of the PUNJAB UNIVERSITY

Number 38 *December 2003*

CONTENTS

Geol. Bull. Punjab Univ. 38, 2003.

DIRECT HRTEM MEASUREMENTS OF EXPANDABILITY OF ILLITE/SMECTITE MIXED LAYER IN KARAK MUDSTONE, KOHAT PLATEAU, PAKISTAN

BY

AKHTAR ALI SALEEMI

Institute of Geology, University of the Punjab, Lahore-54590, Pakistan.

MOHAMMAD ZAHID

Department of Geology, University of Peshawar, Peshawar 25120, Pakistan.

AND

MOHAMMAD ASHRAF SIDDIQUI

Institute of Geology, University of the Punjab, Lahore-54590, Pakistan.

Abstract: *The Karak mudstone sandwiched between Eocene evaporite sequence, is predominantly composed of R=1 ordered mixed layer illite/smectite with 20 to 30% expandibility. Majority of illite/smectite particles are subhedral and show step like growth probably due to dissolutioning of the older smectite particles and neoformation of illite particles. Variation in thickness of individual smectite fringe from 15Å to 10 Å suggests layer by layer transformation of smectite to illite. Smectite content in I/S measured by HRTEM is 26%, and is in consistent with that measured by XRD. Al-pillaring process for sample preparation was found more effective to study I/S by HRTEM.*

INTRODUCTION

Mixed-layer illite/smectite (I/S) has been found in a variety of weathering, sedimentary, diagenetic and hydrothermal environments. The smectite to illite conversion resulting from genetic and hydrothermal alteration, is an important reaction in low-temperature geological environments. The transition from smectite to illite has been widely documented by XRD studies. From the pioneering study of Hower et al. (1976), there has been general agreement that this process involves interstratified (I/S) intermediates, with the proportion of illite in mixed-layer I/S increasing as a function of increasing temperature, time and burial depth of the basin. Although Moore and Reynolds (1989) described four models for this conversion, no single model can explain all of the observations of the smectite to illite conversion. Transmission electron microscopy (TEM) has been used to obtain lattice-fringe images of mixed-layer illite/smectite (I/S) by many investigators (e.g. Lee et al., 1985; Ahn and Peacor, 1986; Klimentidis and Mackinnon, 1986; Yau et al., 1987; Huff et al., 1988; Ahn and Peacor, 1989; Murakami et al., 1993; Dong and Peacor, 1996; Dong et al., 1997; Yan et al., 2001; Bauluz et al., 2002).

Although 001 lattice fringes of 2:1 phyllosilicates are easily imaged using samples for which X-ray diffraction (XRD) patterns show mixed layering of illite and smectite, individual layers of illite or smectite can not be unambiguously identified. Differences in interlayer spacing are so subtle as to be non-diagnostic under normal imaging conditions (Ahn and Peacor, 1986). A major cause of this ambiguity is the dehydration and collapse of smectite interlayer under high vacuum. The collapse gives smectite a layer thickness of 10 Å, the same as that of illite: thus unambiguous distinction of individual smectitic and illitic interlayer is not possible. Efforts have been made to distinguish smectite from illite by intercalation of laurylamine (Yoshida, 1973; Lee and Peacor, 1986) and n-alkylamine (Bell, 1986; Vali and Köster, 1986; Vali and Hesse, 1990; Vali et al., 1991) in order to keep smectitic interlayers expanded, but with limited success. Method of Guthrie and Veblen (1989a, 1989b, 1990) based on over focused image was successfully applied to highly ordered I/S. In the present study we have successfully pillared the smectite layers by Al and as a result smectite layers remained expanded under high vacuum.

EXPERIMENTAL

Sample descriptions

The sample used in this study is a representative of Karak mudstone. The Karak mudstone is named after its type locality near Karak town (lat. 33° 7′ N; long. 71° 6′E), Kohat District, Pakistan. The mudstone is 3 to 20 m thick and located between Early and Middle Eocene Bahadur Khel salt and Jatta Gypsum (Wells, 1984). Chaudhry and Ashraf, (1979) described it as bentonite and named it as Karak Bentonite. However Saleemi and Ahmed (2000) showed that it lacks the essential attributes of either bentonite or fuller's earth. The Karak mudstone is soft, sticky, plastic colloidal clay. It has a greasy and splintery appearance when fresh. Locally, it is used as a detergent for clothes-washing purpose. When wet, it can be molded into any shape. On drying it contracts and develops cracks. On weathered surfaces, it crumbles to small, loose pieces. The colour of mudstone varies from greenish blue to grayish and bluish gray. At some places near its contact with salt, sulphur is deposited giving a yellow color to the contact. Some of the exposures near the base show a dark bluish gray colour due to the presence of bituminous matter. The mudstone also has thin partings of gypsiferous clay and gypsum. Saleemi and Ahmed (2000) have shown that the Karak mudstone is mainly composed of detrital clays of varied composition and concentration along with the flakes of detrital muscovite and fine grains of quartz and feldspar dispersed through the matrix.

X-ray diffraction

The < 2 μm fraction was separated from the sample according to Stokes' Law of settling and subsequently saturated with Mg by adding 5 ml of 10% solution of magnesium chloride ($MgCl_2$). Oriented mounts were prepared by smearing the clay suspension onto glass sildes, following the method described by Moore & Reynolds (1989). In addition to being run as air dried, the oriented mounts were also run following glycolation (vapor pressure method) at 70 °C overnight. XRD scans were made on a Philips PW 1700 diffractometer utilizing Co Kα radiation at a scan speed of 0.5θ/min. Samples were scanned from 2° to 30° 2θ. The composition of illite-smectite was determined by comparing the simulated X-ray traces with the observed ones. Illite-smectite structures were modeled using the NEWMOD computer program developed by R.C. Reynolds (Department of Earth Sciences, Dartmouth College, Hanover, New Hampshire).

Tranmission electron microscopy (TEM)

Morphology of illite-smectite particles was examined by transmission electron microscopy (TEM). For TEM samples were prepared following the procedure of Nadeau et al. (1985). Clay fractions of < 1 μm were diluted and spread over a piece of freshly cleaved mica, dried shadowed with Pt at an angle of 10° and coated with carbon. The shadowed film was then floated on water and uplifted (fished out) on Cu grids.

To investigate illite-smectite particles under higher resolution transmission electron microscope < 1 μm clay fraction was A1 pillared. $AlCl_3$ aqueous solution was prepared by dissolving the A.R grade chemicals in deionised water. Hydroxy-A1 solution was prepared by slow addition of 0.2M NaOH solution to a 0.2M $AlCl_3$ $6H_2O$ solution with vigorous stirring at room temperature. The OH/A1 molar ratio was 2.40. Vigorous stirring was essential to prevent accumulations of OH ions, which might cause precipitation of $Al(OH)_3$ in the form of gibbsite. The resulting hydroxy-A1 solution was aged at room temperature over one and a half months to form $[AlO_4Al_{12}(OH)_{24}(H_2O)_{12}]^{7+}$ polymer (A113) as pillaring agent. It was observed that it turned turbid at first in spite of vigorous stirring, but after several days again became transparent.

Pillaring process (preparation of hydroxy-Al intercalated clays) was mostly accomplished by the method previously described by Lahav et al (1978) and Shabtai and Lahav (1980). Clay suspension of 200 mg per litre was used. The hydroxy-A1 solution was 6.8 ml/200 mg clay. The solution was added to clay suspension at the rate of 0.2 m1/min with vigorous stirring, causing flocculation at a certain stage. After addition the suspension was aged for 10 days in a polypropylene bottle. The resulting product was separated by centrifugation and washed repeatedly by deionised water until free of chlorides as determined by $AgNO_3$. Square embedding moulds were part filled with Spur resin mixture, which were then polymerized to give a flat surface. A drop of clay suspension was layered onto the flat surface. Thus, the grains were oriented parallel to the surface of the resin (Ahn and Peacor, 1985). Before impregnating the samples in Spur resin they were dried over three days in a 70°C for 16 hours in the same oven. The polymerised blocks were removed from the moulds, reoriented and cut to give a transverse profile of the samples sandwiched between the two layers of resin. Sectioning was carried out on Reichert Ultramicrotome using a diamond knife to give sections of 70 nm thickness and the sections were collected on 300 mesh Cu. grids. A thin layer of evaporated carbon was applied to the sections on the grids to stabilize the resin under the electron beam. Lattice fringe images were obtained at 100 KV using JEOL CX 100 electron microscope. Same microscope was used for the TEM examination.

RESULTS AND DISCUSSION

Clay mineralogy

Almost all analysed samples were composed of predominantly illite/smectite mixed-layer followed by subordinate amounts of kaolinite, illite/mica and Chlorite. Quartz is the only non clay mineral, which is present in 2μm fraction.

The samples from Karak mudstone do not show a 17 Å peak on glycolation. Instead they show a maxima in the region between 17 Å and 10 Å that contains a dominating component of second order superstructure reflection (002*) i.e. a combination of the superlattice 002 of the 27 Å phase and 001 of the 10 Å phase (Fig. 1). The position of this maxima between 12 Å and 13 Å indicates R1 ordering (Reynolds & Hower, 1970).

Variations in the low angle peak positions, widths, and intensities of peaks occurred with changes in the value of N, the range of thicknesses of unit layers making up the diffracting domain is the interference function. With all the variables held constant, the computed patterns (NEWMOD) for very thick domains (N = 9-14) produced relatively narrow peaks with shifts in the high 2θ direction and a low angle reflection at 32.7 Å. N values of 5-12 and 3-9, produced broader peaks with different relative intensities and shifts in the low 2θ direction. The higher angle peak near 17° was not affected. R1 ordering was assumed in the calculations of diffractograms and best fit patterns were achieved for N = 3-9, which suggests a minimum size for diffracting crystals. It is possible that actual three dimensional crystals may have thicker domains than the assumed ones and may have been made up of many domains. Diffractograms of samples investigated show consistent smectite proportion in illite-smectite mixed layer, which varies between 25 to 30%.

Morphology of illite-smectite by TEM

Transmission electron microscope photomicrographs are presented in Fig. 2. Unfortunately most of the particles show coalescence probably due to inadequate sample dilution. This aggregation of the particles hampered the efforts to measure the dimensions of the individual particles. However, close inspection of the photographs revealed two features. Firstly the majority of the particles are subhedral thin laths of varying length and width and only little grain show irregular shape. This type of morphology is a very common feature of illite-smectite having R=1 ordering with low expendabilities (e.g. Inoue et al., 1987, 1988,: Nadeau et al., 1985). Secondly it appears that many grains show step like growth probably due to dissolutioning of the older smectite particle and neoformation of illite particles.

Fig. 3 shows well resolved lattice fringe images of thin crystals (cystallites). These crystallities consist of sets of layers of strictly parallel, defect free and regularly spaced 10 Å layers. In terms of shape they are mostly straight and are in abundance. These crystallities are assumed to be illite. In this study these are called coherent scattering domains from XRD point of view. Interruption to the regular 10 Å periodicity was treated as crystallite boundaries. Many of these have spacing of 15 Å or greater and were considered as smectite layers. In the lower left corner of the Fig. 3 crystallites show irregularity in structure as they are curved and twisted in a felt like configuration. Moreover, compaction has resulted in a kinked like folded crystallites. Similar structural features have also been observed in HRTEM study of illite-smectite from COST 1 well by Bell (1986).

Figs. 4a-c are the enlargements of Fig. 3. and show that individual crystallite layers are sub parallel and are characterized by low grain boundary angles. The fringe lattices of one crystallite terminate along outer layers of an adjacent crystallite. Fig. 4a also shows typical features of edge dislocations also reported by other workers (e.g. Lee et al., 1985; Ahn and Pecoar, 1985, 1986; Huff et al., 1988). Crystallites seem to be spilt off separately at the ends of crystals or merge with adjacent crystallite along low angle boundaries. Thus, as a whole the large domain in the photomicrograph appears to be a composite of smaller unit, which nevertheless retain some internal coherence of their own. Rare small dislocations within the crystallite can also be observed. These dislocations are probably due to compositional anomalies or represent imperfections in scattering order of individual layers similar to interfaces between coherent domains. The thickness of the fringe sometimes changes as it is traced along its length (Fig. 4c). A fringe starting as a smectite interlayer (15 Å) on left side of photomicrograph becomes illitic (10 Å) interlayer on the right side of photomicrograph (shown by arrows). This part of collapsed smectite may be considered due to non effective Al pillaring, but many other smectite layers maintained their spacing (15 Å) constant through out their length. Therefore, it is more likely that the collapsed part may be converted illite from smectite rather than simply a collapsed part due to high beam energy. If it is the case it can be suggested that illitization of smectite layers have taken place through layer by layer transformation of smectite to illite without dissolution and precipitation. In brief, this study suggests that both dissolution and precipitation and solid state mechanism were involved in the smectite to illite conversion.

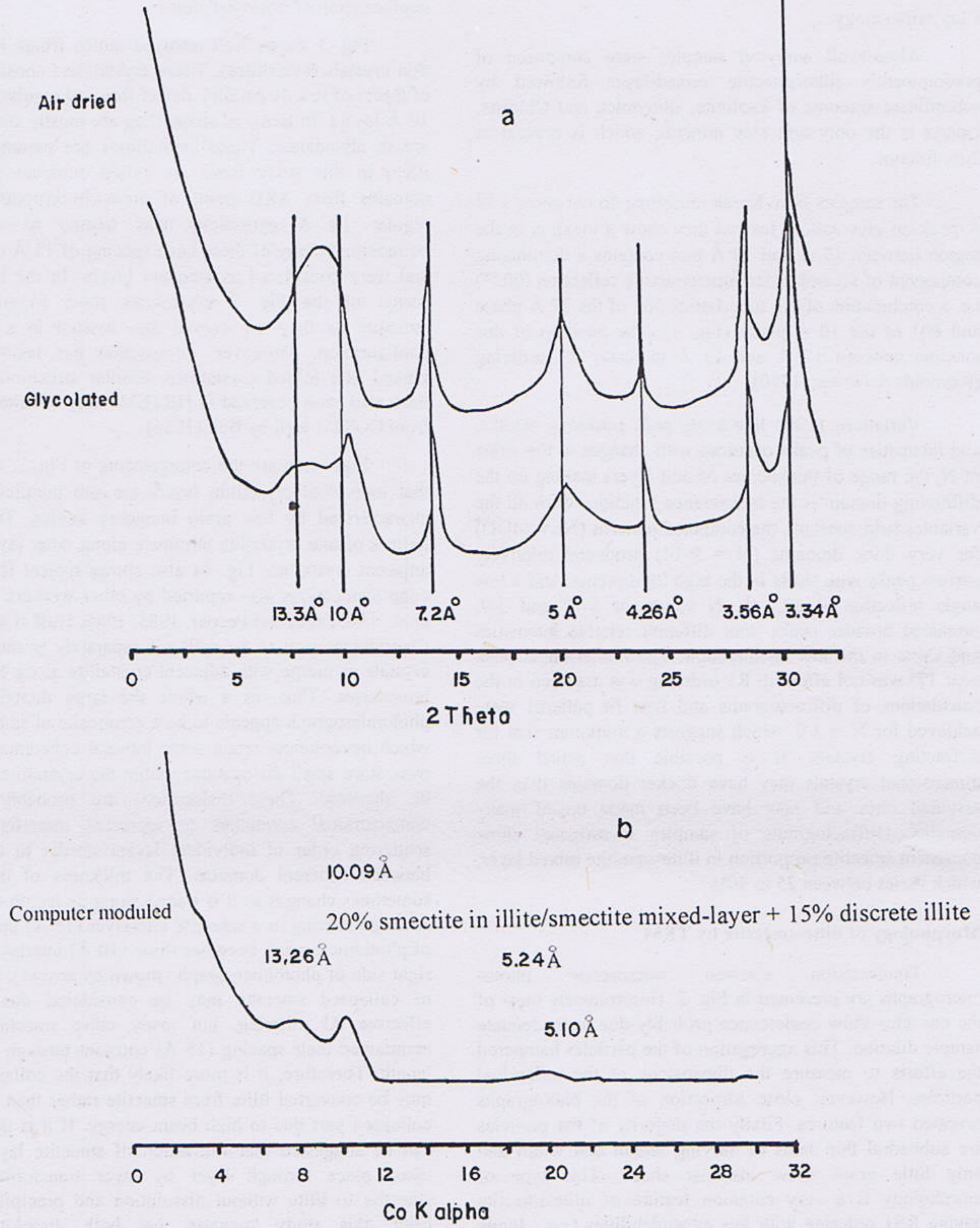

Fig. 1 Typical X-ray diffraction tracings of < 2μm air dried and glycolated fraction of Karak mudstone, peak positions and intensities indicate R=1 ordering (a). Computer generated (NEWMOD) XRD pattern of ordered illite/smectite mixed layer (b).

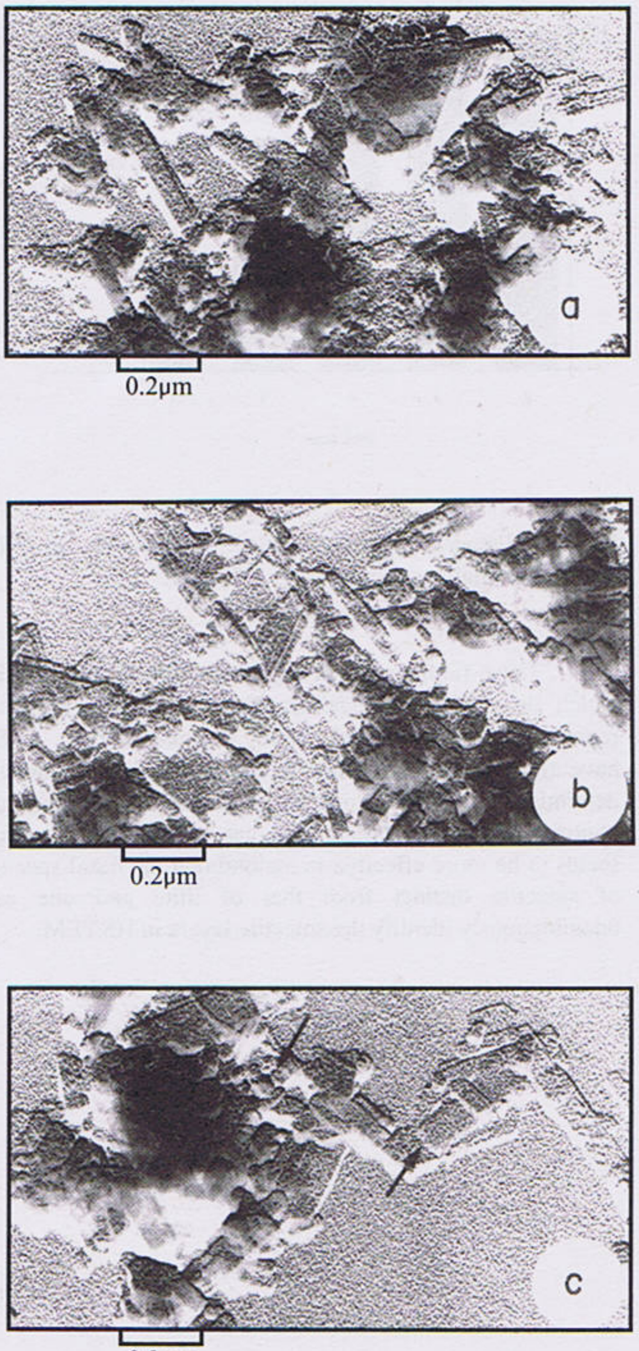

Fig.2:- TEM microphotographs of <1μm clay fraction from Karak mudstone showing lath shaped morphology, characteristics of illites/smectite having low expandability. Some particles with irregular boundaries probably are of kaolinite (eg. Photomicrograph c, same microphotograph shows step like growth (indicated by arrow).

Fig. 3:- Direct lattice image of Al-pillared illite/smectite from Karak mudstone. Imaged area showing predominance of thin packets consisting of 10Å illite with intercalations of 15Å expanded smectite. In the left corner of the microphotograph crystallites are folded (see text for explanation). Non imaged area is due to beam damage.

In this study 54 illite crystallite were measured by treating a sequence of defect free, regular 10 Å fringe lattices as coherent domain. As such these would be expected to coherently scatter an incident beam of X-rays. Histogram of these measurements is presented in Fig. 5, which shows that majority of illite crystallities are 2-4 layers (i.e. 20-40 Å) thick with < 20% of the measured population having 5 or 6 layers. The mean thickness of the population is 3.5 layers i.e. most crystallities are either 3 or 4 layers thick.

In order to compare the smectite content of the illite-smectite specimen observed by HRTEM with that observed by XRD, illite and smectite layers were directly counted in the HRTEM photomicrographs 62 smectite layers were found to be present in 242 illite-smectite layers, which suggests 26% smectite in illite-smectite layers.

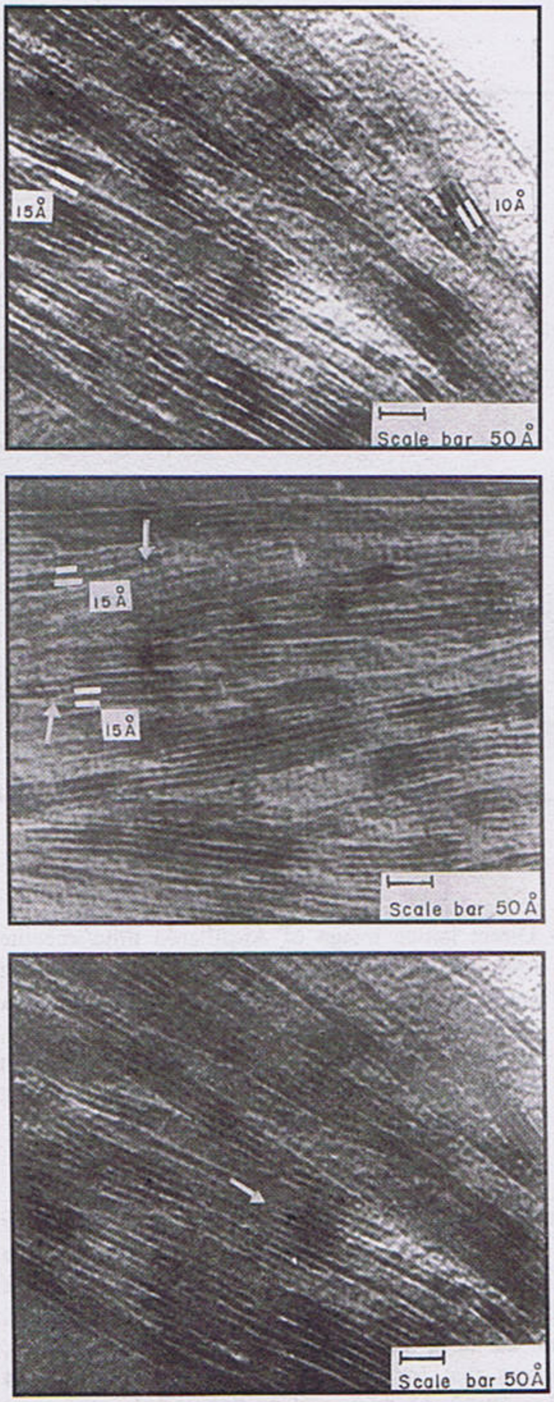

Fig.4:- HRTEM microphotographs showing individual illite and smectite layers characterized by 10Å and 15Å interlayer distance (a) smectite layers showing dislocation indicated by arrows (b) and 15Å smectite interlayer converting to 10Å illite (c). Interlayer thickness change is shown by arrow direction.

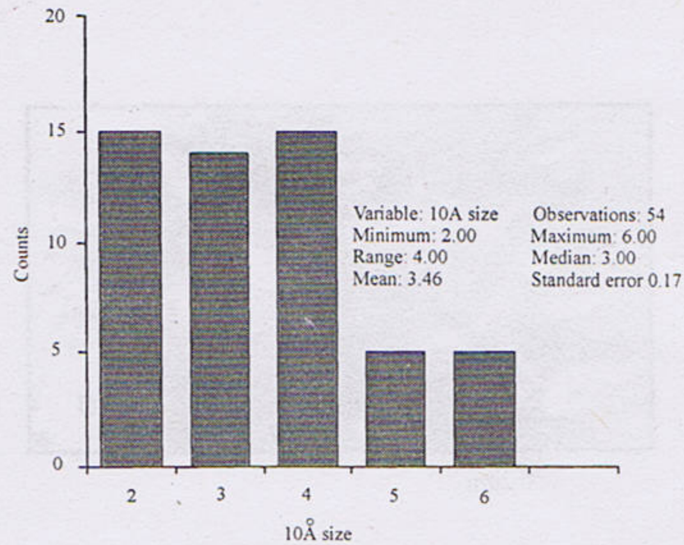

Fig.5:- Histogram showing range of thickness of illite crystallites measured by HRTEM.

These findings are in consistent with those of XRD, which show 25% expandability for this sample. Previous reports (e.g. Srodon, et al., 1990; Murakami, et al, 1993) have also shown consistency in the percentage of smectite determined by HRTEM and XRD. In this study a different approach in sample preparation has been adopted, which seems to be more effective in maintaining the basal spacing of smectite distinct from that of illite and one can unambiguously identify the smectite layers in HRTEM.

REFERENCES

Ahn, J. H. and Peacor, D. R. 1985. Transmission electron microscopic study of diagenetic chlorite in Gulf Coast argillaceous sediments. *Clays and Clay Miner.*, **33,** 228-236.

Ahn, J. H. and Peacor, D. R. 1986. Transmission and analytical electron microscopy of the smectite to illite transition. *Clays and Clay Minerals.*, **34,** 165-179.

Ahn, J. H. and Peacor, D. R. 1989. Illite/Smectite from Gulf Coast Shales; a reappraisal of transmission electron microscope images. *Clays and Clay Miner.,* **37,** 542-546.

Bell, T. E. 1986. Microstructures in mixed layer illite/smectite and its relationship to the reaction of smectite to illite. *Clays and Clay Miner.,* **34,** 146-154.**34,** 146-154.

Bauluz, B,. Peacor, D. R. and Ylagan, R. F., 2002. Transmission electron microscopy study of smectite illitization during hydrothermal alteration of a rhyolitic hyaloclastite from Ponza, Italy. *Clays and Clay Miner.*, **50,** 157-173.

Chaudhry, M. N. and Ashraf, M. 1979. Petrology of the Karak Bentonites- Kohat District, N.W.F.P, Pakistan. *Geol. Bull. Punjab Univ.,* **14,** 1-26.

Dong, H. and Peacor, D. R 1996. TEM observations of coherent stacking relations in smectite: Evidence of MacEwan crystallites and dominance of 2M1polytypism. *Clays and Clay Miner.*, **44,** 257-275.

Dong, H., Peacor, D. R. and Fred, R.L. 1997. Phase relations among smectites. R1 illite- smectite and illite. *Amer Mineral,* **82,** 379-391.

Guthrie, G. D., Jr. and Veblen, D. R. 1989a. High -resolution transmission electron microscopy applied to clay minerals. In L., M, Coyne, D. F. Blake. and S. McKeever, Eds., Spectroscopic characterisation of minerals and their surfaces. *American Chemical Society Symposium Series,* **415,** 75-93.

Guthrie, G. D., Jr. and Veblen, D. R. 1989b. High -resolution transmission electron microscopy of mixed layer illite/smectite; Computer simulations. *Clays and Clay Miner,* **37,** 1-11.

Guthrie, G. D., Jr. and Veblen, D. R. 1990. Interpreting one dimensional high resolution transmission electron micrographs of sheet silicates by computer simulation. *Amer Mineral,* **75,** 276-288.

Hower, J., Eslinger, E. V., Hower and M., Perry, E. A. 1976. Mechanism of burial metamorphism of argillaceous sediments; 1 Mineralogical and chemical evidence. *Geol. Soc. Amer. Bull.,* **87,** 725-737.

Huff, W. D., Whiteman, J. A. and Curtis, C. D. 1988. Investigation of K-bentonite by X-ray powder diffraction and analytical transmission electron microscopy*: Clays and Clay Miner,.* **36,** 83-93.

Inoue, A., Kohyama, N., Kitagawa, R. and Watanabe, T. 1987. Chemical and morphological evidence for the conversion of smectite to illite. *Clays and Clay Miner,* **35,** 111-120.

Inoue, A., Velde, B., Meunier, A. and Touchard, G. 1988. Mechanism of illite formation during smectite-to-illite conversion in hydrothermal systems. *Amer Mineral,* **73,** 1325-1334.

Klimentidis, R. E. and Mackinnon, D. R. 1986. High resolution imaging of ordered mixed-layered clays. *Clays and Clay Miner,* **34,** 155-164.

Lahav, N., Shani, U. and Shabtai, J.1978. Cross-linked smectites. I-Synthesis and preparation of hydroxy-aluminium montmorillonite. *Clays and Clay Miner,* **26,** 108-115.

Lee, J. H., Ahn., J. H. and Peacor, D. R. 1985. Textures in layered sillicates. Progressive changes through diagenesis and low temperature metamorphism. *J. Sed. Pet,* **55,** 532-540.

Lee, J. H. and Peacor, D. R. 1986. Expansion of smectite by laurylamine hydrochloride: Ambiguities in transmission electron microscope observations. *Clays and Clay Mineral,* **34,** 69-73.

Moor, D. M. and Reynolds Jr. R. C. 1989. X-Ray Diffraction and the identification and analysis of clay minerals. *Oxford university Press, Oxford.* pp 135-138.

Murakami, T., Sato, T. and Watanabe, T. 1993. Microstructure of illite/smectite at 123 K: A new method for HRTEM examination. *Amer Mineral,* **78,** 465-468.

Nadeau, P. H., Tait, J. M., McHardy, W. J. and Tait, J. M. 1985. The conversion of smectite to illite during diagenesis: evidence from some illitic clays from bentonites and sandstones. *Min. Mag.,* **49,** 393-400.

Reynolds, R. C. Jr. and Hower, J. 1970. The nature of the interlayering in mixed layer illite-montmorillonites. *Clays and Clay Miner.* **18,** 25-36.

Saleemi, A.A. and Ahmed, Z. 2000. Mineral and chemical composition of Karak mudstone, Kohat Plateau, Pakistan: implicatios for smectite illitization and provenance. *Sedimentary Geology,* **130,** 229-247.

Shabtai, J. and Lahav, N. 1980. Cross-linked montmorillonite molecular sieves: *US. Patent,* **4, 216,** 188.

Srodon, J., Andreoli, C., Elsass, F. and Robert, M, 1990. Direct high resolution transmission electron microscopic measurements of expandability of mixed-layer illite/smectite in bentonite rock. *Clays and Clay Miner,* **38,** 372-379.

Vali, H. and Hesse, R. 1990. Alkylammonium ion treatment of clay minerals in ultra thin section: A new method for HRTEM examination of expandable layers. *Amer Mineral,* **75,** 1433-1446.

Vali, H. and Köster, H. M. 1986. Expanding behaviour, structural disorder, regular and random irregular interstratification of 2:1 layer-silicates studied by high-resolution images of transmission electron microscopy. *Clay Mineral,* **24,** 827-859.

Vali, H., Hesse, R. and Kohler, E. E. .1991. Combined freeze etch replicas and HRTEM images as tool to study fundamental particles and the multiphase nature of 2:1 layer silicates. *Amer Mineral,* **76,** 1973-1984.

Yan, Y., Tillick, D. A., Peacor, D. R. and Simmons, S. F. 2001. Genesis of dioctahedral phyllosillicates during hydrothermal alteration of volcanic rocks: The Broadlands hydrothermal system, New Zealand. *Clays and Clay Mineral,* **49,** 141-155.

Yau, Y. C., Peacor, D.R., and McDowell, S. D. 1987. Smectite to illite reaction in Salton Sea Shales: A transmission and analytical electron microscopy study: *J. Sed. Petrol,* **57,** 335-342.

Wells, N. A. 1984. Marine and continental sedimentation in the early Cainozoic Kohat Basin and north-western Indo-Pakistan. Ph.D. thesis, University of Michigan.

Yoshida, T. 1973. Elementary layers in the interstratified clay minerals as revealed by electron microscopy: *Clays and Clay Miner,* **21,** 413-420.

Geol. Bull. Punjab Univ. 38, 2003.

PETROGRAPHY AND GEOCHEMISTRY OF THE NAGARPARKAR COMPLEX, SOUTHEASTERN SINDH, PAKISTAN

BY

SYED ALIM AHMAD
Institute of Geology, University of the Punjab, Quaid-e-Azam Campus, Lahore, Pakistan

ABDUL MATEEN
Pakistan Institute of Engineering and Applied Sciences, P.O Nilore, Islamabad, Pakistan.

AND

MUHAMMAD NAWAZ CHAUDHRY
Institute of Geology, University of the Punjab, Quaid-e-Azam Campus, Lahore, Pakistan

Abstract: *The rocks of Nagarparkar Igneous Complex fall into two distinct magma associations. The older sequence represents plutonic sub-alkaline tholeiitic magma association of gabbro, diorite, granodiorite, adamellite and granites. The younger magma series form an alkaline bimodal volcanoplutonic association comprising mafic suite of alkali basalt/dolerites, trachybasalt, phonotephrite, while felsic members consist of alkaline rhyolites and alkaline granites.*

The so called Shield elements exposed to the west of the Aravalli Orogen, in Kirana, Nagarparkar, Jodhpur, Malani, Tosham, Mount Abu and Erinpura are neither a part of the Aravalli Orogen nor do they belong to the Vindhyan Basin. These volcanoplutonic and sedimentary rocks represent a distinct cratonic rift assemblage. They were deposited in extensional basins formed as a result of rising of the mantle plume around 1000 ma and probably can be linked up with opening of the Mozambique ocean and break up of Rodinia Super continent during 850-750 Ma. This basin is named by us as Malani-Kirana Basin.

INTRODUCTION

The Nagarparkar Complex, which crops out in the extreme southeast of Thar desert near the Runn of Kutch, is a part of widespread Late Proterozoic Malani Igneous suites extending from western Rajasthan to Sindh Province in Pakistan (Fig: 1). The Nagarparkar Complex constitutes two distinct magma series; the older series represents the plutonic subalkaline association of gabbros, diorite, granodiorite and granites, while the younger volcanoplutonic magma series represents pulses of biomodal suites comprising alkali basalts/dolerites and alkali rhyolites/granites. Earlier geological accounts of rocks and associated china clay deposits and other economic resources of Nagarparkar are given elsewhere (Wynne, 1867; Fermor, 1932; Pascoe, 1960; Kazmi and Khan, 1973; Kella, 1983; Butt et al., 1989). Detailed geology and petrographic accounts are presented by a number of workers (Butt et al., 1992; Muslim et al., 1997, Jan et al., 1997) who differentiated various mafic and felsic rock units, particularly granites and rhyolites. Butt et al. (1994) correlated the granites with the Late Proterozoic Mount Abu Granites and proposed that the granites are anatectic products. Jan et al. (1997) concluded that the Nagarparkar Igneous Complex is a product of several distinct batches of mafic and felsic magmas of alkaline affinity.

Nagarparkar Igneous Complex constitutes a distinct anorogenic igneous cratonic rift assemblage of widespread magmatic activity (Chaudhry et al., 1999). The complex does not represent Indian Shield elements as previously believed by several workers (Heron, 1913; Davies and Crawford, 1971; Shah, 1973; Kochhar, 1984;Muslim et al., 1997). The igneous rock suites of Nagarparkar Complex may be petrogenetically correlated with the Malani Igneous suites, particularly granites from Mount Abu, Jalore, Siwana and Erinpura (Srivastava, 1988;Eby and Kochhar, 1990;Sarkar et al., 1993;Kochhar et al., 1995;Rathore et al., 1996; 1999;Bhushan and Chittora,

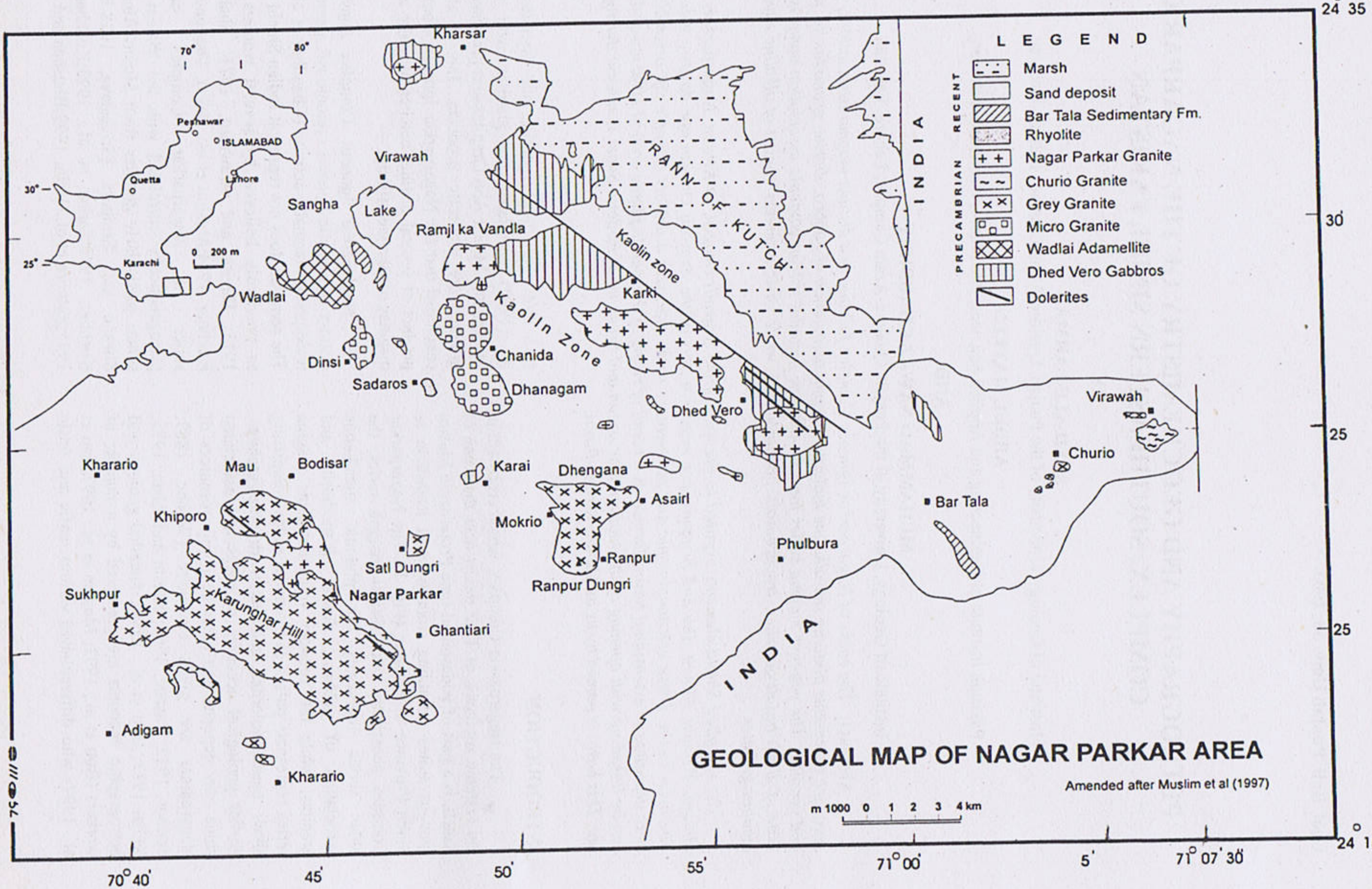

GEOLOGICAL MAP OF NAGAR PARKAR AREA

Amended after Muslim et al (1997)

1999). This paper presents the petrographic and geochemical data in an attempt to seek interpretation of the petrogenesis of the Nagarparkar Complex.

GEOLOGICAL SETTING

The Nagarparkar Complex is situated at the extreme southeast of Thar desert of Sindh near the Runn of Kutch (24° 15' to 24° 30' latitude, 70° 37' to 71° 07' longitude and covers an area of about 450 sq km (Fig.1). The earliest accounts of the geology of the Nagarparkar rocks are recorded in Geological Survey of India (Wynne 1867, Fermor 1932). A detailed map of the area and description of the basic intrusions and granitic rocks are presented by Kazmi and Khan (1973) who defined the Nagarparkar igneous complex as Precambrian basement. Detailed description of geology and petrographic data of various rock units of the Nagarparkar Complex are presented by several workers (Shah, 1977, Butt et al., 1989, 1992; Muslim et al., 1997; Jan et al., 1997). These workers are of the opinion that the Nagarparkar Complex is a part of Precambrian fragment of the Western Indian Shield. The granites of the complex are considered to be the extension of the post-Aravalli magmatism in the Late Proterozoic. They may have been generated as a consequence of sinistral shear along the Narmada-Son lineament and crustal anataxis in the continental anorogenic environment (Butt et al., 1992, Jan et al., 1997). The basement may have undergone a tectono-metamorphic event before the emplacement of the granites.

However, the recent tectono stratigraphic observations on Kirana Volcanics (Chaudhry et al., 1999) and the present geochemical investigations have indicated that the Nagarparkar Complex and the Kirana Volcanics do not represent Indian Shield elements. The igneous rock suites of the Nagarparkar Complex constitute a distinct cratonic rift assemblage of widespread magmatic activity. They may be petrogenetically correlated with the Malani Igneous suites (Srivastava, 1988; Eby and Kochhar, 1990; Rathore et al., 1996; 1999; Bhushan and Chittora, 1999). The volcanoplutonic and sedimentary rocks were emplaced in extensional basin. The episodic igneous activity in the Nagarparkar and Kirana in Pakistan may be linked with opening of the Kirana-Malani Basin formed by rifting of Greater Gondwana (Chaudhry et al., 1999). Present geological and geochemical investigations have shown that the Nagarparkar Complex may be defined in terms of two distinct magma associations. The older plutonic sequence represents the subalkaline tholeiitic magma series of gabbro, diorite, granodiorite, adamellite and granites. While the younger volcanoplutonic association is comprised of bimodal alkaline mafic and felsic rock suites. On the basis of petrographic studies and geochemical data, the Nagarparkar Complex has been divided into the following rock units:

Subalkaline rocks association consists of Dhedvero Gabbros and diorites, granodiorite, Wadlai Adamellite, Nagarparkar Granite and aplite/porphyry dykes bimodal alkaline rock association is comprised of mafic component of alkali basalt, trachybasalt and dolerite dykes and the felsic rock units named as Sadarous Rhyolite/Grey Granites, and Churio Granites.

Subalkaline Association

Dhedvero Gabbros and Diorites: The gabbroic intrusions occur near Dhedvero, Karai, Karki, Parodhra and Ramji Ka vandi areas. They are dark green massive and generally medium-grained. At places, particularly around Dhedvero, they are highly weathered, sheared and show foliation. Butt et al., 1992 and Jan et al., 1997 defined this mafic unit as metabasites or amphibolites and related dykes based upon the field observations and suggested that it has suffered epidote-amphibolite facies metamorphism. However, this is not so, their argument is not supported by mineralogical and petrological evidence of such a high-grade metamorphism.

Present field investigations and petrographic studies clearly indicate that the gabbroic intrusions locally have been subjected to intensive weathering and alteration, particularly near Dhedvero, chloritization and epidotization is generally observed but no evidence of amphibolite facies metamorphism is observed in all the studied samples as claimed by previous workers (Butt et al., 1989; Muslim et al., 1997; Jan et al., 1997). On the contrary, most of the exposures in Karai and Karki exhibit rather fresh, compact and unaltered intrusions of gabbroic rocks. Petrographically two distinct varieties are identified as normal gabbros and hornblende gabbros.

Within the Dhedvero gabbroic intrusions, several related mafic dykes occur which range in composition from hornblende gabbros, gabbroic diorite to quartz diorite. They are medium- grained, contain hornblende and plagioclase as the major phases and show slight alteration.

Wadlai Adamellite: Typical adamellites are exposed in Wadlai area. They also occur near Mokrio locality Butt et al. (1992) included this unit in their pink granites, which contain higher plagioclase content. Jan et al., (1997) coined the term 'Mottled' pink granite for this adamellite rock found NE of Mokrio village. In fact, most of the Wadlai rock sequence is comprised of adamellite. The rock is medium to coarse-grained, petrographic observations show that it is an alkali adamellite and not normal adamellite. (Aegirine appears in some thin sections e.g. S No.A892, Table.1). Moreover peralkalinity index of all adamellites falls below 0.87index as indicated in Fig No.6.

Nagarparkar Granite: The main unit occurs near Nagarparkar town along the northeastern margin of Karunghar Hill. Other exposures of this unit are found in Bhodisar, Dinsy, Waravai Dhedvero and NE of Kharsar, the pink granite is medium to coarse grained, mostly homogenous leucocratic and exhibit spheroid weathering surfaces. The whole body in Nagarparkar and Bhodisar is intruded by aplite and acid porphyry dykes as well as doleritic dykes. Such dykes have been reported by pervious workers as well (Kazmi and Khan, 1973; Butt et al., 1992; Muslim et al., 1997).

Aplitic and Acid Porphyry Dykes: Several small dykes of felsic composition are found intruding the older lithologies, particularly in Dhedvero and Nagarparkar localities. They range from rhyolitic porphyry to aplite and microgranites. Best exposures of acid porphyry and microgranite dykes occur in Dhedvero, Chanida, Dhanagam Ghantiari and Dinsy

Alkaline Association

Basalts and Dolerites: This mafic rock unit comprised of basalt and dolerite occur as dykes and small intrusions within the major gabbroic rocks particularly near Karai and Dhedvero areas and in the major granitic rock units. They exhibit crosscutting relationships. In Karai section, dolerites occur as dyke swarm traversing in two different directions. Fine-grained dolerites and lamprophyritic dykes (chemically identified as K-phonotephrite) have been found intruding the Grey Granite. Several workers have described mafic dykes as a separate unit younger than granites (Kazmi and Khan, 1973; Muslim et al., 1997; Jan et al., 1997). All samples falls in alkali basalts, trachybasalt, and phonotephrite indicated in Fig No.2. Moreover aegirine and riebeckite is appearing in some thin sections (S.NoA889 T.No.1).

Sadarous Rhyolites: Major outcrops of this unit occur near Sadarous and Dungri-in the form of domal shape plugs, small bodies of rhyolite unit are also found associated with the Grey Granite and the granitic stocks in Dinsy and near Mokrio. The rhyolite unit is homogeneous, dark grey and dark brown in colour, fine-grained, subporphyritic at places glassy-looking and apparently banded.

Grey Granite: This grey granite covers the major portion of Karunghar Hill, forming a large plutonic body striking in the NW-SE direction. The exposures of this unit are found at many places including Karai, Dungri, Ghantiari, Rarko, Karai, Adhigam and Mau. The Granite is undeformed; medium to coarse grained, contains xenoliths of dolerite and is characterized by peralkaline mineralogy (riebeckite and aegirine are present in most of the sample studied)

Churio Granite: This granite unit occurs as isolated outcrops in Churio and Virawah. It is coarse grained, off-white to high pink in colour, leucocratic and shows alkaline character. This type of granite is also exposed at Mokrio, Sadarous and Dungri.

AGE RELATIONSHIP

To date no published radiometric age data is available on the Nagarparkar rocks. Recent systematic geological and geochronological studies have lead to establish the correlation of various litho-tectonic units in the Western Trans Aravalli-Delhi orogenic belt stretching from western Rajasthan and Gujarat in India and the extreme south to Nagarparkar Sindh in Pakistan (Heron, 1913; Shah, 1973; Pareek, Srivastava, 1988; Virdi, 1997). The late-Proterozoic tectono stratigraphic history of Kirana-Nagarparkar-Malani cratonic rift Basin is marked by widespread plutonic-volcanic activity and sedimentation (Chaudhry et al. 1999). This episodic igneous activity in the Nagarparkar may be related with rifting of Rodinia supercontinent. The igneous rocks of Nagarparkar Complex may be petrogenetically correlated with the granites of Mount Abu, Jalore and Siwana (Crawford, 1970; Srivastava, 1988; Kochhar et al., 1995; Bhushan and Chittora; 1999).

PETROGRAPHY

Accounts of the petrography of various rock types of the Nagarparkar Complex are given by Butt et al., 1992; Muslim et al., 1997 and Jan et al., 1997. This petrographic account is based on the study of 115 representative samples collected from different rock units of the complex based on petrographic features and modal mineralogy. Summary of the petrographic data is presented in Table 1. A brief description of the petrography of the rocks is given as follows.

Mafic Rocks

Two distinct types of gabbros are identified on the basis of mineralogy (a) normal gabbros having plagioclase ± olivine + pyroxene (augite) + Fe- Ti-oxide + apatite + sphene (b) hornblende gabbros consisting of plagioclase + hornblende ± biotite +

Table 1

Model compositions of representative igneous suites from Nagarparkar alkaline complex.

	Basalts/dolerites		Gabbros		Diorites		Granodiorites		Alkali Rhyolites		Adamallites		Grey granites		Offwhite granite		Pink granite	
Group	Karai-Dhedvero		Karai-Dhedvero		Nagarparkar		Churio-Mokrio		Dungari		Wadlai		Karunghar hill		Churio-Mokrio		Nagar-Dhedvero	
Areas	Dinsy	Wadlai	Karai	Karai	Nagar	Dhedvero	Mokrio	Rarko	Dungari	Sadarous	Wadlai	Wadlai	Mokrio	Karunghar	Mokrio	Mokrio	Sadarous	Nagar
Sample.No	A856	A889	A857	A866	A943	A925	A910	A899	A852	A871	A884	A892	A913	A952	A902	A907	A875	A957
Minerals																		
Quartz	nil	0	0	nil	3	11	21	23	12	8	30	30	30	37	31	34	26	36
Plagioclase	29	17	59	53	26	47	47	45	7	nil	33	34	20	3	18	27	29	5
Perthite	nil	0	0	nil	0	0	0	0	35	nil	20	12	30	47	41	32	15	50
K-felspar	nil	7	0	nil	5	9	6	4	6	7	12	15	13	0	nil	nil	25	0
Hornblende	tr	0	0	tr	9	7	3	3	nil	nil	1	1	tr		1	1	1	0
Pyroxene	12	0	31	42	18	9	8	12	2.5	0	1.5	3	2.5	3	0	2.5	1	2
Nephenline		8	0	nil	0	0	0	0		nil	nil	nil	nil	0	nil	nil	nil	0
Biotite	nil	pr	0	nil	0	2	0	4	2	nil	1	2	2	3	3	2	1	2
Sphene	nil	pr	0	nil	0	tr	2	0	0.5	nil	0.5	1	0.5	tr	0.5	0.5	nil	tr
Olivine		8	6	nil	0	nil		0		nil	nil	nil	nil	0	nil	nil	nil	nil
Aegirine	nil	7	0	nil	0	0	4	3	Tr	nil	nil	1	nil	2	2	tr	2	2
Riebeckite	nil	pr	0	nil	0	0	0	4	2	nil	nil	nil	nil	3	2	nil	nil	1
Epidote	7	0	0	nil	6	0	6	0	nil	nil	nil	nil	nil	0	nil	nil	nil	0
Act-tre	nil	0	0	nil	0	0		pr	nil	nil	nil	nil	nil	0	nil	nil	nil	0
Chlorite	47	0	0	nil	0	8	pr	pr	2	nil	nil	nil	nil	0	nil	nil	nil	0
Muscovite	nil	0	0	nil	0	0	0	0	Tr	nil	nil	nil	nil	0	nil	nil	nil	0
Iron	5	3	3	5	5	8	3	3	1	2	0.5	1	2.3	2	2	2	1	2
Calcite	nil	0	0	nil	3	0	0	0	nil	nil	nil	nil	nil	0	nil	nil	nil	0
Sericite	tr	0	0	nil	0	0	tr	0	nil	nil	0.5	tr	nil	0	nil	tr	nil	0
Zircon	nil	0	0	nil	0	0	0	0	Tr	nil	0.5	tr	tr	0	tr	tr	tr	0
Apatite	nil	0	0	nil	0	0	0	0	Tr	nil	tr	tr	tr	0	tr	nil	tr	0
Mic-crys	nil	50	0	nil	25	nil	nil	nil	30	83	nil	nil	0	0	0	nil	tr	0
Total	100	100	99	100	100	101	100	101	100	100	100.5	100	100.3	100	100.5	101	101	100
Phenocryst	100	35	100	100	60	nil	nil	100	100	15	100	100	100	100	100	100	80	100
Groundmass	0	65	0	0	40	nil	nil	0	nil	85	0	0	0	0	0	0	20	0

chlorite ± epidote ± quartz + apatite + sphene. Texturally they are subophitic. Olivine is recorded in few samples. Augitic pyroxene occurs as phenocrysts and shows reaction/alteration to hornblende and chlorite. Hornblende is strongly pleochroic from yellowish green to brownish green and generally fresh and shows alteration to chlorite. Plagioclase laths are subhedral with corroded margins and its composition ranges from labradorite to andesine. Butt et al. (1989) recorded the presence of graphic patches in gabbroic rocks and suggested tholeiitic affinity.

Diorites are comprised of plagioclase and hornblende as the major mineral phases. Quartz, biotite, opaque iron oxide and sphene as essential minor constitute. Plagioclase shows zoning. Granodiorite contain hornblende, biotite and K-feldspar as essential mineral phases.

Felsic Rocks

Nagarparkar Granite is medium to coarse grained homogeneous and exhibits equigranular to subequigranular texture. The rock is composed of quartz + perthite (locally contains plagioclase) + biotite + magnetite ± aegirine (at the contact of Grey Granite) ± sphene. Perthitic texture predominates. Rapakivi texture was not observed in any sample, though it has been reported by Muslim et al., 1997. However, granophyric texture and myrmekitic intergrowths are common. The granite exhibits variable degree of alteration to sericite and kaolin.

Wadlai Adamellite is equigranular, medium-grained and consists of quartz perthitic K-feldspar and plagioclase. Mafic minerals include biotite, hornblende and chlorite. K-feldspar is partially sericitized. Subporphyritic texture and perthitic intergrowths are common.

Grey Granite is composed of quartz + perthite ± plagioclase + aegirine + riebeckite ± biotite + magnetite. Accessory to trace minerals include sphene, zircon, apatite and allanite. The whole unit is medium to coarse grained and pegmatite growth is also observed. Texturally the rock is generally equigranular to subporphyritic. The feldspars exhibit myrmekitic and granophyric intergrowths. Graphic intergrowth of quartz and feldspar is also observed in many samples.

Churio Granite is coarse grained mineralogically and texturally similar to Grey Granite. Some samples exhibit more than one generation of quartz and K-feldspar. The feldspar shows extensive alteration to kaolin, particularly around Virawah.

Sadarous Rhyolites is composed of quartz + K-feldspar + perthite (as phenocrysts as well as groundmass) ± riebeckite ± aegirine ± magnetite. Other type of rhyolites occur as dykes and are comprised of quartz + K-feldspar + plagioclase + magnetite + sphene + apatite. Microphenocrysts of quartz and perthite or K-feldspar are embedded in a microcrystalline groundmass. The groundmass is generally devitrified to microcrystalline aggregate of quartz and alkali feldspar. Strongly pleochroic bluish riebeckite and minor amount of brown biotite appear in most of the rhyolite samples. The phenocryst phase constitutes up to 25% of the rocks. Spherulitic and micrographic textural intergrowths of quartz and K-feldspar are common in groundmass. Rounded spherulites have radiating growth of alkali feldspar and quartz. Rhyolites are generally related to Grey Granite. Rhyolitic and aplitic dykes are fine-grained, strongly porphyritic and contain phenocrystic mineralogy of perthite and plagioclase with minor amount of quartz.

GEOCHEMISTRY

Major and trace element contents in various rock units from Nagarparkar Complex were determined by standard X-ray fluorescence technique. Average data of major and trace element compositions for rock suites is listed in Table 2. All major elements have been recalculated on an anhydrous basis as recommended by IUGS (Le Maitre et al, 1989) after adjustment of Fe_2O_3 contents according to the recommendation of Middlemost (1991) for oxidation condition of magma generation.

The gabbros in the Nagarparkar Complex, particularly in Dhedvero area have been affected by low-grade metamorphism. The analytical data was evaluated with a preserved primary mineralogy among the studied rocks to check the elements mobility during metamorphism.

The field relations indicate that the Nagarparkar Complex experienced two distinct magma episodes. The older plutonic sequence constitutes magma series comprising of gabbro, diorite, granodiorite and granites. The younger magma episode represents alkaline volcanic activity.

The major rock units have been classified on the basis of petrography and major element chemistry. The analytical data have been plotted on the standard geochemical classification diagrams of total alkali versus silica (Fig 2, TAS diagram after Le Maitre 1989,Middlemost 1991) and K_2O versus SiO_2 (Fig 3, after Rickwood 1989). The sub-alkaline-alkaline dividing line of Miyashiro (1978) has been marked to

Table 2

Average major and trace element compositions of rock suites from Nagarparkar alkaline complex

	Alkaline magma association				Subalkaline magma association						
	Alkali basalts & dolerites	Sadaros alkaline rhyolites	Karunjhar gray alkaline granites	Churio potassic alkali granites	Dhedvero gabbros	Diorites	Granodiorites	Wadlai adamellites	Nagar pink granites	Aplite dyke	Average A-type Granites•
No. of Samples	[6]	[7]	[9]	[5]	[12]	[3]	[4]	[7]	[6]	[1]	[148]
Major elements (wt. %)											
SiO_2	49.02	77.73	77.42	75.96	50.06	56.89	65.34	75.60	78.17	78.96	74.82
TiO_2	2.42	0.17	0.15	0.28	1.39	1.84	0.86	0.25	0.18	0.24	0.17
Al_2O_3	15.49	11.57	11.57	11.93	16.70	15.23	16.54	13.41	11.82	14.13	13.90
$Fe_2O_3^t$	13.77	2.17	2.05	2.62	11.34	9.96	4.80	1.76	2.20	1.59	1.68
MnO	0.21	0.05	0.04	0.06	0.18	0.16	0.11	0.06	0.05	0.03	0.03
MgO	5.49	0.12	0.13	0.23	7.73	4.01	2.41	0.32	0.15	0.45	0.13
CaO	7.88	0.22	0.28	0.58	10.32	6.55	5.00	0.95	0.36	1.01	0.77
Na_2O	4.19	3.24	4.04	3.27	2.08	3.49	3.48	3.79	3.30	2.93	1.72
K_2O	1.56	4.85	4.42	5.19	0.59	1.82	1.47	3.89	3.76	0.66	5.66
P_2O_5	0.600	0.001	0.006	0.024	0.248	0.533	0.205	-	-	0.032	0.07
Trace elements (ppm)											
Rb	38	147	138	111	16	52	17	102	134	149	-
Sr	646	20	12	46	407	440	405	85	17	129	48
Ba	439	409	130	170	266	559	437	660	125	843	352
V	226	-	-	-	214	163	80	-	-	-	6
Cr	5	-	-	19	200	44	19	-	-	-	-
Co	32	-	-	172	50	40	41	-	-	174	-
Ni	19	-	-	6	118	30	17	-	-	15	-
Cu	26	22	-	-	52	18	9	-	-	-	-
Zn	121	117	125	89	82	98	68	71	158	34	-
Ga	23	25	28	23	17	20	22	20	26	16	-
Y	26	92	94	65	20	31	19	46	98	46	75
Zr	412	721	568	381	127	226	200	232	702	192	528
Nb	32	34	38	28	6	8	-	13	-	17	37
Th	-	17	17	14	-	-	-	11	15	16	23
Ce	87	140	112	163	42	69	57	86	150	101	137
Nd	42	71	58	64	19	23	28	33	74	36	-

- A-type granites, average of 148 samples (Whalen et al., 1987) define magma series. (Fig 2) According to these diagrams, the rocks of Nagarparkar complex fall into two distinct magma associations: (a) Sub-alkaline gabbro-diorite-granodiorite-granite association. (b) Bimodal alkaline basalt/trachybasalt–alkaline rhyolites/granites association.

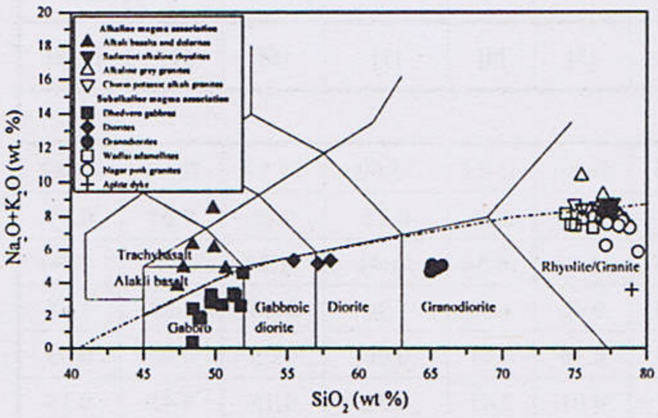

Fig.2:-Total alkali-silica classification diagram (TAS:Le Bas et al., 1986; Le Maitre et al., 1989) for Nagarparkar alkaline igneous Complex. The dotted dividing line between alkalic and sub alkalic rock series is after Irvine and Baragar (1971).

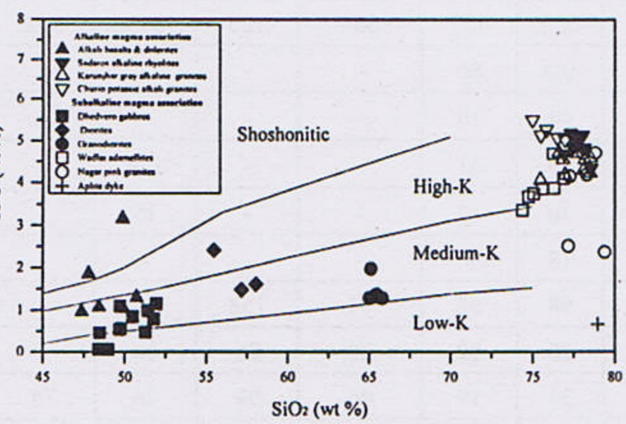

Fig.3:-K_2O versus SiO_2 (wt%) diagram for the igneous rocks of the Nagarparkar alkaline igneous Complex with boundaries for the division into compositional fields of the low-K Tholeiite (low-K), Calc-alkaline (medium-K), high-K Calc-alkaline (High-K) and Shoshonitic suits (after Peccerlillo and Taylor 1976; Rickwood 1989).

The salient geochemical characteristics of Nagarparkar Complex observed are described below:

Nagarparkar Complex constitutes two distinct magma series, the older represents plutonic association of sub-alkalic gabbro, diorite, granodiorite and granite. The younger volcanoplutonic magma series represents pulses of bimodal volcanic suite comprising alkaline basalt and alkali rhyolite intruded into older plutonics. The alkaline granites are an integral part of this association. The older plutonic associates exhibit tholeiitic as well as calc-alkaline trend (Fig. 4, 9).

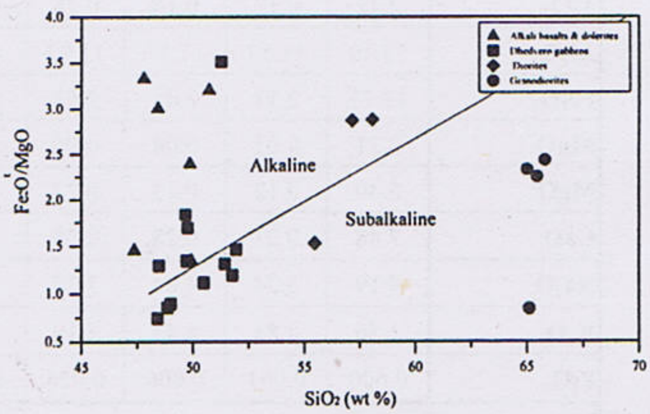

Fig.4:-Classification of Tholeiitic and Calc-alkaline series within igneous rocks of Nagarparkar alkaline igneous Complex. The dividing line between the two series is taken from Miyashiro (1974).

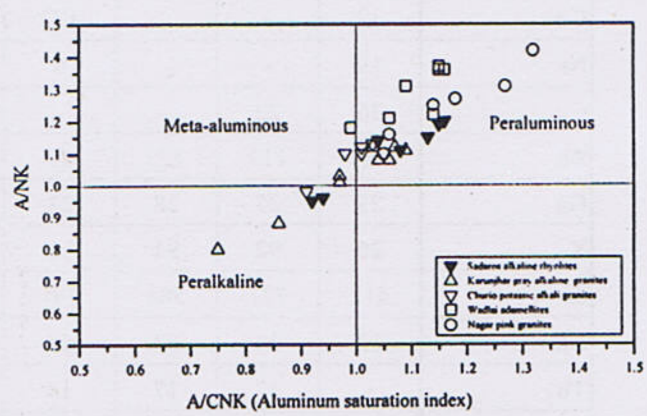

Fig.5:-Plot of Shand Index [Plot of A/NKmol.% $Al_2O_3/(Na_2O+K_2O)$] versus A/CNK (mol.% $Al_2O_3/CaO+Na_2O+K_2O$) for Nagarparkar alkaline igneous Complex.

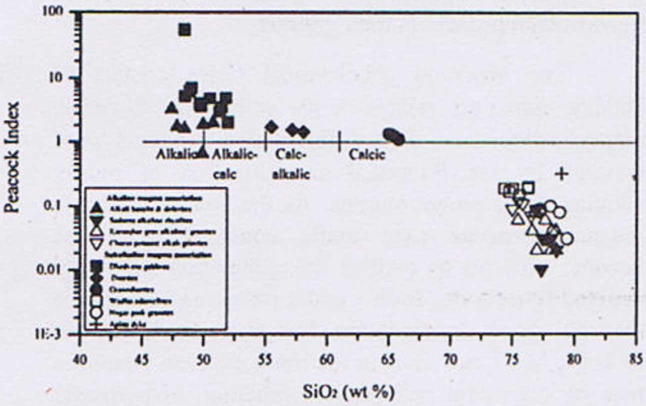

Fig.6:- Peacock Index (CaO/Na_2O+K_2O) versus SiO_2 after Brown (1981) for the igneous rocks of the Nagarparkar Alkaline Igneous Complex showing the calcic trend for the felsic suites

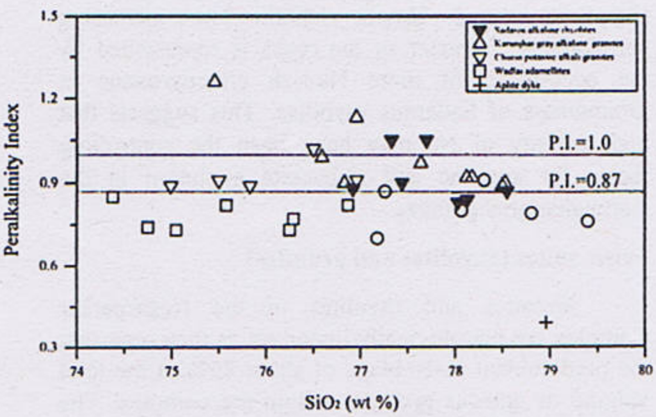

Fig.7:- Plot of Peralkalinity Index [mol% $(Na_2O+K_2O)/Al_2O_3$] versus SiO_2 for Nagarparkar Felsic rocks. The limit at P.I=0.87(minimum value for alkaline granites) is after Liegeois and Black (1987).

Gabbros, basalts/alkali basalts, and trachybasalt to K-phonotephrite represent the mafic rocks. These rocks are generally sub-aphyric to holocrystalline and sub-alkalic tholeiitic to mildly alkaline in nature. The mildly alkaline trend is indicated by the appearance of nepheline in S.NoA889 (Table.1). Mg number varies from 70.27% to 29.9% indicating that surface rocks represent alkaline differentiates.

Sub-alkaline mafic gabbroic intrusions are less differentiated, MgO content varies from 10.01% to 6.6% mostly MgO > 8. The chromium varies from 16 to 371 ppm and nickel varies from 34 to 78 ppm. The bimodal magmatic trend is depicted in Fig.4. The felsic end members are typically potassic rich rhyolites and granites. On the basis of FeO^t/MgO vs. SiO_2 wt. % diagram (Fig.4) the Nagarparkar mafic rocks also exhibit characteristic tholeiitic as well as calc-alkaline trend suggesting distinct, magma generations from alkaline trend to K-rich granite differentiate.

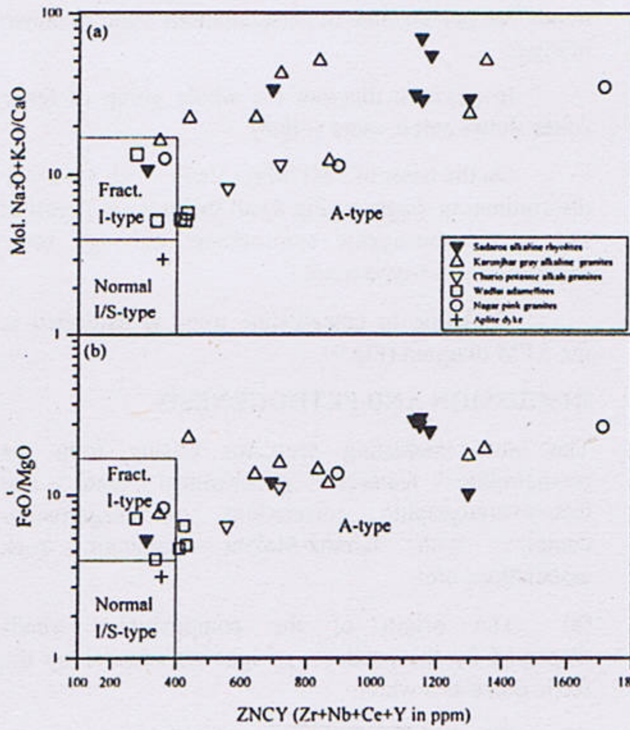

Fig 8:- FeO/MgO versus Zr+Nb+Ce+Y discrimination diagram (after Whalen et al., 1987) for Nagarparkar felsic rocks.

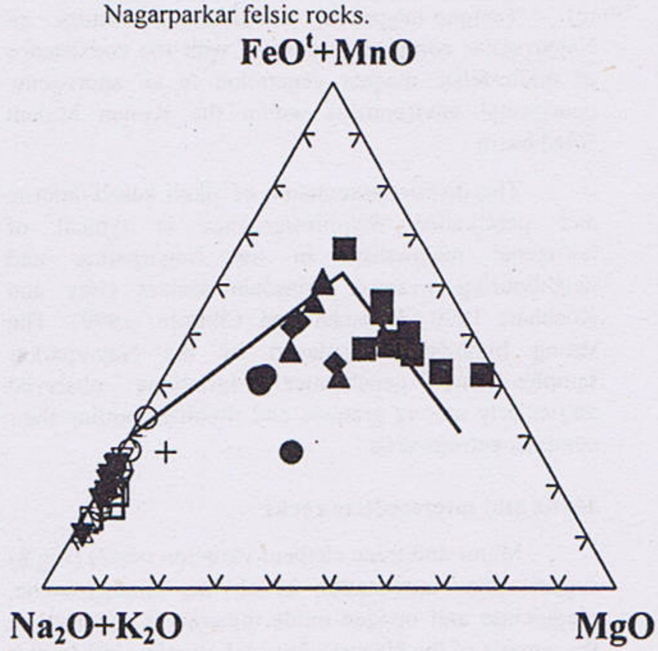

Fig.9:- AFM Diagram (based on Irvine and Baragar (1971) showing the major element compositional diversity in mafic and felsic rocks from Nagarparkar Alkaline Igneous Complex.

The alkalinity in the rhyolites and granitic rocks has been defined on the basis of per alkalinity index (Fig 7). Majority of the rocks fall above the limit. Moreover, presence of normatic acmite, alumina saturtation index and appearance of aegirine and riebeckite in the modal mineralogy suggest per alkaline trend. The per-alkaline to per-aluminous trend is shown in Fig.5.

In peacock diagram the whole group of felsic suites shows calcic trend (Fig.6).

On the basis of FeO^t/MgO Vs Zr + Nb + Ce + Y discrimination diagram (Fig 8) all the granites/rhyolites fall in an anorogenic environment although some samples shows I-type trend.

Tholeiitic to calcalkaline trend is exhibited in the AFM diagram (Fig.9).

DISCUSSION AND PETROGENESIS

The most interesting problems arising from the petrographic features, geochemical data and tectonostratigraphic correlations of Nagarparkar complex with Kirana-Malani magmatic rock associations are:

(a) The origin of the compositional trends displayed by the products of igneous suite or by the felsic rocks as a whole

(b) The genetic relationships if any, between mafic and felsic rocks

(c) Tectono-magmatic evolutionary history of Nagarparkar complex in context with the coexistence of mafic-felsic magma generation in an anorogenic continental environment within the Kirana Malani rifted basin

The distinct association of alkali basalt/dolerite and peralkaline rhyolites/granites is typical of norogenic magmatism in the Nagarparkar and neighbouring western Rajasthan sectors (Eby and Kochhar, 1990; Bhushan and Chittora, 1999). The strong bimodality displayed by the Nagarparkar samples and geochemical variations observed particularly among granites and rhyolites outline their complex petrogenesis.

Mafic and intermediate rocks

Major and trace element variation trends (Fig 8) suggest that fractionation of olivine, clinopyroxene, plagioclase and opaque oxide minerals is involved in the genesis of the Nagarparkar mafic rocks. Although it is possible to model a realistic crystal fractionation path for magmatic suites, the significant spread of same trace element compositions suggests the involvement of additional process in their genesis.

The observed geochemical characteristics of alkaline suites are related to the continental tholeiitic magma association. The differentiated products were evolved by the fractional crystallization of mildly alkaline mafic parent magma. As the amount of felsic magma dominate over mafic constituents, it has become difficult to explain the generation of highly evolved felsic rocks from a mafic parent magma source through simple fractionation. However, the behaviour of FeO^t, MgO and TiO_2 in the more evolved transition may be consistent with the fractionation of pyroxene and Fe-Ti-oxides in agreement with petrographic features. The degree in Mg-number has also been recognized in mafic phases. The evolution of clinopyroxene towards more aegirine rich compositions in felsic suites was governed by theFe^{3t} / Fe^{2t} ratio. This, in turn, was controlled by high alkali activity (Paul and Donglas, 1965) and/or high oxygen fugacity (Stephenson and Upton, 1982). The increasing peralkalinity character of the rocks is represented by the occurrence of more Na-rich clinopyroxene in groundmass of Sadarous rhyolites. This suggests that high activity of Na may have been the controlling factor for aegirine and riebeckite evolution in the Karunghar grey granites.

Felsic suites (rhyolites and granites)

Granites and rhyolites in the Nagarparkar Complex are petrologically important as they represent the predominant assemblage of about 85% of the total volume of igneous products within the complex. The geochemical variations displayed by the felsic rocks are the result of similar differentiation processes. These processes have generated an increase in SiO_2, total alkalis, Rb, Zr, Nb, Y and LREE and a decrease of Al_2O_3, MgO, CaO, Sr and Ba. It can be seen that the felsic rocks show decrease in normative femic minerals with increasing normative quartz. The Fe-Mg bearing phases were separating along with the alkaline feldspar. The less peralkaline and low-Fe trend indicate that an alkaline phase was coprecipitating with feldspar. This phase was either aegirine augite or alkali feldspar.

Felsic rocks in the Nagarparkar Complex range from subalkaline tholeiitic granodiorite adamellite and aplite to the alkaline/peralkaline granites and rhyolites. Four main hypotheses are generally considered for genesis of felsic magma in extensional setting. (a) Fractional crystallization of basaltic liquids at shallow depth (Carmichael 1964; Macdonald et al. 1990) (b) Assimilation or contamination of continental crust by ascending mantle melts (c) melting of the continental crust (anataxis) (d) partial melting of earlier mafic magmas underplated at the base of the crust.

The geochemical data collectively reveals a complex petrogenic history particularly of peralkaline rhyolites and granites. The preferred interpretation of this history accounts for the observed geochemical trends. Partial melting of intrusive mafic material at mid-crustal level generates intermediate composition magma, which then undergoes fractional crystallization. This two-stage process probably has generated diorite, granodiorite and adamellite. The peralkaline granites and rhyolites may have been generated in anorogenic environment. The alkaline source is ubiquitous and widespread at the base of; the lithosphere and the upper asthenosphere (Liegeois and Black, 1987). The alkaline magmatism is linked to major lithospheric structures.

Tectonic Implications

Discriminate functions based on major element distribution have been used to define the basic magma types and their geodynamic significance. Within the limits of such method, the geochemical data and petrography has suggested that Nagarparkar – Kirana region have been affected from Late Proterozoic time by either compressional or tensional processes. These processes produced geochemically well defined orogenic and anorogenic magmas. Local development of transitional magma type also occurs as due, possibly, to the overlapping of complex mantle processes. It must be emphasized that for a correct interpretation of the available data, it is necessary to separate both chronologically and spatially, the geodynamic process leading to a complex Neoproterozoic mantle evolution beneath NE Gondwana from the tectonic events directly linked to the magma generation and volcanism in Kirana – Nagarparkar and Western Rajasthan.

The Kirana, Malani, Nagar Parkar, Mount Abu and Tusham lie west of the Trans - Aravalli belt. At about 1000 Ma, it is believed that rifting started due to a big mantle plume in the NE Gondwana. This was accompanied by wide spread igneous activity west of the Aravalli region. Extension of the crust resulted in wide spread igneous activity and deposition of Marwar Super group in India and Machh super group in Pakistan (Chaudhry et al 1999).

The hot spot activity due to which wide spread volcanism and plutonism took place appears to have started at around 950 ma. The centers of these activites were Tosham (940 ± 20, modal age, Kochhar 1974, calculated isochron age of 770 ma, Eby 1990), Diri and Gurapratap Singh in Pali district (779 ± Ma), Kirana (873 ± 40 – 870 ± 40), Nagarparkar (800 – 750 Ma, Davies and Crawford 1971), Malani (745 ± 40, Crawford and Compston, 1970), Siwana and Jalore (750 ± 14 ma, Rathore et.al.,1991)

The Kirana–Malani Basin has preserved the records of the Pan–African Orogeny ascribed as Pan–African-tectonothermal episode by Kennedy (1964) extending from 950 ma to 500-±10 ma. The opening of this basin can be linked with opening of the Mozambique and rifting of the Rodinia Super continent (Stern 1994). The episodic igneous activity of basalt–Andesite–Dacite–Rhyolite suites and successive anorogenic bimodal alkaline magmatism is related tectonic evolution and possibly to initial rifting of Greater Gondwana (Chaudhry et al., 1999)

CONCLUSIONS

The rocks of Nagarparkar Complex fall into two distinct magma associations. The older sequence represents plutonic sub-alkaline tholeiitic magma associations of gabbro–diorite-granodiorite-adamellite and granites. While the younger magma series form an alkaline bimodal volcano plutonic association, comprising mafic suites of alkali basalt, a trachybasalt, K-phonotephrite and felsic members consists of alkali rhyolites and alkali granites. The metamorphism in the Nagarparkar complex does not exceed lower green schist facies. No amphibolite facies metamorphism was observed anywhere (as reported by Muslim et al., 1997;Butt et al., 1992). The volcanoplutonic assemblages at Nagarparkar areas do not represent shield elements or are a part of the Vindhyan Basin or Aravalli Orogen.

AKNOWLEDGEMENTS

This research work was carried out under financial support of Punjab University. Geological Survey of Pakistan is hereby highly acknowledged for providing facilities at Nagarparkar.

REFERENCES

Bhushan, S. K., 1985. Malani volcanism in western Rajasthan: *Indian. Jour. Earth. Sciences*, **12,.(1)** 58-71.

Bhushan, S. K and Chittora.V.K., 1999. Late Proterozoic bimodal volcanic assemblage of Siwana subsidence structure, western Rajasthan, India. *J. Geol. Soc. India*,.**53**,433-452.

Butt, K.A., Nazirullah, R. and Syed, S.A., 1989. Geology and Gravity interpretation of Nagar Parkar area and its potential for surfacial uranium deposits. *Kashmir. Jour. Geol*., **6&7**,41-50.

Butt, K.A., Jan, M.Q. and Karim. A. 1992. Late Proterozoic rocks of Nagar Parkar, Southeastern Pakistan. A preliminary petrologic account. In: Ahmad, R and Sheikh, A, M. (Eds). *Geology in South Asia-1, Islamabad*, 106-109.

Chaudhry, A.K., Gopalan, K. And Sastry, C.A., 1984. Present status of geochronology of the Precambrian rocks of Rajasthan. *Tectonophysics*. **105**, 131-140.

Crawford, A.R. and Compston, W., 1970. The age of the Vindhyan System of Penisular India. *Quart. Jour. Geo. Soc. London*, **125**,351-372.

Chaudhry, Ṁ.N, Ahmad, S.A. and Mateen, A., 1999. Some postulates on the tectonomagmatism, tectonostratigraphy and economic potential of Kirana-Malani-Basin, Indo-Pakistan. *Pakistan. Jour. of Hydrocarb. Res.* **11**, 29-35.

Davies, R.G. and Crawford, A.R., 1971. Petrography and age of the rocks of Buland hills, Sargodha Districts West Pakistan, *Geol. Mag;* **108 (3)**, 235-246. U.K.

Dolan, P. Edgar, D.C. B. and Sherlin, B.J., 1987. Pakistan Regional Geology and Petroleum exploration potential. *Dolan and Associates. Non-Exclusive Report. London.*

Eby, G.N. and Kochhar. 1990. Geochemistry and petrogenesis of the Malani igneous suite, north Penisular India.*Jour.Geol.Soc.India*.**36**, 109-130.

Farah, A., Mirza, M.A., Ahmad, M.A. and Butt, M.N. 1979. Gravity field of the burried shield, in the Punjab Plain Pakistan. *Bull.Geol. Soc. Am.* **88:** 1147-1155.

Farah, A. and Jafree, S.A.R.1965. Regional gravity survey of Thatta district, Hyderabad division, West Pakistan. *Records: Geological Survey of Pakistan*.**15.**

Fermor, L. L.1932. General report of the Geological Survey of India for the year 1931. *Records: Geological Survey of India*, **No. LXVI (1)**, 1-150.

Gansser, A. 1964. Geologic and tectonic maps of the Himalayan region. (Wiley interscience) London.

Gopalan, K. And Choudhry, A.K. 1984. The crustal record in Rajasthan. *Proceedings of the Indian Academy of Sciences. Earth. Planet. Sic.* **93**, 337-342.

Gopalan, K., Macdougall, I.D., Roy, A. B. And Murali, A.V.1990. Sm-Nd evidence for 3.3 Ga old rocks in Rajasthan, India. *Precambrian Res.* **48:** 287-297.

Gopalan, K., Macdougall, J.D., Roy, A.B and Murali, A.V. 1990. Sm-Nd evidence for 3.3 Ga old rocks in Rajasthan, N.W. India. *Precambrian Research.* **48:** 287-297.

Heron, A.M. 1913. The Kirana and other hills in the Chej and Rachna Doabs. *Memoirs, G.S.I, Records,* **43:(3)** 229-236.

Heron, A. M. 1953. The Geology of Central Rajputana. Mem. Geol., Surv. Inida, Vol. 79, 1-339.

Irvine, T.N and Baragar, W.R.A. 1971. A guide to the chemical classification of the common volcanic rocks. *Can. J. Earth. Sci*.**8**, 523-548.

Jan, M.Q., Laghari, A. and Khan, M.A. 1997. Petrography of the Nagar Parkar Igneous Complex.Tharparkar, Sind, Pakistan. *Geol, Bull, Uni, Peshawar*.**30**, 227-249.

Kazmi, A. and Khan, R.A. 1973. The report on the geology, mimeralogy and mineral resources of Nagar-Parkar, Pakistan, *Geological Survey of Pakistan, Information release,***64.**

Kella, S. C. 1983. Nagarparkar China clay deposits:Proceedings,2nd National Seminar on development of Mineral Resources ,1.

Khan, Z. K. and Chaudhry, M.N. 1991. Engineering Geological and Petrographic Evaluation of Metadolerites of Buland Hill and Chak 123 Quarries of Kirana Hills, District, Sargodha, Pakistan. *Kashmir Journ. Geol:* **8, 9,** and **181-184.**

Kochhar, N.1973. On the occurrence of a ring dyke in the Tosham igneous Complex, Hisar (Haryana). *Jour. Geol. Soc. Ind.*.**14(2)**, 190-193.

Kochhar, N.1974. The age of the Malani series. *Jour. Geol. Surv. India:* **15**, pp316-317.

Kochhar, N., 1984. Malani igneous suite: Hotspot magmatism and Cratonization of the northern part of Indian Shield. *Journ. Geol. Surv. India,* **25 (3)**, 155-161.

Kochhar, N. 1998. Malani igneous suite of rocks. J. Geol. Soc. India, **51(1)**,120 p.

Kennedy, W. Q., 1964. The structural differentiation of Africa, in the Pan-African (+500 Ma) tectonic episode. *Leads Univers. Res. Inst. Afr. Geol. Annu. Rep:***8**, 48-99.

Le Bas M.J, Le Maitre,R.W., Streckeisen, A and Zanettin, B., 1986. A chemical classification of volcanic rocks based on the total alkali silica diagram. *Jour. Petrol:* **27**,745-750.

Le Maitre R .W., Baterman P., Dudec A., Keller J.,Lameyre Le Bas M. J, Sabine P. A, Schmid R.,Sorensen H., Streckeisen A., Wooley A. Rand Zanettin B.,1989,*A classification of igneous rocks and glossary of terms.* Blackwell, Oxford.

Liegeois J.P and Black R.,1987.Alkaline magmatism subsequent to collision in the Pan-African belt of the Adrar des Iforas (Mali).In Alkaline Igneous Rocks (edited by Fitton .J.G and Upton B.G.J). Spec. Publ. 30.381-401, Geol. Soc.

Menke, W.H. and Jacob, K.H. C. 1976. Seismicity patterns in Pakistan and North India associated with continental collision. Bull. Seismal. Soc. Amer. 66, 5.1695-1712. ElCerrito, Col.

Miyashiro, A.1978 Nature of alkalic volcanic rock series. *Contrib. Mineral. Petrol:* **66**, 91-104.

Middlemost, E.A.K., 1991. Towards a comprehensive classification of Igneous rocks and magmas. *Earth Science Reviews:* **31**,73-87.Elsevier Science Publishers, B. V, Amsterdam, Australia.

Muslim, M., Akhtar, T., Khan, Z.M., and Khan, T., 1997. Geology of Nagar Parkar area, Thar Parkar District, Sindh, Pakistan, *G.S.P. Release:* **605.**

Naqvi, M.S and Rojers, J. J. W., 1987. *Precambrian Geology of India.* Oxford University press,New York, 1-234 p.

Pascoe, E. 1959. A manual of the Geology of India and Burma, II: Govt of India Printer Calcutta.

Peacock, M. A., 1931, Classification of igneous rock series. *J, Geol.*, **39**, 65-67.

Peccerillo, R. and Taylor, S.R., 1976. Geochemistry of Eocene calc-alkaline rocks from the Kastamonu area, northern Turkey. *Contrib. Mineral. Petrol:* **58**, 63-81.

Rathore, S. S. Trivedi, J.R. and Venkateshan, R., 1991. Rb/Sr age of Jalore and Siwana granites*: Resolution of Thermal Events by Ar40-39 study. 5th National Symposium on Mass Spectroscopy, Ahmadabad*, 10, 3.

Rathore, S. S., Venkatesan, T. R. and Srivastava, R. K. 1996. Rb-Sr and Ar-Ar systematics of Malani volcanic rocks of southwest Rajasthan: Evidence for a younger post-crystallization thermal event. Proc. Indian Acad. Sci. (Earth Planet. Sci.), **105**, 131-141.

Rathore, S. S., Venkatesan, T. R. and Srivastava, R. K. 1999. Rb-Sr isotope dating of Neoproterozoic (Malani Group) magmatism from southwest Rajasthan, India: Evidence of younger Pan-African thermal event by ^{40}Ar-^{39}Ar studies. Gondwana Res. **2**, 271-281.

Rickwood, P.C., 1989. Boundary lines within petrologic diagrams, which use oxides of major and minor elements. *Lithos:* **22**,247-263.

Sarkar,G.,Bristal,P.K.,Guha,D.B.,Jain.s.s.,Banerjee,s.,Bhushan.S.K.,Chittora.V.K and Bhattacharjee, J. 1993. Geochemistry of Granites and felsic volcanic rocks of Delhi fold belt. GSI. Rec. v 126.pt 231-33.

Seeber, L., and Armbruster, J., 1979. Seismicity of the Hazara arc in Northern Pakistan. Farah, A and Dejong, K. A (Eds) *Geodynamics of Pakistan:*131-147; Geol. Surv. Pakistan; Quetta.

Srivastava, K. R., Magmatism in the Aravalli Mountain Rajasthan, India: Geological Society of India. Memoir 9,.77-93.

Shand, S.I., 1949 *Eruptive Rocks.*New York, John Wiley.

Shah, S.M.I., 1973. Occurrence of Gold in the Kirana group, Sargodha (Punjab) Pakistan. *Inform Release, GSP, Quetta, Pakistan:* **68**, 1-14.

Stern, R.J., 1994. Arc assembly and continental collision in the Neoproterozoic east African orogen: Implications for the consolidation of Gondwanaland. *Annu. Rev. Earth & Planet. Sci:* **22**, 319-351.

Virdi, N.S., 1997. Upper proterozoic geotectonic events in the Trans-Aravalli regions and their signatures in the Lesser Himalaya In: Wijayanda, N.P. Cooray, P.G and Mosley, P(eds) *Geology in South Asia II.* Geological Survey and Mines Bureu Srilanka, Professional paper 7.

Wynne A.B., 1867. Memoir on the Geology of Kutch; *Geological Survey of India, Memoir:* **9**, 293.

Whalen, J. B., Currie, K. L and Chappel, B. W., 1987. A-type granites: Geochemical characteristics, discrimination and petrogenesis. *Contrib. Mineral. Petrol:* **95**.407-419.

Yeats, R.S and Lawrence, R.D., 1984. Tectonics of the Himalayan thrust belt in Northern Pakistan. In: Maq, B. U and Milliman, J. D (eds), *Marine Geology and Oceanography of the Arabian Sea and Coastal Pakistan* Von Nostrand, New York,.177-198.

Geol. Bull. Punjab Univ. 38, 2003.

ALTERATION AND METAMORPHISM OF THE PANJAL VOLCANICS IN NORTHWESTERN HIMALAYA, PAKISTAN.

BY

M. SABIR KHAN, MOHAMMAD ASHRAF
Institute of Geology University of Azad Jammu and Kashmir, Muzaffarabad, Pakistan.

AND

AKHTAR ALI SALEEMI
Institute of Geology, University of the Punjab, Lahore-54590, Pakistan.

Abstract:- *The Panjal volcanics are tholeiitic to mildly alkalic rocks. The basaltic lava flows of these rocks show continuous compositional change from low temperature sea water chemical exchange to the development of rocks with spilitic characters. The rocks were further altered and metamor-phosed during Himalayan orogeny.*

The Panjal volcanics are altered to lower greenschist facies. Major minerals assemblages are chlorite, epidote, albite and actinolite. Based on the mineralogy these rocks may be divided into chlorite rich and epidote rich mineral assemblages. Both the chlorite and epidote rich assemblage show chemical changes in composition compared with their assumed basaltic precursors. The change involves addition of K, Na, Si and loss of Ca. Severe alteration leads to spilitization of rocks with release of Ca from calcic plagioclase and inversion of plagioclase to albite.

The lithology and geochemistry of the Panjal volcanic rocks suggest that they were thoroughly altered by hydrothermal and metamorphic processes. Chemically, the Panjal volcanics are greatly enriched in Na and K. The elements Na, K, Ca, Sr and Ba demonstrate large variations in the Panjal volcanics. Na_2O varies from 0.05 to 4.57 wt.%, K_2O from 0.11 to 2.78 wt.%, CaO varies from 4.82 to 10.35 wt.%, Ba from 24 to 1847 ppm, Sr from 42 to 423 ppm and Rb upto 224 ppm. The geochemical data mainly suggest an increase in Na, K, Si and a decrease in Ca.

The alteration of the Panjal volcanic rocks resemble with that observed in recent submarine volcanics. The mineralogy of these rocks was mainly controlled by water/rock ratio during alteration. Subsequent Himalayan regional metamorphism had only a minor effect on the geochemistry of the rocks and had only readjusted the mineralogy of the rocks to the conditions of lower greenschist facies.

INTRODUCTION

In the western and eastern part of Hazara-Kashmir Syntaxis, the Panjal volcanics are bound by a regional thrust system (Fig. 1). The Panjal volcanics are alterd and metamorphosed to lower greenschist facies metamorphism.

A major problem in the study of altered and metamorphosed basalts like the Panjal volcanics is to identify their environment of alteration especially when alteration due to seawater/ basalt interaction has been over printed by later orogenic metamorphism.

Previously geology of the Panjal volcanics was studied by Lydekker (1878, 1883), Middlemiss (1911), Wadia (1928, 1934), Ganju and Rajnath (1939), Ganju (1943), Calkins et al. (1975), Bhat & Zainuddin (1978, 1979), Honegger et al. (1982), Greco (1989), Ghazanfar and Chaudhry (1984, 1985).

The distribution and general chemical characteristics of the Panjal volcanic rocks around the apex of Hazara-Kashmir Syntaxis have been discussed by Butt et al. (1985), Khan and Ashraf (1989), Khan et al. (1991), Chaudhry and Ashraf (1980), Papritz and Rey (1989), Ashraf and Khan (1991) and Khan (1994).

The purpose of this study is to identify alteration assemblages and to deal with the mineralogical and chemical changes that took place during the formation of greenschist facies metabasalts by hydrothermal alteration.

GEOLOGICAL SETTING

NW Himalaya has been divided from south to north into three tectonic subdivisions, Sub-Himalaya, Lesser

Himalaya and Higher Himalaya (Gansser 1964, Greco 1989).

In this area the Subhimalaya are composed of sediments of the Murree Formation and Siwaliks with inliers of Cambrian, Paleocene and Eocene rocks (Fig.1). These rocks form the core of the Hazara-Kashmir Syntaxis. To the north Sub-himalaya is bound by the Main Boundary Thrust (Fig.1). The Main Boundary Thrust cuts the steep dipping beds of Tertiary rocks. The NE dipping rocks of the Lesser Himalaya overrides the Subhimalayan rocks along this thrust.

The Lesser Himalaya in the region consists of the Agglomeratic slate, the Panjal volcanics (lava flows), associated sedimentary rocks and metasediments of Tanol formation (of Ghazanfar et al. 1983) with granitic intrusions (Fig. 2). Dolerite and amphibolite dykes and sills are common in the Agglomeratic slates and metasediments. These rocks form a major tectonic unit in the apex and eastern side of Hazara Kashmir Syntaxis in the Lesser Himalaya (Fig.2).

The Panjal volcanics are bound by the Panjal Thrust on the northeast and the Main Boundary Thrust in the southwest. The Panjal volcanics have been thrust over the younger sediments of the Murree Formation (Fig. 1).

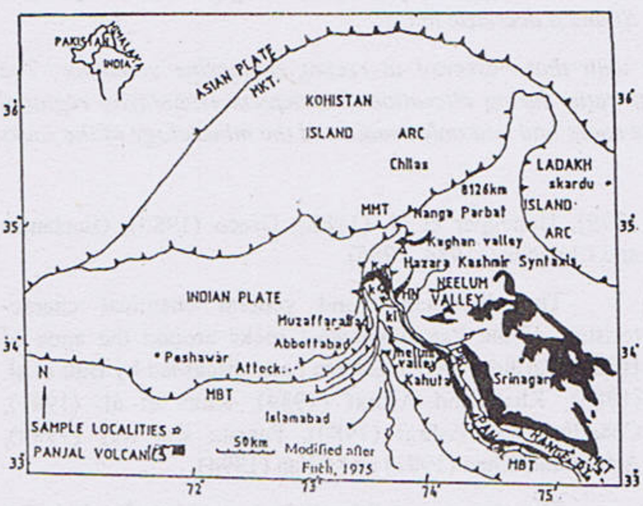

Fig.1 Distribution of the Panjal Volcanics in the NW Himalayas Stippled area. Occurrence of the Panjal Volcanics, MMT Main Mantle Thrust, MKT Main Karakoram Thrust, MCT Main Central Thrust, PT Panjal Thrust. MBT Main Boundary Thrust.

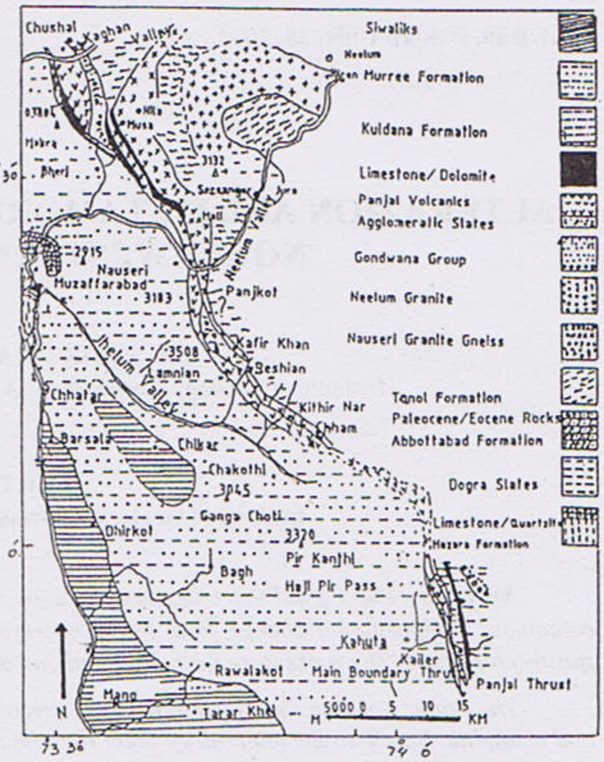

Fig.2 Geological Map of Kahuta-Jhelum-Neelum and Kaghan Region of North West Himalaya Pakistan.

The tectonic setting of these rocks have been identified from within plate to shallow oceanic environment (Khan et al. 1991; Khan and Ashraf 1989; Khan, 1994; Chaudhry et al. 1995).

In the study area (Fig. 2) a sequence of Agglomeratic slates with predominantly massive lava flows (Panjal volcanics) are exposed on the eastern and western flanks of the Hazara-Kashmir Sntaxis. The Panjal volcanics are alterd and metamorphosed to lower greenschist facies metamorphism. The area between the Panjal Thrust and the Main Boundary Thrust comprises a lower unit of Agglomeratic slates followed by the Panjal volcanics with associated carbonate rocks.

The Agglomeratic slates are heterogeneous in appearance than the Panjal volcanics, having particles of varying size and composition like, slates, granite gneiss, limestone, chalcedony and feldspar crystals.

The volcanic rocks comprise, massive basaltic lava flows with pillow structures. These rocks are tholeiitic to mildly alkalic in nature. The pillows, varying in size from 25 to 140 cm show a zoned structure. The inner part of the pillow is greenish-grey and lighter towards the margins with increasing albitization. The Panjal volcanics are characterized by interbedded limestone and bedded chert. The thickness of bedded chert ranges from few cm to more than a meter.

The Panjal volcanics show a thickness of less than few meters to more than a kilometer. These rocks extend along the Main Boundary Thrust from Kahuta in the southeast to Kaghan in the northwest, where they are terminated by the Panjal Thrust. They have an associated belt of Nauseri granite gneiss (Fig.2) of Cambrian age (Khan et al. 1994).

A Permian to Triassic age for the Panjal volcanics in the Lesser Himalaya is based on (a) Baig (1991) used Ar^{40}/Ar^{39} and obtained ages of the mafic Panjal volcanics in Hazara area from 284 ± 4 to 262 ± 1 Ma and (b) correlation of these rocks with lithologically similar basalts and carbonate rocks in Baramula and Srinager region where a Permian to Triassic age has been accepted (Wadia, 1934).

The Higher Himalayas consist of highly crystalline metamorphic and magmatic rocks. To the north they are separated from the Kohistan island arc sequence by the Indus Suture zone while in the south the Main Central Thrust (MCT) separates them from the Lesser Himalaya (Fig.1).

PETROGRAPHY

The Panjal volcanics are greenish grey or greyish to reddish brown coloured rocks. They are compact, hard, massive and fine grained. Some lava flows show blocky and schistose character. The rocks are variably vesicular. The vesicular infillings include chalcedony, epidote, chlorite and quartz. Amygdules are rounded to subrounded, ovoid and elongated. The amygdules as large as 5 cm are encountered. The lava flows are crosscut by epidote and calcite veins.

Microscopic examination of thin-sections of the Panjal volcanic rocks show textural and alteration characters. Mineralogically these rocks are plagioclase phyric with relict of pyroxene and their alteration products (Table 1). The plagio-clase occur as microphenocrysts and microlites. Plagioclase alters to clay minerals, chlorite and epidote.

The ground mass is very fine grained of altered plagioclase, chlorite, epidote, and sericite. Opaque minerals such as hematite and magnetite are present in these rocks. Plagioclase crystals are set in a fine matrix. Porphyritic chlorite is abundant in some of lava flows.

The petrographic results of these rocks reflect their alteration. The rocks are altered with ubiquitous chlo-rite, albite, epidote, actinolite, quartz and carbonates.

Table 1.
Petrographic composition of the Panjal volcanic rocks

								K(16)	Kc(16)	Lm(18)	Nus(16)	Mn(16)
	1	2	3	4	5	6	7	1	2	3	4	5
Plagioclase	45	20	8	30	45	38	25	20-51	8-45	6-35	8-45	10-35
Pyroxene	6	25	-	-	-	-	-	2-25	-	-	-	-
Epidote	15	25	40	22	20	28	30	12-35	10-40	10-45	20-60	10-35
Chlorite	20	24	45	40	16	24	40	10-30	25-45	15-60	15-38	18-51
Sericite	6	3	-	-	10	5	-	2-12	2-5	1-15	2-10	1-12
Quartz	-	2	1	-	1	-	-	1-2	1	1-3	1-2	1-8
Calcite	-	-	1	-	2	-	-	1	0.5-1	1-2	1-8	0-1
Actinolite	-	-	-	1	-	-	-	0-1	0-1	1-4	3-10	1-2
Sphene	-	-	5	2	3	3	2	2-12	3-7	2-12	1-2	1-10
Chal/Chert	-	-	-	1	2	-	-	1-2	0-1	0-1	1-2	1-3
Hamatite	3	1	-	3	1	2	2	1-5	1-4	1-3	1-2	1-3
Magnetite	4	-	-	1	-	-	-	1-4	1-5	0-1	0-1	1-4
Clay Mins.	-	-	-	-	-	-	-	2-6	-	-	-	-

K, Kahuta; Kc and Lm, Jhelum valley; Nus and Mn, Nelum valley.
Numbers in paranthesis represent number of samples.

Seawater/basalt interaction has caused alteration of the glassy and cryptocrystalline ground-mass of the Panjal volcanics to form chlorite. Sea floor metamorphism involves partial or complete devitrification of volcanic glass and its replacement by clay minerals, albite, chlorite, silica and carbonates (Dimroth and Lichtblau, 1979). The presence of chlorite patches in the Panjal volcanics probably reveal the presence of volcanic glassy matter. Modal olivine has not been found in these rocks. It is suggested that Olivine was replaced by chlorite whereas calcic plagioclase changed to albite by an exchange of Na and Si for Ca and Al. The replacement of plagioclase by epidote, sodic plagioclase and even albite and chlorite suggests that significant amount of calcium was released from the Panjal volcanics. Epidote is formed from CaO which is released from feldspar during the process of alteration at low oxidation conditions (Cann, 1969, Condie et al. 1977). Clino-pyroxene by Hydrothermal alteration of basalts involves the loss of Ca (Wolery and Sleep, 1976; Humphris and Thompson, 1978). Pyroxene (Augite) in the Panjal volcanics have been replaced by actinolite and chlorite while iron ore is replaced by sphene.

GEOCHEMISTRY

Those samples were selected for study which show minimum effects of low temperature weathering. The rocks were selected from Kahuta, Jhelum, Neelum and Kaghan areas (Fig. 1). A total of 122 rock samples collected from lava flow sequence, were analysed for major (ICP) and trace elements by inductively coupled plasma (ICP-MS).

The petrography of the Panjal volcanic rocks indicate strong alteration. Further evidence is given by the geochemistry of the volcanics. The chemical composition of the samples are reported in Table 2. The Panjal volcanics in the Kaghan and Azad Jammu and Kashmir Himalayas show total alkalies (Na_2O+K_2O) ranging from 1.38 to 5.91% wt.%. In some areas the Panjal volcanics reveal Na_2O enrichment ranging from 1.23 to 4.57 wt.%. In one rock it is 0.05 wt. % Table 2).

However, not withstanding alteration most of major and trace elements concentration in the Panjal volcanics show igneous signatures. Similarly Ti, P and Zr which are considered to be immobile during low-grade alteration (Fig. 3) suggest that their presence in these rocks is of magmatic origin. The studies of the Panjal volcanics indicate their submarine tectonic setting (Khan, 1994; Khan and Ashraf, 1989; Chaudhry et al. 1992). Considering this tectonic setting these volcanics were effected by the seawater-rock interaction.

Reactions in seafloor conditions are controlled by different processes. Experimental studies indicate that the water/rock (w/r) ratio is one of the basic factors in the seawater/rock system (Janecky and Seyfrid, 1983; Reed, 1983; Hajash and Chandler, 1981; Hajash and Archer, 1980; Mottle and Holland, 1978; Seyfried and Bischoff, 1977). The high w/r and low w/r ratios produce different mineral assemblages. The permeable and porous parts of the volcanic rocks such as fractures, pillow matrix and vesicles are more sensitive to high w/r ratios in contrast to massive and unfractured lava flows with least population of vesicles are characterized by low w/r ratios. The change in w/r ratios will be reflected in different mineral assemblages.

The Panjal volcanic rocks are composed of chlorite-epidote-albite and actinolite. These assemblages correspond to w/r ratios >50 provided that the conditions are comparable with those in the experimental studies (Fig. 4). However, in other rocks which contain chlorite-epidote-albite and albite-epidote-chlorite indicate variable w/r ratios (Fig. 4). The Panjal volcanics show dark schlieren, at many places, in Kahuta, Muzaffarabad and Kaghan areas. These dark schliern can also be interpreted as combined effect of high w/r ratios, hydrothermal alteration and a subsequent effect of Himalayan regional metamorphism.

The alteration product of the Panjal volcanics is indicated by mineral assemblages of albite-chlorite-epidote-actinolite-sphene-quartz-calcite. These assemblages crosspond to a w/r ratios ranging from 50 to <10 (Fig.4). The presence of chlorite and epidote indicate a w/r ratios of 50 to < 10 in the Panjal volcanics. The higher content of Na and Si in these rocks also support this argument.

In the Panjal volcanics the alteration is refelceted by Na enrichment and depletion in Ca during basalt/seawater interaction. Hydrothermal alteration caused chemical changes in these rocks. Na, K, water and Si were added while Ca was removed. Alteration is also indicated by variable amount of Sr, Ba and Rb (Table 2). Other workers (e.g., Hart, 1973, Hart, 1970; Hart 1969; Hart et al. 1974; Frey et al. 1974, Berry et al. 1992) have also reported enrichment in Na_2O and K_2O and depletion in calcium during alteration of oceanic basalts with sea water at low temperature. Sea water alteration of pillow lavas can add Na, Rb, and Sr, to the rocks with removal of Ca from it (Loeschke, 1976, Cawood, 1984).

Table 3 shows the chemical gain and loss of these rocks during hydrothermal alteration. These fluxes were calculated by assuming constant aluminum and comparing the composition of these rocks with that of mid ocean ridge basalts. As no fresh rock is available therefore, it was assumed that mid ocean ridge basalt may represent their basaltic precursor. Valuse of fluxes obtained by comparing the Panjal volcanics with mid ocean ridge basalts may give qualitative changes in the chemical composition of the Panjal volcanics in terms of mass of oxides/100 cm3 of rock.

Table 2.

Chemical analysis of the Panjal volcanics of the Lesser Himalaya.

(MORB Values are after Humphris at al. 1985)

Wt. %	1	2	3	4	5	6	7	129A	MORB
SiO_2	41.01	50.52	48.93	50.58	48.88	50.10	44.38	50.70	5.40
TiO_2	1.48	1.81	1.25	1.63	1.28	2.69	1.77	21.66	1.36
Al_2O_3	14.79	14.87	14.85	14.32	11.93	11.72	16.82	8.90	15.19
Fe_2O_3	9.85	11.39	10.31	11.24	9.69	15.44	12.60	3.51	10.10
MnO	0.16	0.15	0.15	0.17	0.17	0.23	0.20	2.34	0.18
MgO	5.12	4.63	7.49	7.22	5.82	3.14	8.99	0.72	8.96
CaO	10.35	4.82	7.07	5.87	8.56	6.87	6.51	5.93	11.48
Na_2O	0.05	4.57	2.78	2.27	3.16	2.82	2.85	1.23	2.30
K_2O	2.78	1.34	0.07	0.32	0.12	0.16	0.11	0.15	0.09
P_2O_5	0.21	0.27	0.17	0.22	0.15	0.41	0.13	0.05	0.14
LOI	12.80	5.4	6.7	5.1	10.10	6.0	5.0	5.40	
Ba	371	499	39	61	24	24	24	1847	
Sr	81	414	423	358	180	180	84	42	
Rb	-	-	-	-	-	-	-	244	
Li	-	-	-	-	-	-	-	49	
Na_2O+K_2O	2.83	5.91	2.85	2.59	3.28	2.98	2.96	1.38	

Average analyses of the Panjal volcanics

(1) Kahuta (2) Khatir Nar (3) Lamnian (4) Nauseri (5) Manj Hotor (6) Kaghan.

Wt. %	(n=18) 1	(n=16) 2	(n=18) 3	(N=13) 4	(N=16) 5	(N=13) 6
SiO_2	49.40	50.42	50.12	49.74	48.88	50.10
TiO_2	1.42	1.43	1.53	1.66	1.67	1.61
Al_2O_3	15.49	16.03	15.08	14.28	15.08	15.22
Fe_2O_3	10.58	10.55	10.97	12.07	12.03	11.09
MnO	0.16	0.15	0.17	0.17	0.22	0.18
MgO	6.13	6.29	6.22	5.88	6.44	6.77
CaO	7.86	6.14	7.71	7.78	7.91	7.44
Na_2O	2.71	4.12	3.08	2.95	3.13	3.64
K_2O	1.53	1.52	1.01	1.19	0.90	0.74
P_2O_5	0.16	0.18	0.17	0.18	0.16	0.16
LOI	4.31	2.90	3.45	3.78	3.04	2.76
Mg #	57.50	58.10	56.90	53.20	55.50	58.70
Ppm						
Ba	352	306	220	215	260	178
Sr	373	368	282	218	178	170

(number in paranthesis indicate number of analyses)

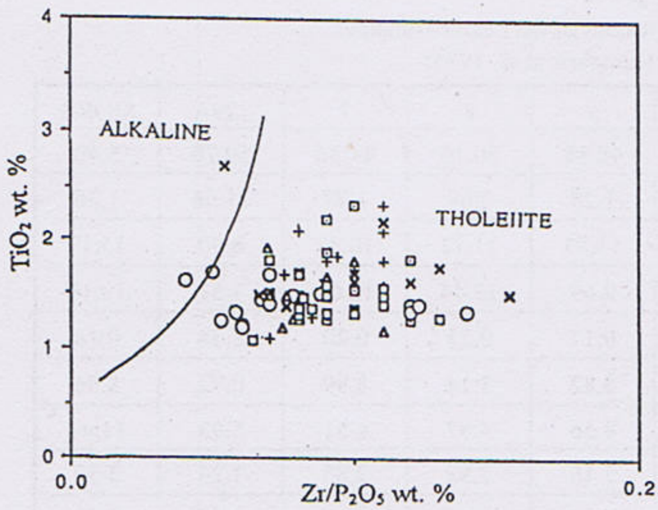

Fig.3 TiO_2 versus Zr/P_2O_5 plot showing tholeiitic to weak alkaline character of the Panjal volcanics. Fields are after Winchester and Floyd (1976) Symbols as in Fig. 2.

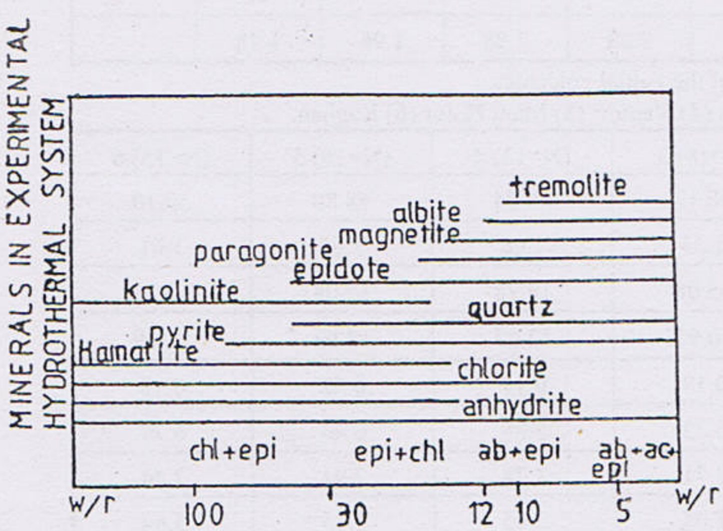

Fig.4 Mineral assemblage formed in a reaction between the Panjal volcanic rocks and sea water at varying water/rock 9w/r) ratios under hydrothermal conditions 9T=300°C). Modified after Mottl and Holland 1978; Reed 1983. The lower portion of the diagram shows the approximate mineral assemblage of the Panjal volcanic rocks. Chl., chlorite, epi. Epidote, ab. Albite, ac. Actinolite.

The change in chemical composition due to alteration are reflected by high loss-on-ignition (LOI) values in some of the Panjal volcanic rocks. The Panjal volcanics in a few samples show high loss on ignition. Many authors (EmbeyIsztin et al. 1993; Speed, 1991, Floyd et al. 1991; LeRoex et al. 1983) have shown that high LOI indicates alteration in volcanic rocks. The chlorite, epidote and carbonate reflect high loss on ignition (Floyd et al. 1991). Floyd et al. (1991) used LOI as an alteration index and defined three alteration classes on the basis of LOI values, at <4 wt. % mild alteration, 4-8 wt. % strong alteration and >8 wt. % severe alteration. Their criteria is used for alteration classification of the Panjal volcanics. Table 1 shows that four Panjal basaltic rocks have LOI values from 5 to 5.4 wt.% while two samples (3, 6) have LOI values 6 and 6.7 wt.% respectively (Table 2). Two rock samples 1 and 5 (Table 2) have LOI 12.80 and 10.1 wt.% respectively. These two rocks show severe alteration. The Panjal volcanic rocks 1 and 5 are from the Kahuta and Nauseri areas respectively. These severely altered Panjal volcanic rocks imply elemental mobility at some places. Remaining rocks have LOI values ranging from 1.6 to 3.6 wt. % (analyses are not given in Table). Therefore, most of the Panjal volcanics are mildly altered rocks.

Mobility of Na, K, Sr and to some extent Ca, due to alteration processes in the Panjal volcanics are shown by an irregular scatter of these elements in the differentiation index plots (Fig. 5). This elemental mobility in the Panjal volcanics may have been caused by hydrothermal alteration, spilitization and metamorphism related with both sea floor and enhanced by regional metamorphism during Himalayan orogeny.

The slight decrease of Ca and Sr with differentiation index probably reveal breakdown of Ca rich plagioclase and pyroxene producing variable CaO and Na_2O contents. The K_2O contents in the Panjal volcanics are highly variable. This variation of K_2O suggests mobility of this element. Seawater alteration can cause K-enrichment in rocks (Bevins and Roach, 1979, Erlank and Kable, 1976). Abbotts (1981) also noted mobility of K, Rb, Ba and Sr due to alteration of the basaltic rocks. However, the K_2O content in some rocks may also be due to presence of biotite. Spilitization and mobility of alkalies was very intensive and comprehensive in some of the Panjal volcanic rocks. As a result these rocks were moved out of the igneous spectrum (Fig. 6).

In the Panjal volcanics the mineral assemblage is albite+chlorite+ epidote+quartz±calcite±actinolite and sphene. However in some lava flows plagioclase is more calcic as indicated by modal mineralogy. This mineral assemblage also correspond to the lower greenschist facies metamorphism.

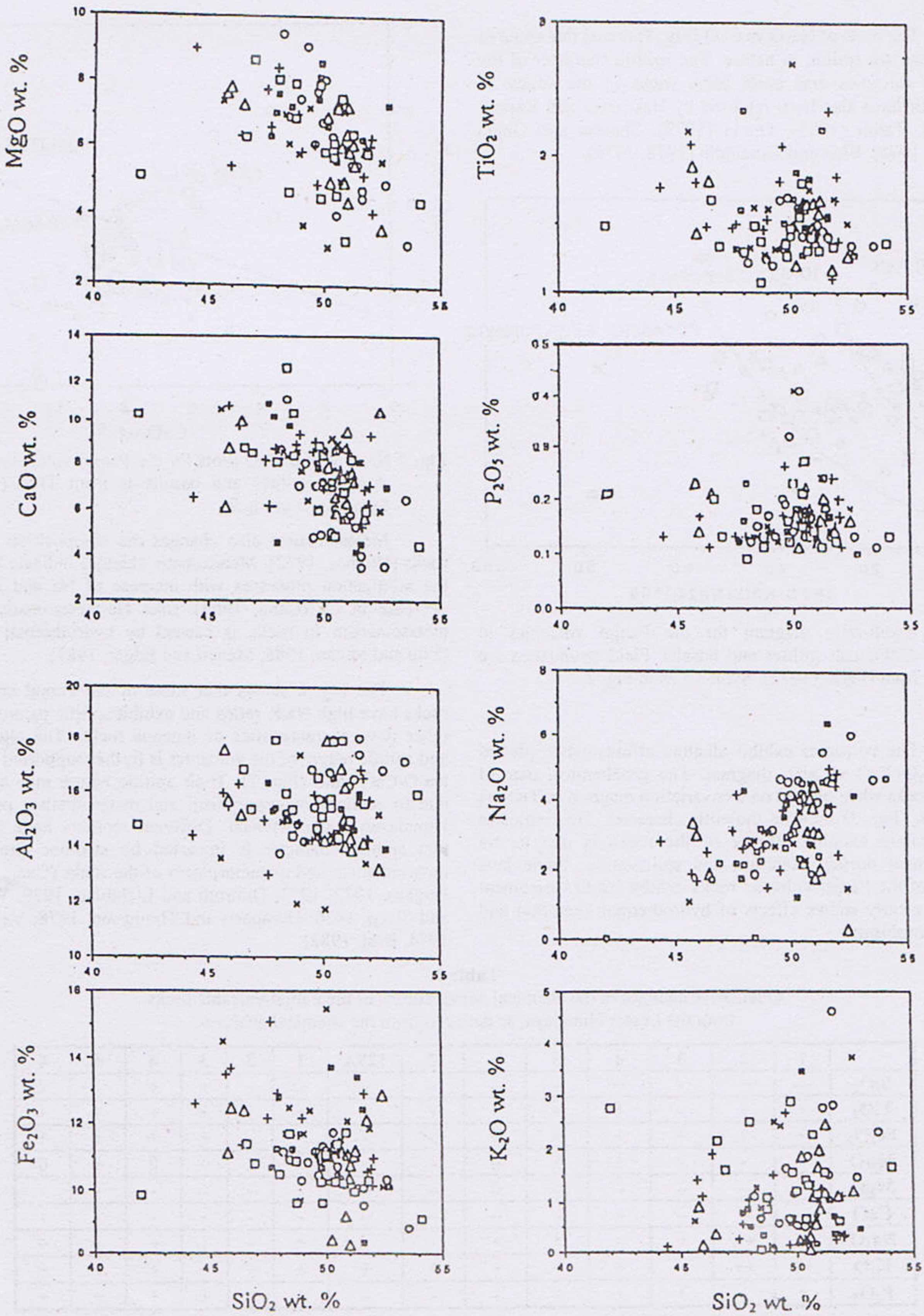

Fig.5 Harker type variation diagrams, with SiO_2 as abscissa, showing compositional variation for the Panjal volcanic rocks. Symbols as in Fig. 2.

The plots of Na_2O vs CaO (Fig. 7) reveal that some of the rocks are spilitic in nature. The spilitic character of the Panjal volcanics and other basic rocks in the valley of Kashmir have also been reported by Nakazawa and Kapoor (1973), Taron (1982), Gupta (1979), Sharma and Gupta (1972, 1975), Bhat and Zainuddin (1978, 1979).

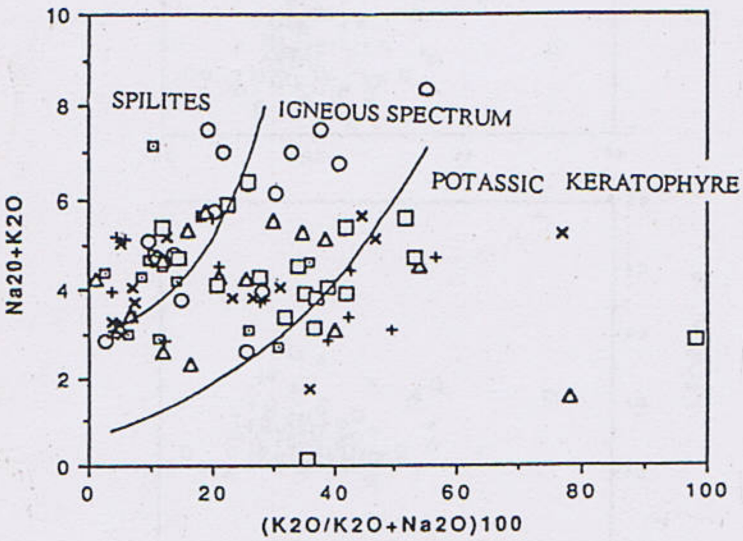

Fig.6 Alkali-ratio diagram for the Panjal volcanics to distinguish spilites and basalts. Field boundaries are from Huges (1972). Symbols as in Fig. 2.

The volcanics exhibit alkaline affinity when plotted on Na_2O+K_2O vs SiO_2 diagram. The geochemical data of these rocks when plotted on a covariation diagram of TiO_2 vs Zr/P_2O_5 (Fig. 3) indicate tholeiitic character. This indicates that mainly alkaline affinity of the rocks is due to Na enrichment during alteration and spilitization. Some lava flows of the Panjal volcanic rocks exhibit Na_2O enrichment which clearly shows effects of hydrothermal alteration and metamorphism.

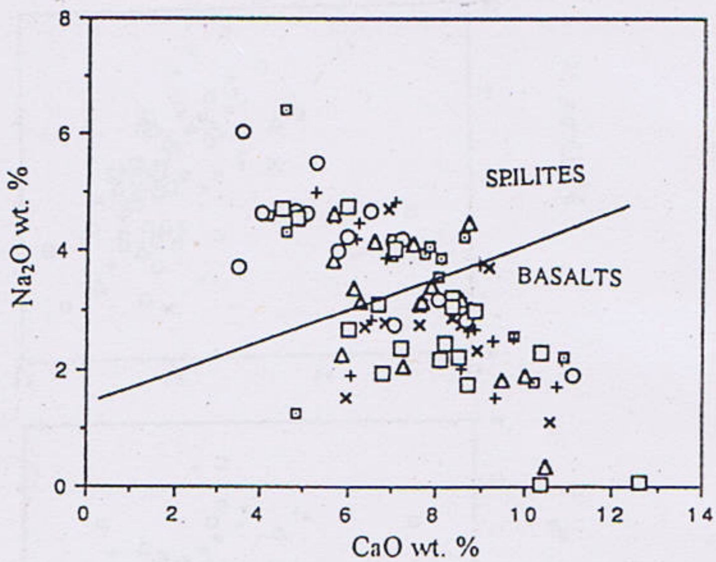

Fig. 7 Na_2O versus CaO plots for the Panjal volcanics. Line dividing spilites and basalts is from Tron (1982). Symbols as in Fig.2.

Metasomatism also changes the composition of the rocks (Hughes, 1972). Metasomatic changes indicate mainly the albitization processes with increase of Na and Si and decrease in Ca (Cann, 1969). Like Na-metasomatism, K-metasomatism in rocks is caused by hydrothermal fluids (Eilu and Idman, 1988, Meneil and Edgar, 1987).

The Fig. 6 shows that some of the Panjal volcanic rocks have high Na/K ratios and exhibit spilitic nature while other have characteristics of igneous rocks. The alteration and spilitic nature of the volcanics is further supported by the Na_2O/CaO ratio (Fig. 7). Their spilitic nature may also be due to seafloor metamorphism and metasomatism prior to Himalayan metamorphism. Different workers have argued that spilitic character is imparted by seafloor alteration, metasomatism and metamorphism of the rocks (Cann, 1969; Hughes, 1972, 1973, Dimroth and Lichtblau, 1979; Wolery and Sleep, 1976, Humphris and Thompson, 1978; Vallance, 1974, Best, 1982).

Table 3.
Qualitative changes in the chemical compositions of the Panjal volcanic rocks from the Lesser Himalaya, as deduced from the chemical analyses.

	1	2	3	4	5	6	7	129A	1	2	3	4	5	6
SiO_2	---	+	-	++	-	--	-	-	-	-	+	+	-	-
TiO_2	+	+	-	+	+	+	-	-	+	-	+	+	+	+
Fe_2O_3	+	+	+	+	+	+	-	-	+	-	+	+	+	+
MnO	-	-	-	+	+	0	-	-	-	-	-	0	+	0
MgO	--	--	--	--	--	0	--	--	-	-	-	-	-	-
CaO	--	--	--	--	-	--	--	--	-	-	-	-	-	-
Na_2O	-	++	+	-	+	+	-	-	+	+	+	+	+	+
K_2O	++	++	-	+	+	+	+	+	+	+	+	+	+	+
P_2O_5	+	+	+	+	+	-	-	-	+	+	+	+	+	+

0 = Change not known; + = tends to increase; + + = clearly increases; - = tends to decrease;
- - = clearly decreases.

CONCLUSIONS

The Panjal volcanics in the Lesser Himalaya on the eastern and western Hazara-Kashmir Syntaxial bend are highly altered with the variable development of chlorite and epidote. On the basis of relict primary assemblage, they were originally plagioclase-clino-pyroxene phyric basalts.

The major and trace elements of the Panjal volcanics which have been affected by alteration processes are Na, K, Ca, Sr and Ba. These elements demonstrate large variations in their concentration in the Panjal volcanics (Table 1). Na_2O varies from 0.05 to 4.57 wt.%, K_2O from 0.11 to 2.78 wt.%. CaO varies from 4.82 to 10.35 wt.%, Ba from 24 to 1847 ppm, Sr from 42 to 423 ppm and Rb from <2 to 224 ppm (Table 1).

The Panjal volcanics have undergone low grade metamorphism and alteration during sea water/rock interaction which have affected their chemical composition variably.

Alteration, spilitization and metasomatism are responsible for the anomalous enrichment and depletion of mobile elements in the Panjal volcanics. Himalayan metamorphism had only locally readjusted the mineralogy of the rocks to greenschist facies.

ACKNOWLEDGEMENT

Authors are grateful for the financial support from the Pakistan Science Foundation grant No. AJK/33 for studies of the basic rocks in the Lesser Himalaya.

REFERENCES

Abbotts, I. L., 1981 Masirah (Oman) ophiolite sheeted dykes and pillow lavas: geochemical evidence of the former ocean ridge environment. *Lithos,* **14,** 283-294.

Ashraf, M., and Khan, M. S., 1991 Geology of Panjal volcanics in Azad Jammu and Kashmir, Pakistan. *Min. Assoc. Canada. SEG. Abst. Programs,* **16,** A5, P9.

Baig, M. S., 1991 Geochronology of Pre-Himalayan and Himalayan tectonic events, northwest Himalay *Pakistan. Kashmir J. Geol.* **8 & 9,** pp. 197.

Berry, R. F., Huston, D. L., Stolz, A. J., and Hill, A. P., 1992 Stratigraphy, structure and volcanic-hosted mineralization of the Mount Windsor subprovince, north Queensland, Australia. *Econ. Geol.* **87,** 739-763.

Best, M. G., 1982 Igneous and metamorphic petrology. Freeman, W. H., New York, 460p.

Bevins, R. E., and Roach, R. A., 1979 Pillow lava and isolated pillow breccia of rhyodacite composition from the Fishguard volcanic Group Lower Ordovician, S. W. Wales, United Kingdom. *J. Geol.* **87,** 193-201.

Bhat, M. I., and Zainuddin, S. M., 1979 Origin and evolution of the Panjal volcanics. *Him. Geol.* **9,** part 2, 421-461.

Bhat, M. I., and Zainuddin, S. M., 1978 Geochemistry of the Panjal Traps of Mount Kalol, Lidderwat , Pahalgam, Kashmir. *Geol. Soc. India,* **19,** 403-420.

Butt, K. A., Chaudhry, M. N., and Ashraf, M., 1985 Evidence of an incipient Palaeozoic ocean in Kashmir, Pakistan. *Kashmir J. Geol.* **3,** 87-103.

Calkins, J. A., Offield, T. W., Abdullaha, S. K. M., and Ali, S. T., 1975 Geology of the southern Himalaya in Hazara, Pakistan and adjacent areas. *U.S.G.S. Professional Paper* 716-C., 29p.

Cann, J. R., 1969 Spilites from the Carlsberg Ridge Indian Ocean. *J. Petrol.* **10,** 1-19.

Coward, P. A., 1984 A geochemical study of metabasalts from a subduction comlplex in eastern Australia. *Chem. Geol.* **43,** 29-47.

Chaudhry, M. N., and Ashraf, M., 1980 The volcanic rocks of Poonch District, Azad Kashmir. *Geol. Bull. Univ. Peshawar,* **13,** 121-128.

Chaudhry, M. N., Ghazanfar, M., Walsh, J. N., and Hussain, M., 1992 The Panjal Sea, Kashmir Hazara microcontinent and Hercynide geology of northwest Himalaya in Pakistan. *Pakistan J. Geol.* No.1, .81-99.

Chaudhry, M. N., Khan, M.S., Walsh, J. N., and Ghazanfar, M., 1995 Petrology and geochemistry of the Panjal volcanics. *Pakistan J. Geol.* No. 1, 81-99.

Condie, K.C., Viljoen, M. J., and Kable, E. J. D., 1977 Effects of alteration on element distribution in Archean tholeiites from the Barberton greenstone belt, South Africa. *Contrib. Mineral. Petrol.* **64,** 75-89.

Dimroth, E., and Lichtblau, A. P., 1979 Metamorphic evolution of Archean hyaloclastites, Noranda area, Quebec, Canada, 1, comparison of Archean Cenozoic sea-floor metamorphism. *Can. Jour. Earth Sci.* **16,** 1315-1340.

Eilu, P., and Idman, H., 1988 Hydrothermal alteration in the lower part of an early Proterozoic greenstone complex at Palovaara, Enontekio, northwestern Finland. *Bull. Geol. Soc. Finland,* **60,** part-2, 115-127.

Embey-Isztin, A., Downes, H., James, D. E., Upton, B. G. J., Dobosi, G., Ingram, G. A., Harmon, R. S., and Scharbert, H. G., 1993 The petrogenesis of Pliocene alkaline volcanic rocks from the Pannonian Basin, eastern central Europe. *J. Pet.* **34,** part 2, 317-343.

Erlank, A. J., and Kable, J. D., 1976 The significance of incompatible elements in Mid-Atlantic Ridge basalts from 45o N with particular reference to Zr/Nb. *Contrib. Mineral. Petrol.* **54,** 281-291.

Fuchs, G., 1975 Contributions to the geology of the North Western Himalaya. Abh. Geol. Bundensanstalt, **32,** 1-59.

Floyd, P. A., Kelling, G., Gokcen, S. L., and Gokcen, N., 1991 Geochemistry and tectonic environment of basaltic rocks from the Misis ophiolitic melange, south Turkey. *Chem. Geol.* **89,** 263-280.

Ganju, P. N., 1943 The Panjal Traps; Acid and basic volcanic rocks. *Proc. Indian Acad. Sci.* **18,** section B, PP. 125-131.

Ganju, P. N., and Rajnath, 1939 Study of the Panjal Trap in the neighbourhood of Srinagar, Kashmir. *Proc. 26th Indian Sci. Cong.* part-3, pp. 105.

Gansser, A., 1964 Geology of the Himalayas. Wiley - Interscience, London, 289p.

Ghazanfar, M., and Chaudhry, M. N., 1985 A third suture in northwest Himalaya. *Kashmir J. Geol.* **3,** 103-108.

Ghazanfar, M., and Chaudhry, M. N., 1984 A Paleozoic ophiolite and island arc sequence of Hazara - Kashmir syntaxis, District Mansehra. *Kashmir J. Geol.* **2,** No. 1, 37-38.

Ghazanfar, M., Baig, M. S., and Chaudhry, M. N., 1983 Geology of Tithwal-Kel, Neelum valley, Azad Kashmir. *Kashmir J. Geol.* **1,** No. 1, 1-10.

Greco, A. M., 1989 Tectonics and metamorphism in the Western Himalayan syntaxis area (Azad Kashmir, NE-Pakistan). Ph.D Dissertation ETH - Zurich , Nr. 8779, Zurich, 193p.

Gupta, K. R., 1979 Petrogenessis of spilitic-keratophyre suite, Bafliaz volcanics, Western Pir Panjal, Kashmir Himalaya. *Him. Geol.,* **9,** part-2, 498-511.

Hajash, A., and Archer, P., 1980 Experimental seawater-basalt interaction: effects of cooling. *Contrib. Mineral. Petrol.* **75,** 1-13.

Hart, S. R., 1969 K, Rb, Cs, contents and K/Rb, K/Cs ratio of fresh and altered submarine basalts. *Earth Planet. Sci. Lett.* **6,** 295-303.

Hart, R., 1970 Chemical exchange between seawater and deep ocean basalts. *Earth Planet. Sci. Lett.* **9,** 269-279.

Hart, R. A., 1973 A model for chemical exchange in the basalt-seawater system of oceanic layer. *Can. J. Earth Sci.* **10,** 295-303.

Hart, S. R., Erlank, A. J., and Kable, E. J. D., 1974 Sea-floor basalt alteration: some chemical and Sr isotopic effects. *Contrib. Mineral. Petrol.* **44,** 219-230.

Honegger, K., Dietrich, V., Frank, W., Gansser, A., Thoni, M., and Trommsdorff, V., 1982 Magmatism and metamorphism in the Ladakh Himalayas (the Indus-Tsangpo suture zone). *Earth Planet. Sci. Lett.* **60,** 253-292.

Hughes, C. J., 1973 Late Precambrian volcanic rocks of Avalon, Newfoundland- A spilite/keratophyre province: recognition and implications. *Can. J. Earth Sci.,* **11,** 272-282.

Hughes, C. J., 1972 Spilites, Keratophyres and the igneous spectrum. *Geol. Mag.* **109,** part-6, 513-527.

Humphris, S. E., and Thompson, G., 1978 Hydrothermal alteration of oceanic basalts by seawater. *Geochim. Cosmochim. Acta,* **42,** 107-125.

Humphris, S. E., Thompson, G., Schilling, J. G., and Kingsley, R. A., 1985 Petrological and geochemical variations along the Mid Atlantic ridge between 46°S and 32°S: influence of the Tristan da chunha mantle plume. *Geochim. Cosmochim. Acta,* **49,** 1445-1464.

Janecky, D. R., and Seyfrid, W. E., 1983 The solubility of magnesium hydroxide - sulphate - hydrate in seawater at elevated temperatures and pressures. *Am. J. Sci.,* **283,** 831-860.

Khan, M. S., and Ashraf, M., 1989 Panjal volcanics: geochemistry and tectonic setting in Azad Jammu and Kashmir and Kaghan valley. *Kashmir J. Geol.* **6 & 7,** 61-81.

Khan, M. S., Ashraf, M., and Chaudhry, M. N., 1991 Geochemical evidence for an oceanic affinity of the Panjal volcanics in Kaghan valley, Pakistan. *Kashmir J. Geol.* **8 & 9,** 1-18.]

Khan, M. S., Ashraf, M., and Chaudhry, M. N., 1992 Geochemical evidence for an oceanic affinity of the Panjal volcanics in Azad Kashmir and Kaghan area. *First South Asia Geol. Cong. Abst. Programs,* 24p.

Khan, M. S., Ashraf, M., and Raja, M. K., 1994 Petrology of the Nauseri granite gneiss in lower Neelum Valley stste of Azad Jammu and Kashmir. *Kashmir J. Geol.* **11 & 12,** 29-42.

Khan, M. S., 1994 Petrology and geochemistry of the Panjal volcanics in the Azad Kashmir and Kaghan areas of the NW Himalaya, Pakistan. Unpublished Ph.D thesis, Punjab University, Pakistan, 233p.

LeRoex, A. P., Dick, H. J. B., Erlank, A. J., Reid, A. M., Frey, F. A., and Hart, S. R., 1983 Geochemistry, mineralogy and petrogenesis of lavas erupted along the Southwest Indian Ridge between the Bouret tripple junction and 11 degrees east. *J. Petrol.* **24,** 267-318.

Loeschke, J., 1976 Major element variations in Ordovician pillow lavas of the Storm Group, Trondheim region, Norway. *Nor. Geol. Tidsskr,* **56,** No. 2, 141-159.

Lydekker, R., 1878 Notes on the geology of Kashmir, Kishtwar and Pangi: Rec. *Geol. Surv. India,* **11,** 30-60.

Lydekker, R., 1883 The geology of Kashmir and Chamba territories and the British Districts of Kaghan. *Mem. Geol. Surv. India,* **22,** 31-34.

Meneil, A. M., and Edgar, A. D., 1987 Sodium-rich metasomatism in the upper mantle: implications of experiments on the pyrolite-Na_2O rich fluid system at 950oc, 20 kb. *Geochim. Cosmochim. Acta,* **51,** 2285-2294.

Middlemiss, C. S., 1911 Sections in the Pir Panjal Range and Sind valley. Rec. *Geol. Surv. India,* **41,** part-2 115-144.

Mottl, M. J., and Holland, H. D., 1978 Chemical exchange during hydrothermal alteration of basalts by seawater. *Geochim. Cosmochim. Acta,* **42,** 1103-1115.

Nakazawa, K., and Kapoor, H. M., 1973 Spilitic pillow lava in Panjal Trap of Kashmir, India. Mem. *Fac. Sci. Mineral.* **39,** No. 2, 83-98.

Papritz, K., and Rey, R., 1989 Evidence for the occurrence of Permian Panjal Trap basalts in lesser and higher Himalayas of the western syntaxis area, NE Pakistan. *Eclogae Geol. Helv.,* **82,** part-2, 603-627.

Reed, M. H., 1983 Seawater-basalt reaction and the origin of greenstones and related ore deposits. *Econ. Geol.* **78,** 466-485.

Seyfrid, W., and Bischoff, J. L., 1977 Hydrothermal transport of heavy metals by seawater: the role of seawater/basalt ratio. *Earth Planet. Sci. Lett.* **34,** 71-77.

Sharma, T. R., and Gupta, K. R., 1975 Petrology and petrochemistry of splite-keratophyre suite of Thanamandi area of Rajouri District, Jammu and Kashmir State. *Geol. Surv. India, Misc. Publ.,* No. 24, part-1, 230-243.

Sharma, T. R., and Gupta, K. R., 1972 On the spilite-keratophyre rocks of Thanamandi area, Kashmir Himalaya. *Him. Geol.* **2,** 452-467.

Speed, R. C., 1991 Oceanic crust of the Kyoto University, Ser. Geol. Grenada Basin in the southern Lesser Antilles Arc platform. *Jour. Geophys. Res.* **96**, . 3835-3851.

Taron, P. B., 1982 Spilitic basaltic composition of Himalayan lavas- A study. Contemp. *Geosc. Res. Himalaya,* **2,** 19-24.

Vallance, T. J., 1974 Spilitic degradation of a tholeiitic basalts. *J. Petrol.* **15,** part-1, 79-96.

Wadia, D. N., 1934 The Cambrian-Trias Sequence of North-Western Kashmir (parts of Muzaffarabad and Bramula Districts). *Geol. Surv. India Rec.* **68,** part-2, 121-176.

Wadia, D. N., 1928 The geology of Poonch state (Kashmir) and adjacent portions of Punjab. *Mem Geol. Surv. India,* **51,** part-2, 184-370.

Wolery, J. J., and Sleep, N. H., 1976 Hydrothermal circulation and geochemical flux at mid ocean ridges. *Jour. Geol.* **84,** 249-276.

Geol. Bull. Punjab Univ. 38, 2003.

STUDY OF SHALLOW GEOLOGICAL STRUCTURES IN THE CORE OF HAZARA KASHMIR SYNTAXIS BASED ON RESIDUAL GRAVITY DATA IN AZAD JAMMU AND KASHMIR PAKISTAN

BY

MOHAMMAD RUSTAM KHAN, MOHAMMAD SABIR KHAN
Institute of Geology Azad Jammu and Kashmir University Muzaffarabad

AND

UMAR FAROOQ
Institute of Geology, University of the Punjab, Lahore-54590, Pakistan.

Abstract: *The residual gravity data has been incorporated for the interpretation of shallow geological structures in the core of Hazara Kashmir Syntaxis. In the western periphery of area Jhelum fault is running along the river Jhelum. The contours trend on residual gravity maps from Muzaffarabad to Tain follows the trend of Jhelum fault. The residual gravity data also indicates the Riasi thrust parallel to Jhelum fault from Tain to Muzaffarabad. The negative contours closure on the residual gravity map in Bagh area shows the low-density fill sedimentary basin of recent age. The modelling of residual gravity data indicates 1.3 km deep sedimentary basin. The contours trend from Bagh to Chikar and from Chikar to Muzaffarabad delineated the Kashmir Boundary Thrust (KBT). The KBT is running from Bagh to Chikar between Murree Formation and Siwaliks whereas in the northeastern side from Chikar to Muzaffarabad Siwaliks has been eroded and exposed the Murree Formation. The gravity modelling also envisage the KBT as a shallow thrust, which penetrates upto the depth of Kuldana Formation. The shales of Kuldana Formation are acting as decollement for the overlaying sedimentary wedge of Murree Formation which is thrusting over Siwaliks along the KBT. The Riasi thrust and KBT are tectonically active. The Coal, Buxite and sulfide bodies have been observed along the Riasi thrust.*

INTRODUCTION

Himalayas are extended from Burma to India and then in Kashmir and Northern Pakistan. In Kashmir and Northern Pakistan these are bended and formed the Nanga Perbat Syntaxis and Hazara Kashmir Syntaxis. The present work focuses in the core of Hazara Kashmir Syntaxis (Fig.1). Powell (1979) integrated the paleomagnetic data with a large scale features (Indian ocean) suggested that the Hazara Kashmir Syntaxis is the product of three comtemporaneously converging elements. These elements are Indo Pakistan plate, Himalaya and the Salt Range cover. According to Powell (1979) the convergence rate between the Indo-Pakistan and Salt Range was larger than those of the Kashmir Himalaya and produced an over print of the later structures in the Hazara Kashmir Syntaxis. The Salt Range also shows anticlockwise rotation. These differential motions led to the formation of Hazara Kashmir Syntaxis. Khan and Ali (1994) and Khan and Ali (1997) suggested that the differential movement low and high angle thrust faults and anticlockwise rotation of the transport direction of Indian plate are responsible for the formation of Hazara Kashmir Syntaxis. They also suggested that 4 km thick Murree Formation is present in the core of Hazara Kashmir Syntaxis.

In the northeastern part of the study area Greco (1989) reported that Su-Himalaya element form the core of Hazara Kashmir Syntaxis which is the molasse, Late Paleocene to Middle Eocene Murree Formation. Older Cambrian and Paleocene rocks exposed along the ridge of the Muzaffarabad anticline is the main structural feature of this element (Fig. 2).

The area under study is highly folded and faulted and a complexity of the structure is developed in response to stresses caused by the collision of Indian and Eurasian plate. In the southwestern part of the studied area Murree Formation thrusts on the Siwaliks rocks. In this area still no systematic work has been done. The present research work mainly focuses in the core of HKS to delineate the shallow geological structure on the basis of residual gravity data. The geological structures of the area are Jhelum strike slip fault, Kashmir Boundary Fault (KBT), Riasi Thrust and the Bagh basin.

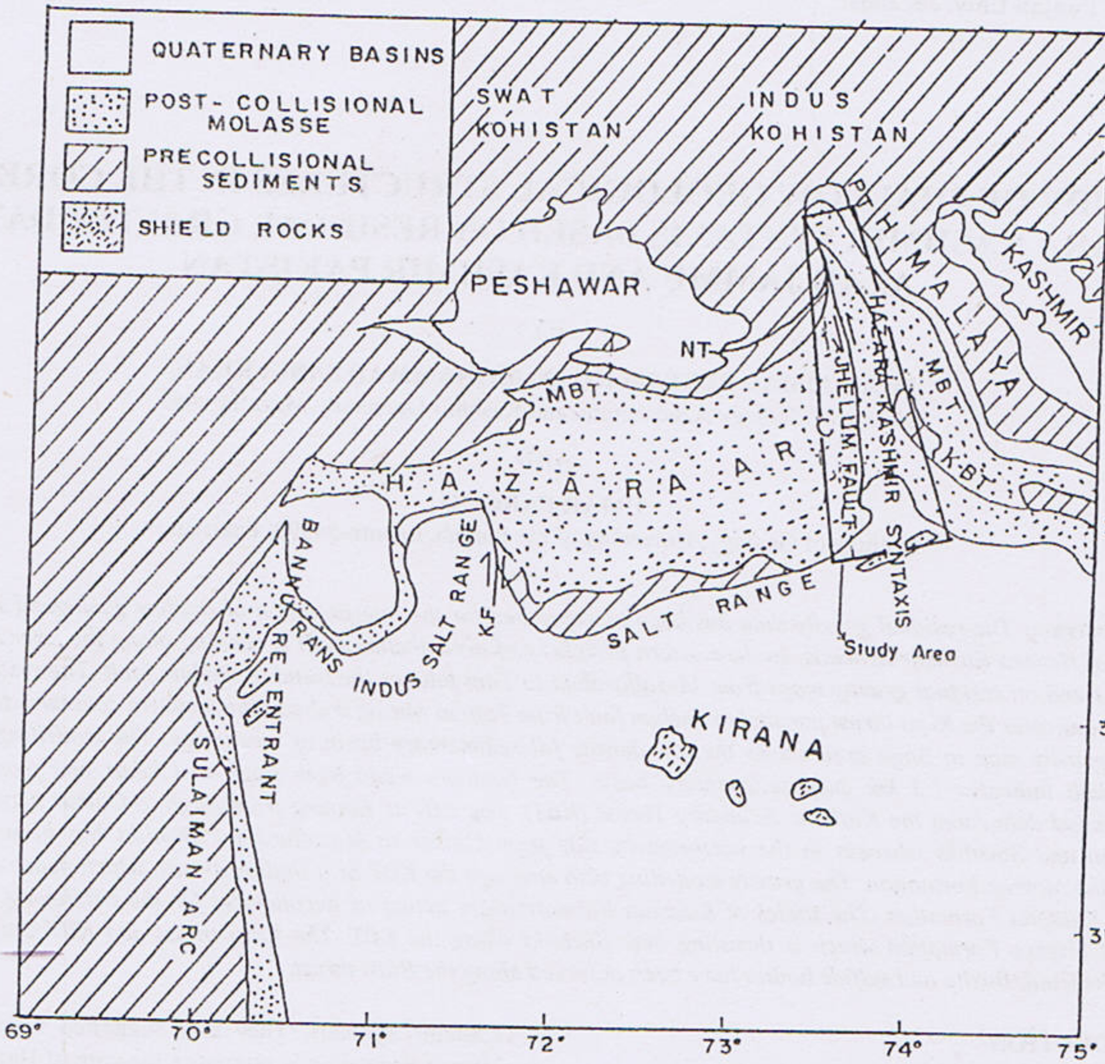

Fig.1. Tectonic map of the area after Chaudhry & Ghazanfar (1992), Khan & Ali (1994) and Seeber et al. (1981) shows the Hazara arc.

TREND- SURFACE ANALYSIS

The Bouguer anomalies map of Khan (1994) shows apparently a complex influence of the surface and deep seated features. To separate the effects the mathematical tool of trend surface analysis was used successfully. Trend surface maps of 1st, 2nd, 3rd and 4th degree have been prepared and goodness of fit and correlation coefficient for each was calculated by using statistical method of Davis (1973). The 4th degree trend surface provided better goodness of fit and correlation coefficient as compared to the lower cases (Table-I). The correlation coefficient is greater than 0.96 and goodness of fit is 0.94. So for the interpretation of shallow geological structures residual gravity map (Fig.3) of 4th degree is selected.

Table-1
Degree of Trend Surface Maps

S. No.	Degree	Goodness of Fit	Correlation Coefficient
1.	1st	0.8066	0.8981
2.	2nd	0.9281	0.9634
3.	3rd	0.9392	0.9691
4.	4th	0.9462	0.9785

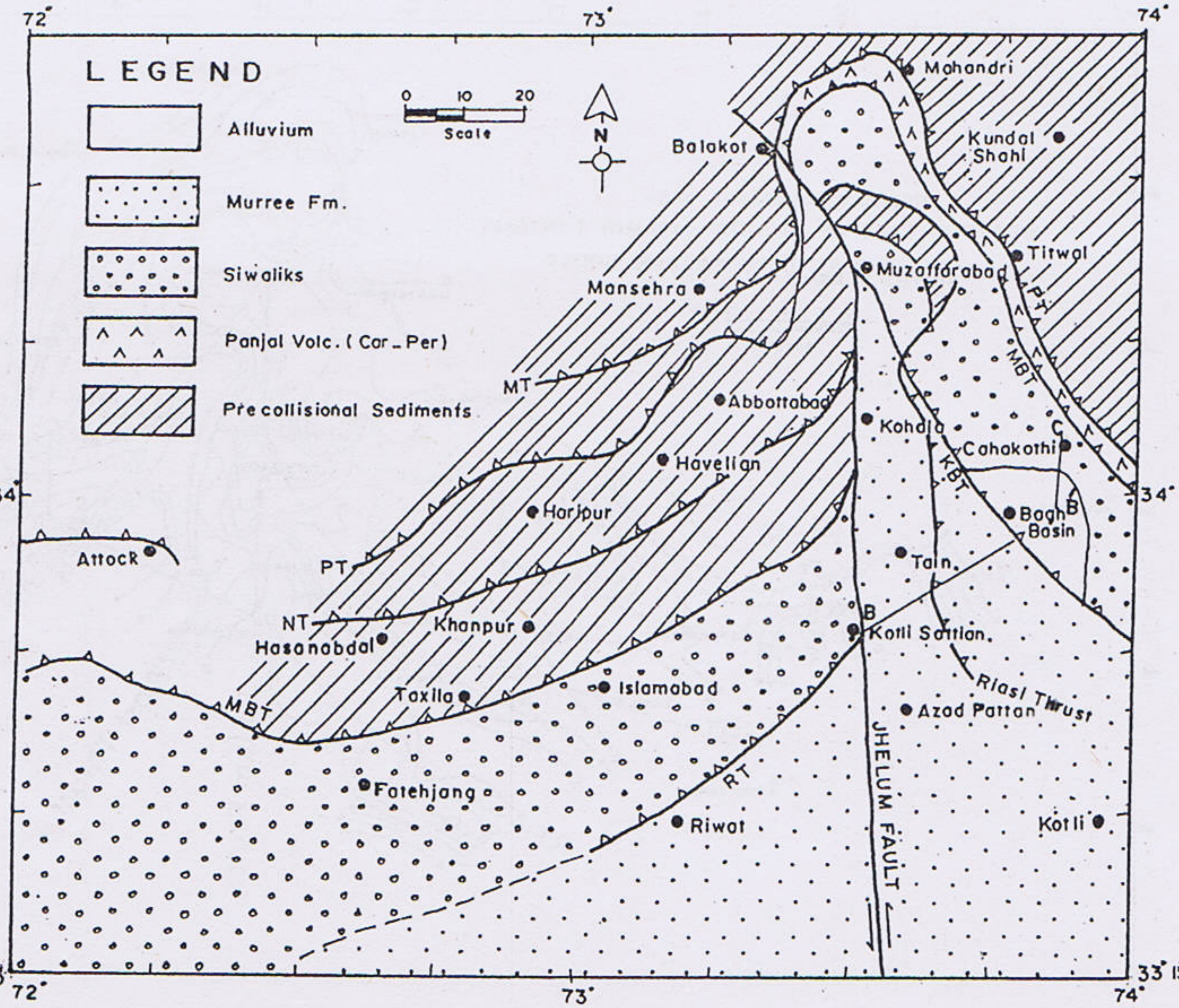

Fig.2. Generalize Tectonic map of Hazara-Kashmir Syntaxis in Northern Pakistan & Kashmir, PT=Panjal Thrust, MBT=Main Boundary Thrust, KBT=Kashmir Boundary Thrust, RT=Riwat Thrust, compiled after Wadia (1928), Latif (1970), Calkins, et al. (1975), Kazmi and Rana (1982). Baig and Lawrance (1987), Chaudhry and Ghazanfar (1992) and Khan (1994). Section B-B′-C is selected for gravity modelling from Kotli Sattian to Bagh and Chakothi.

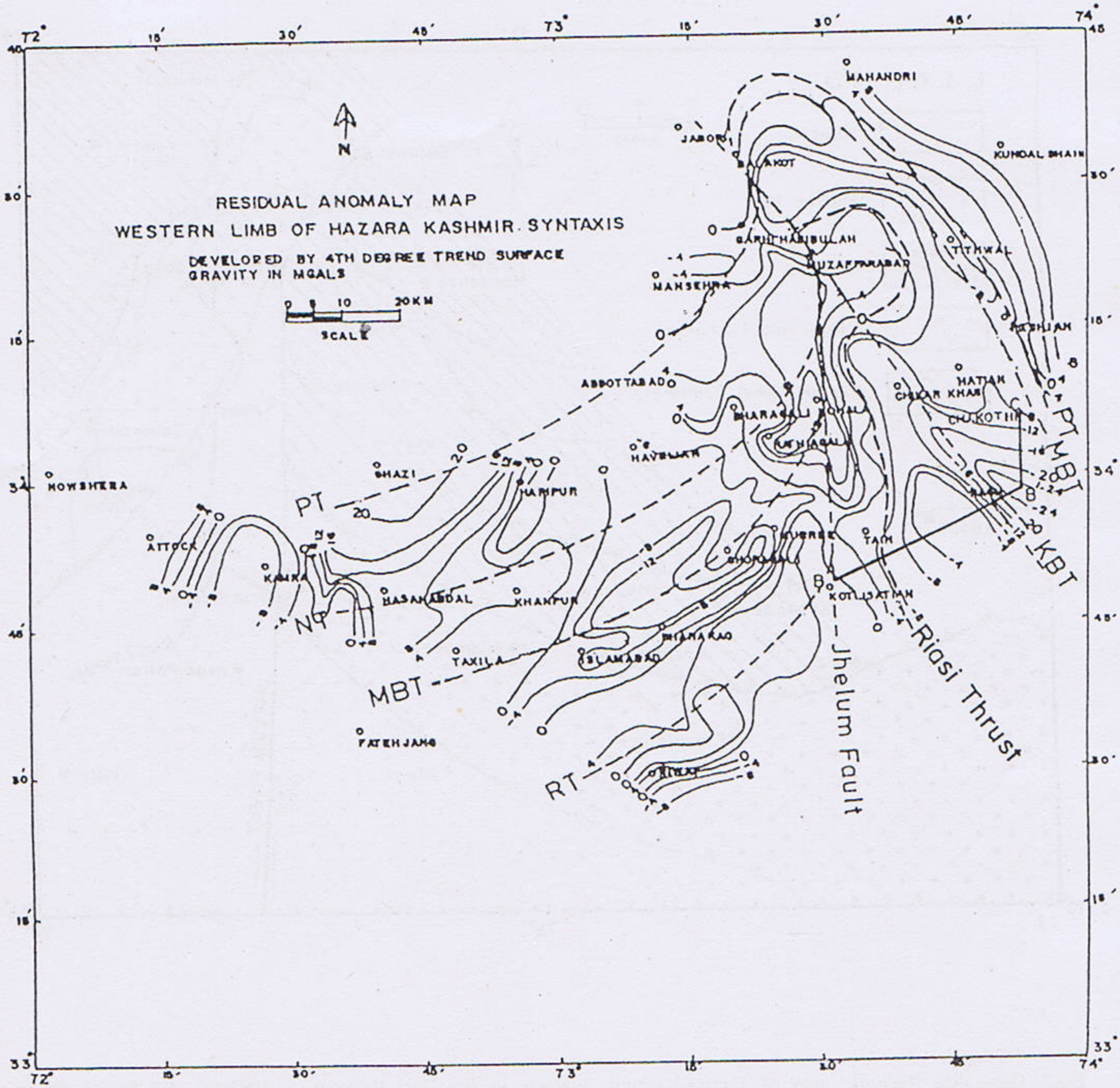

Fig.3. Residual gravity anomaly map, PT=Panjal Thrust, NT=Nathiagali Thrust, MBT=Main Boundary Thrust, KBT=Kashmir Boundary Thrust, RT=Riwat Thrust.

Modelling

Geological model is computed on residual gravity map (Fig.3) along the profile B-B'-C from Kotli Sattian to Bagh and Chikothi Azad Kashmir. The gravity modelling in the core of HKS has been attempted by Talwani et al. (1959) technique using software of Malinconico (1986). In case of gravity modelling the densities assigned to geological bodies are already measured by Khan (1994). Khan (1994) estimated 2.55 ± 0.11 and 2.45 ± 0.1 gm/cc. The densities of Murree Formation and Siwaliks respectively. The present estimated density of the sediments of Bagh basin is 2.1 ± 0.15 gm/cc and the density estimated for the Kuldana Formation is 2.41 ± 0.9. These sedimentary rocks occur in the core of HKS and bounded by Main Boundary Thrust (MBT) in the north and Salt Range Thrust Front in the south (Fig.1). Khan (1994) and Khan and Ali (1997) on the basis of gravity modelling indicated the thick carbonate rocks under the molasse of Murree and Siwaliks in the core of HKS.

QUALITATIVE INTERPRETATION

Residual Anomaly Map

The residual gravity field at a point is related with the local or near surface geological structures having different densities. The residual gravity map of the HKS is presented in fig. 3 and shows gravity variations from -24 mgal to 20 mgal. The contours trend in the southwestern half of the area appears to be NE-SW following generally the trend of Hazara thrust system. In the present study area gravity variation is from 0 mgal to -24 mgal and contours conform the trend of Jhelum strike slip fault from Muzaffarabad to Kotli Sattian. The gravity high and low north-south contours trend from Muzaffarabad to Tain indicates another fault which is parallel to the Jhelum fault (Fig. 3). In the eastern side the contours take a northwesterly trend from Bagh to Muzaffarabad. These contours demarcated the NW-SE trending KBT which is running between Murree Formation and Siwaliks from Bagh to Chikar. In the NW of Chikar Siwaliks have been eroded and exposed the Murree Formation. The negative contours closure in the Bagh area indicate the sedimentary basin. The contours closures also indicate that low-density sediments are filled in this basin.

QUANTITATIVE INTERPRETATION

For the construction of gravity model for shallow geological structures in the core of HKS, gravity data has been incorporating with gross densities zoning of the area in previously known lithostructural information of Wadia (1928), Kazmi and Rana (1982), Khan (1994) and Khan et al. (1997). Modelling along southwest northeast oriented profile B-B'-C from Kotli Sattian to Bagh and Chikothi (Fig.3) computed the structural features such as Jhelum strike slip fault, Riasi thrust, KBT and Bagh basins (Fig.2). In the southwestern part near Tain. Jhelum strike slip fault dips at 85° NW and marks a boundary between Murree Formation and Siwaliks. The density contrast across the Jhelum strike slip fault is 0.11gm/cc. The modelling depicted the Riasi thrust near Tain. In this area Siwaliks are being thrusted under the Murree Formation and the density contrast across the fault is 0.11 gm /cc and dips 28° northeast. In the northeastern side near Bagh KBT dips 30° NE and brings the Murree Formation on the Siwaliks. The density contrast across the KBT is also 0.11gm/cc. In Bagh area the Murree Formation is bended and 1.5 km thick low density sedimentary layer is present in Bagh basin. The density contrast of these sediments with Murree Formation is -0.4 gm/cc. The Murree Formation and Siwaliks are folded and faulted in the study area. The observed dip of the Murree Formation is 0 to 85° in different areas where as the dip of Siwaliks are comparatively gentle. The present study indicates that residual gravity data is only effective upto 5 km depth.

DISCUSSION

The folded and faulted Murree Formation and Siwaliks are present in the core of HKS. In this area the dip of Murree Formation ranges from 0-85° whereas the dip of Siwaliks are comparatively gentle. In the residual gravity map anomaly is found to be 0 mgal in Kotli Sattian and decreases to -24 mgals in the northeastern side in Bagh area. Khan (1994) and Khan and Ali (1997) suggested that Jhelum fault is a strike slip fault and running along the river Jhelum from Muzaffarabad to Salt Range Thrust Front. The gravity model of Khan (1994) from Fatehjang to Kundul shahi along profile A-A' (Fig. 2) computed 80° NW dip of Jhelum strike slip fault in the south of Muzaffarabad. The present gravity model is carried out along profile B-B'-C from Kotli Sattian to Bagh and Chikothi. The modelling is based on residual gravity map (Fig.3) of Khan (1994) and computed 85° NW dip of the Jhelum strike slip fault near Tain. This fault marks a boundary between Murree Formation and Siwaliks. The western block (Murree Formation) of Jhelum strike slip fault is bounded between Main Boundary Thrust in the northwest and Riwat thrust in the southeast. This zone of Murree Formation was in front of the present position of eastern limb of HSK before the origin of HKS. During the evolution of HKS Murree Formation was also bended in the core of HKS. In the 2 Ma Jhelum strike slip fault cut the HKS near the apex and the western block moved southward at a rate of 2 cm/yr (Khan, 1994). The folding, faulting and land sliding along Jhelum strike slip fault and Salt Range Thrust Front indicate that Jhelum strike slip fault is still tectonically active. Khan (1994) suggested that western limb of HKS was in front of the eastern limb of HKS and moved southward due to the differential movement and the stresses caused by the

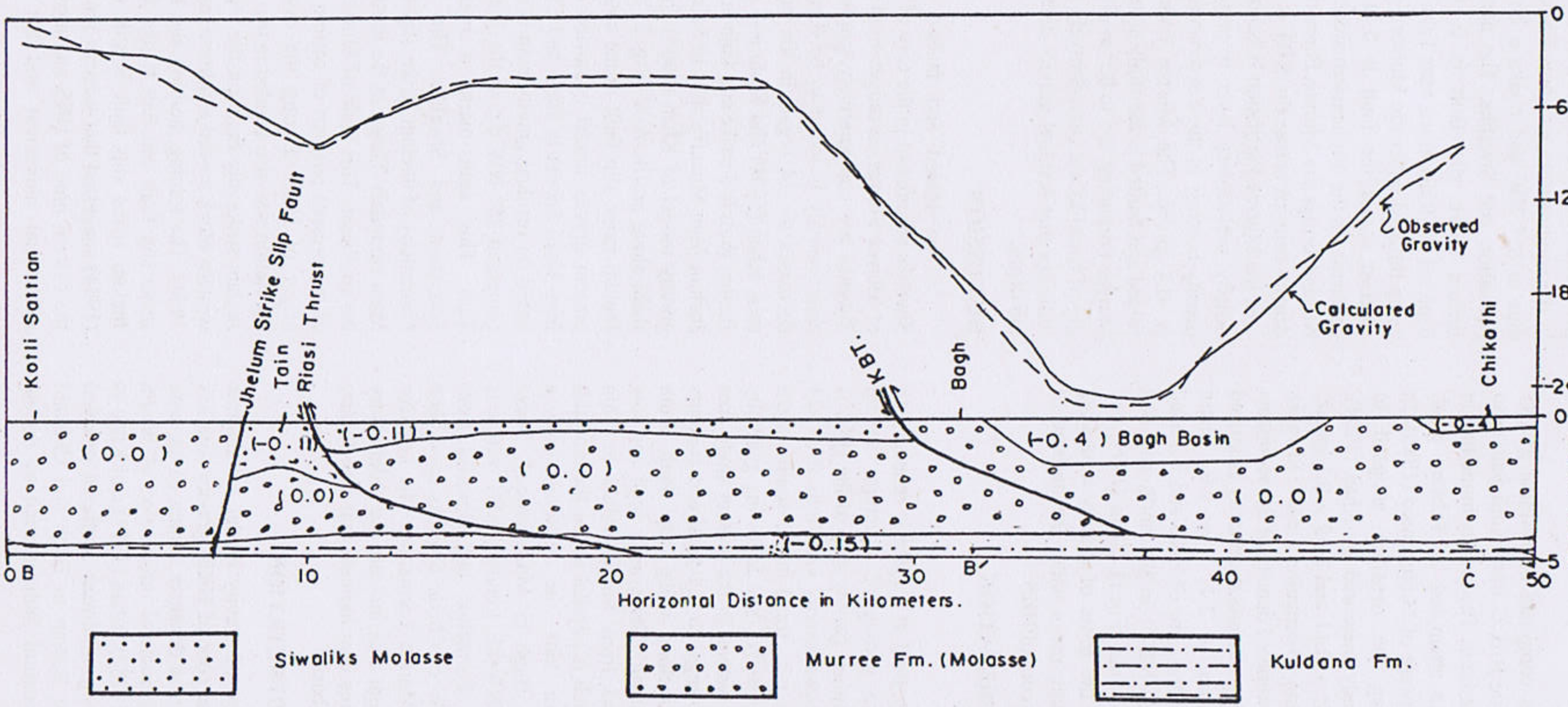

Fig.4. Gravity model along profile B-B′-C from Kotli Sattian to Bagh and Chikathi.

collision of Indian and Eurasian plates. The modelling computed a fault near Tain where Murree Formation is thrusted on the Siwaliks. Verma (1984) indicated the extension of Riasi thrust in Azad Kashmir which joints the river Jhelum near Azad Pattan, 15 km south of village Tain. Chaudhry and Ghazanfar (1991) suggested that KBT is an extension of Riasi thrust. They extended Kotli fault upto Muzaffarabad in the southwest of Bagh. The present study based on gravity data disagree with Chaudhry and Ghazanfar (1991) and shows that KBT is not an extension of Riasi thrust because it is shallow fault and located 30 km northeast of Azad Pattan. In Bagh area at 40 km point modelling shows the KBT dipping 30° NW and running between Murree Formation and Siwaliks. The estimated depth penetration of this fault is 4.5km up to the Kuldana Formation, which is acting as a decollement for the overlying Murree Formation and present throughout the study area between Kotli Sattian to Bagh. In the southwest of Kotli Sattian near Lehtrar Khan (1994, 97) suggested that Kuldana shales are acting as decollement for Murree Formation along the Riwat thrust. The Kuldana Formation is well exposed in Kuldana near Murree in the northwest of Kotli Sattian and also in the northeast of Muzaffarabad. Khan et al. (1997) mapped the Kuldana Formation in the eastern side of study area in Kahuta. The northwest-southeast contours tend on the residual gravity map from Bagh to Chikar and Muzaffarabad delineates the KBT. This fault is running between Murree Formation and Siwaliks from Bagh to Chikar and in the northeast of Chikar Siwaliks have been eroded and exposed the Murree Formation. The contours trend from Tain (15 km north of Azad Pattan) to Muzaffarabad parallel to the Jhelum strike-slip fault (Fig. 3) delineates a fault which could be an extension of Riasi thrust of Verma (1984). The gravity modelling also computed 1.3 km thick sedimentary layer of recent age in Bagh basin. The folding, faulting, land sliding and seismicity in the area indicates that Riasi thrust and KBT are tectonically active. The Coal, Buxite, Fire clay and sulfide bodies are exposed along the Raisi thrust.

CONCLUSIONS

One the basis of residual gravity date the following conclusions are drawn.

Jhelum fault is strike-slip fault and dips 85° NW near Tain.

The gravity data delineates a thrust fault from Muzaffarabad to Tain parallel to the Jhelum strike-slip fault. This fault is an extension of Riasi thrust and dips 28° NE opposite to the Jhelum strike-slip fault.

First time the gravity study demarcated a basin in Bagh Azad Kashmir. The modelling computed 1.3 km thick sedimentary layer of recent age in the Bagh basin.

The KBT is a shallow thrust fault developed due to the stresses caused by the collision of Indian and Erosion plates and the presence of Kuldana shales which acts as a decollement for the overlaying sedimentary wedge. KBT is not an extention of Riasi thrust. Riasi thrust is depicted near Tain 15 km north of Azad Pattan and extended upto the northwest of Muzaffarabad.

The indication of Riasi thrust is valuable for the construction of civil engineering structures and mineral exploration.

REFERENCES

Baig, M.S., and Lawrence, R.D., 1987. Precambrian to Early Paleozoic Orogenesis in the Himalayan, *Kashmir Jour.Geol.*, **5**, 1-22.

Calkins. J. A., Offield, T.W., Abdullah, S. L. M., Shah, T.A., 1975. Geology of the Southern Hazara in Hazara Pakistan and adjacent area. *U.S. Geol. Surv. Prof. Paper*, 716-c, 1-29.

Chaudhry, M.N., and Ghazanfar, M., 1992. Some Tectono Stratigraphic observations on NW Himalayas, *Pakistan, Jour., Geol.*, **1.1**, 1-14.

Davis, J.C., 1973. Statistics and data analysis in geology. John Wiley and Sons, Newyork, 322-358.

Greco, A., 1989. Tectonic and metamorphism of the western Himalayan syntaxis area (Azad Kashmir NE Pakistan) dissertation ETH Zurich, **8779**, 113 p.

Khan, M.R., 1994. Tectonic Modelling of western Hazara and its adjoining areas (gravity modelling) Ph.D thesis Quaid-i-Azam Univ.

Khan, M.R. and Ali, M., 1994. Preliminary modelling of the western Himalaya. *Kashmir Jour. Geol.*, **11-12**, .59-66.

Khan, M.R., and Ali, M., 1997. Tectonic modelling of western Himalaya in northern Pakistan based on gravity study. *Geol. Bull. Punjab Univ.*, **31-32**, .103-113.

Khan, M.S., Ashraf, M. and Chaudhary, M.N., 1997. Geochemical evidence for the tectonic setting of the Panjal volcanics in Azad Kashmir and Kaghan areas. *Geol. Bull. Punjab Univ.*, **31-32,** 43-52.

Kazmi, A.H., and Rana, R.A., 1982. Tectonic map of Pakistan. *Geol. Surv. Quatte, Pakistan.*

Latif M. A., 1970. Explanatory notes on the geology of southeastern Hazara to accompany the geological map. *Jour. Geol. B.A., Sonderbon,* **15,** .5-20.

Malinconico, L.L. Jr., 1986. An interactive modelling programme. Environmental simulation laboratory southern Illinois University Carbondale, IL-62901.

Powell. C. Mc. A., 1979. A speculative tectonic history of Pakistan and surroundings. In Geodynamics of Pakistan. Farah, A., De Jong, K.A., Eds., *Geol. Surv. Quetta, Pakistan,*.**1,** 1-24.

Talwani, M., Worzel, J.L., and Landisman, M., 1959. Rapid. Gravity computation of two dimensional bodies with application to the Mendocino submarine fracture zones. *Jour Geophys. Res.*:**64,** .49-59.

Seeber, L., Armbruster, J., and Quettmyer, R. C., 1981. Seismicity and continental subduction in the Himalaya geodynamics evolution Am. Gephys. Union Geodys., **3,** 215-241.

Verma, R.K., 1984 Gravity Field seismicity and Tectonics of the Indian Peninsula and the Himalayas 169-193.

Wadia D.N., 1928, Geology of Poonch (Kashmir) and adjacent portion of the Punjab. *Geol. Surv. India, Mem.,* **51,** 185-370.

Geol. Bull. Punjab Univ. 38, 2003.

SEDIMENTOLOGY OF THE CHAK JABBI LIMESTONE, KALA CHITTA RANGE, PAKISTAN.

BY

RIAZ AHMAD SHEIKH
Institute of Geology, Punjab University, Lahore. Pakistan.

M. KALEEM AKHTER QURESHI
Geological Survey of Pakistan. Lahore. Pakistan.

AFTAB AHMAD BUTT, SHAHID GHAZI AND KAMRAN MIRZA
Institute of Geology, Punjab University, Lahore. Pakistan.

Abstract: *The Chak Jabbi Limestone north of the Chak Jabbi Rest House, Kala Chitta Range has been systematically measured .The sedimentological studies based on field and laboratory observation revealed a limited number facies throughout the formation The Chak Jabbi Limestone consists of limestones and dolomitic limestones. A remarkable similarity of microfacies has been observed in the Chak Jabbi Limestones and the limestone beds of the underlying Mianwali Formation, representing comparable paleoenvironments.*

INTRODUCTION

The name Chak Jabbi Limestone was introduced by Fatmi (1973) to the lithographic limestone unit overlying the Mianwali Formation in the Kala Chitta Range and it refers to the part of the Kioto Limestone of Cotter (1933). The complete sections of the Chak Jabbi Limestone are present north of the Chak Jabbi Rest House and 1 kilometre southeast of Bagh (Fig. No.1a). At other localities the Chak Jabbi Limestone has a thrusted contact with the younger rocks. The Chak Jabbi Limestone comprises thin to medium bedded (10 cm to 60 cm thick beds) lithographic to sublithographic light grey weathering medium grey limestone (Plate No.1a, Fig No.2). The limestone is fine grained calcisiltite, which shows dolomitization and the dolomitization increases in the upper part where the formation grades into the Kingriali Formation. Certain bioturbated beds having burrows filled by secondary yellow colored dolomite are common in the middle part. Stylolites and stylobedding is frequent in the formation. The lithology is remarkably persistent in the entire area. Both the upper and the lower contacts of the formation are gradational (Plate No.1b). The thickness of the formation as measured at the type locality is 12.5 meters (Fig. No.2).

The Chak Jabbi Limestone is devoid of fossils. However, the Chak Jabbi Limestone is assigned Middle Triassic age on basis of its stratigraphic position and its correlation with The Tredian Formation of the Salt Range, which has been assigned Middle Triassic (Anisian) age by virtue of its age diagnostic faunal assamblage as reported by Balme, (1970) and Masood et al., (1992).

REGIONAL SETTING

During The Paleozoic through Early Mesozoic sedimentaion took place upon the northern margin of the Gondwana bordered by the Tethys. Later, presumably during the Jurassic, the Indo-Pakistan Continent was separated from Gondwana and drifted northward. A shelf system developed, which was influenced by various sea level fluctuations, climatic variations and tectonic instabilities.

The Triassic succession is well exposed in the Kala Chitta Range, the Salt Range, the Trans Indus Ranges, and the Balochistan Basin. In general the Triassic deposits show a superimposed regressive development from bottom to top. The marine sediments of the Mianwali Formation allow to establish a small scale parasequence mosaic in combination with fossil distribution. The Chak Jabbi Limestone is composed of limestone, which is grading upward into the dolomitic limestone. The present research is first attempt to outline the various microfacies, its stratigraphic position and the environmental style.

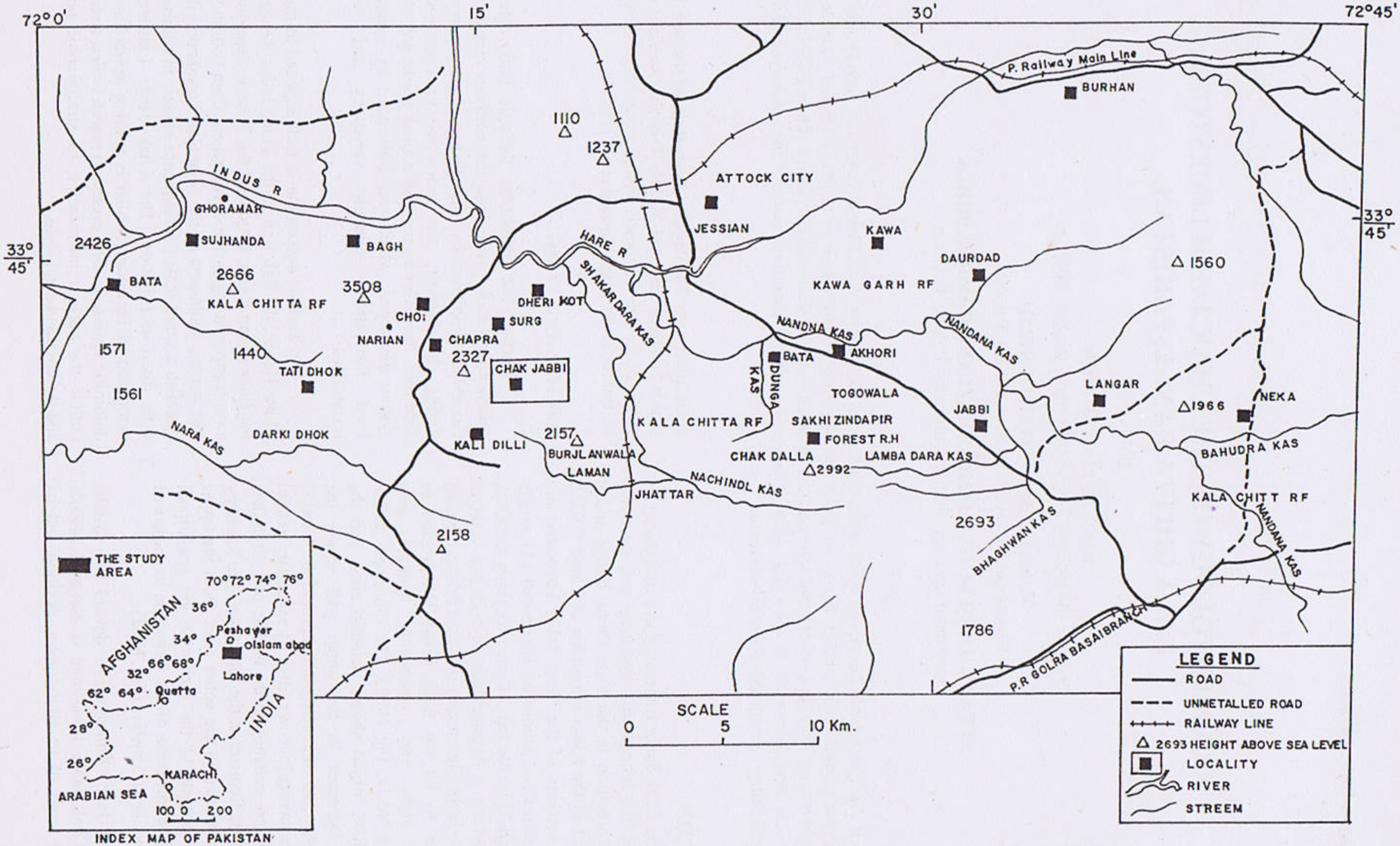

Fig. 1. Map showing location of the Chak Jabbri Limestone in the Kala Chitta Range, Pakistan.2

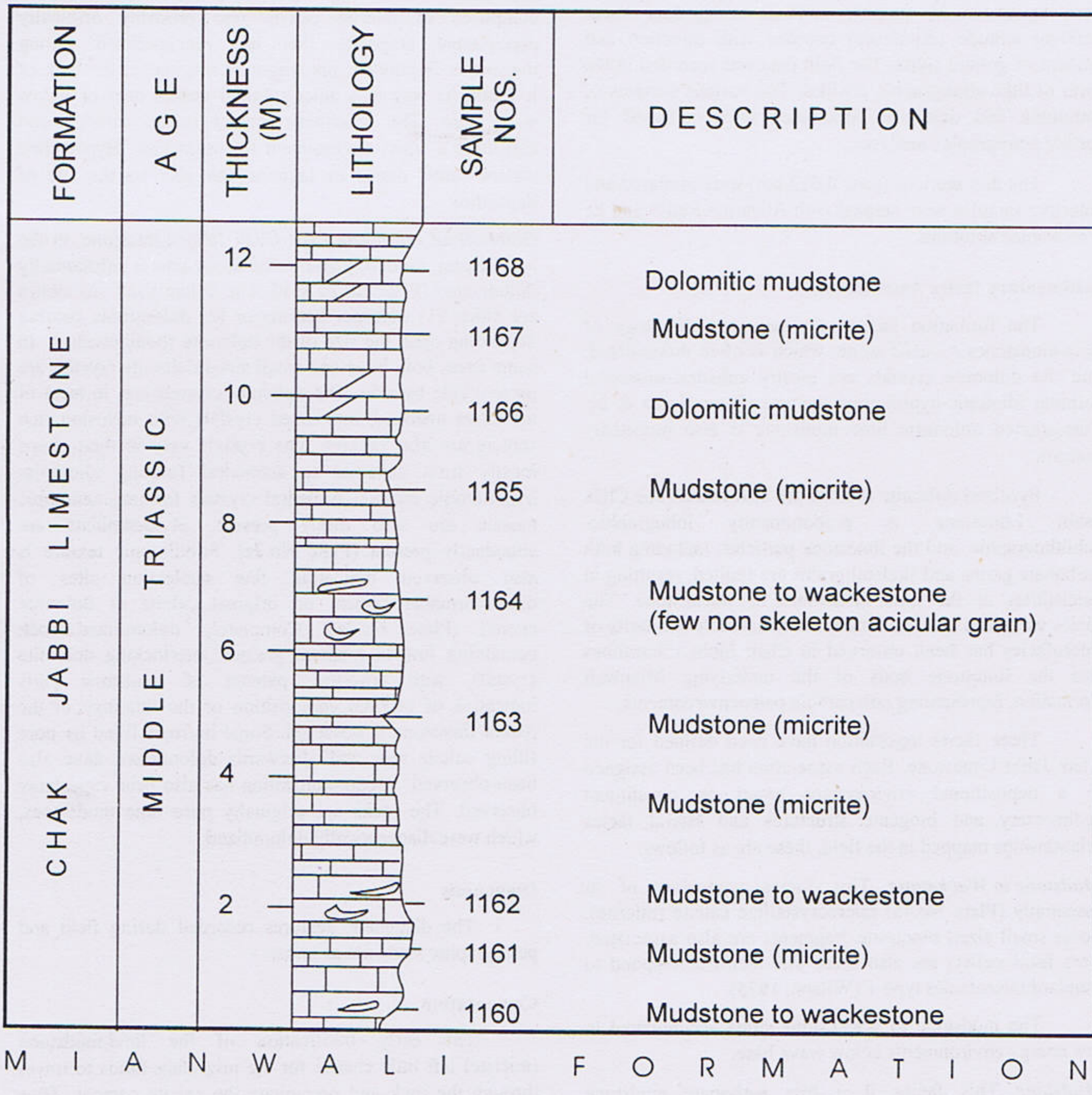

Fig. 2. Lithological section of the Chak Jabbi Limestone, north of the Chak Jabbi Rest house, Kala Chitta Range.

METHODOLOGY

The sections were measured by conventional method using optical distance meter, Brunton compass and measuring tapes. True thickness of the lithologic units has been calculated by graphic methods using data about bedding attitude (dip/strike) coupled with direction and amount of ground slope. The field data was recorded in the form of litho-stratigraphic profiles. The various samples of limestone and dolomitic limestones were collected for further petrographic analyses.

The thin sections (size: 4.5x2 cm) were prepared and selective samples were stained with Alizarine Red-S and K. ferricyanide solutions.

Sedimentary facies Associations

The formation has a very persistent lithology of lime-mudstones / wacke stone, which is often dolomitized, and the dolomite crystals are mostly euhedral-subhedral forming idiotopic-hypidiotopic texture (Plate No.2a & b). Fine-grained dolomitic lime mudstone is also repeatedly present.

Pyritized dolomite rhombs are also found. The Chak Jabbi Limestone is predominantly lithographic-sublithographic, and the limestone particles, including both carbonate grains and skeletal grains are limited, resulting in calcisiltites or the lime mudstones or wackestone. The facies variations are also limited. A remarkable similarity of microfacies has been observed in Chak Jabbi Limestones and the limestone beds of the underlying Mianwali Formation, representing comparable paleoenvironments.

Three facies association have been defined for the Chak Jabbi Limestone. Each association has been assigned to a depositional environment based on constituent sedimentary and biogenic structures and lateral facies relationships mapped in the field, these are as follows:

Mudstone to Wacketone This facies comprises of in essentially (Plate No.4a) microcrystalline calcite (micrite). Some small sized bioclastic fragments are also associated. Rare fecal pellets are also seen. The facies correspond to standard microfacies type-1 (Wilson, 1975).

The mudstone to wackestone strata accumulated in low energy environments below wave base.

Mudstone This facies is a true carbonate mudstone consisting of microcrystalline calcite (Plate No.3a), presumably formed by recrystallization of original aragonitic needles. Small amount of clay mineral and scattered quartz silt grains are also seen especially concentrated as insoluble residue on stylolites, which are abundantly present in this microfacies. The facies corresponds to standard microfacies type 23 (Wilson, 1975).

The pure lime mudstones are indicative of deposition in rather calm waters. The bulk of rock now composed of micrite calcite was probably originally precipitated aragonite that has recrystallized during diagenesis. Wherever, the aragonite originated, the bulk of it found its way into quiet subtidal waters near or below wave base. The conditions appear to be variable and constitute a stress environment for organisms. Hypersaline waters cutoff ponds or lagoons can also be the site of deposition.

Dolomitized mudstone The Chak Jabbi Limestone, in the middle part, randomly and in the upper part is substantially dolomitized (Plate No.2a & b). The dolomitized mudstones are either (1) dolospar bearing or (2) dolomicrite bearing depending upon the size of the dolomite rhombohedron. In some cases both large and small sized dolomite crystals are present side by side. The dolomite crystals are, in most of the cases unzoned, but zoned crystals with inclusion rich centers are also present. The crystals vary in their shape mostly from euhedral to subhedral forming idiotopic-hypidiotopic mosaic. Anhedral crystals forming xenotopic mosaic are also rarely present. Stylocumulate are abundantly present (Plate No.3a). Poikilotopic texture is also observed indicating few nucleation sites of disconformable cement on original calcite or dolomite crystal (Plate No.2a). Completely dolomitized rock containing fine to medium grained interlocking dolomite crystals, with however, patches of mudstone parts indicative of original composition or the lithology of the parent limestone is observed. Some burrows filled by pore filling calcite spar and afterwards dolomitized have also been observed. Dedolomitization has also been repeatedly observed. The rocks are originally pure lime mudstones, which were diagenetically dolomitized.

Diagenesis

The diagenetic features recorded during field and petrographic study are as under: -

Cementation

The early lithification of the lime-mudstone (micrite) left little chance for the migrating fluids to travel through the rock and precipitate the calcite cement. Thus microcrystalline non-ferroan calcite (Folk, 1959) is the only binding material in the Chak Jabbi Limestone. This calcite is dull, opaque and at places changes to microspar. This aggrading crystals range in size from 10-65µm. The pore filling calcite spar, however, has been observed in the cavities, vugs etc.

Plate -1

A

B

A: Thin to medium bedded Chak Jabbi Limestone, Chak Jabbi Rest House section. Kala Citta Range.

B: The contact between the Chak Jabbi Limestone (1) and the overlying Kingriali Formation (2). The pen marks the contact. Photograph taken north of Chak Jabbi Rest House, Kala Citta Range.

Plate -2

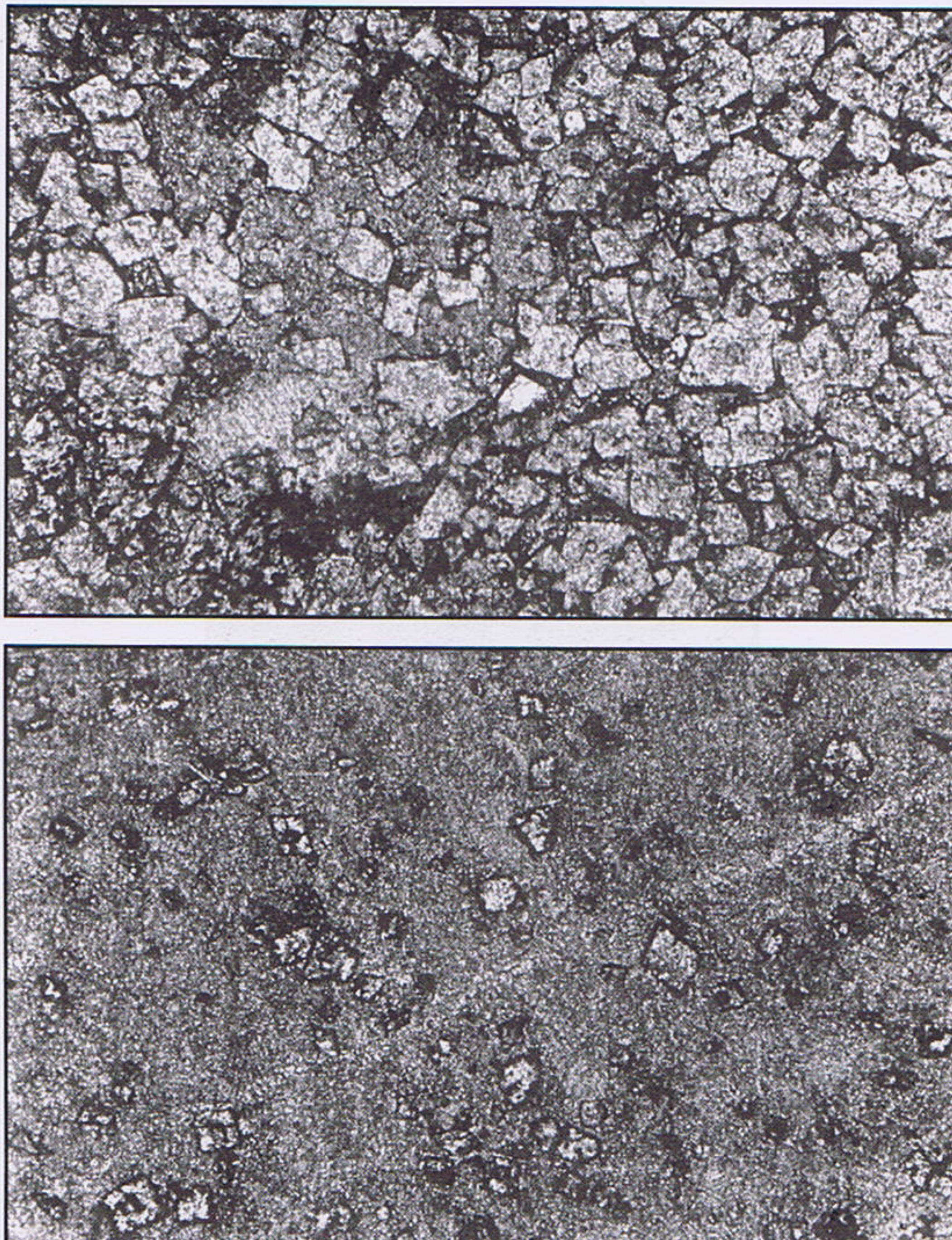

A

B

A: Photomicrograph showing partial dedolomitization in the xenotopic-hypidiotopic crystal mosaic in the dolomitized mudstone of the Chak Jabbi Limestone (Sample, Kala Chitta Range. (PPL). Scale bar 250μm.

B: Randomly distributed, euhedral-subhedral, zoned and unzoned dolomite crystals in the dolomite carbonate mudstone of the Chak Jabbi Limestone (sample Chak Jabbi section, Kala Citta Range. (PPL). Scale bar 550μm.

Plate -3

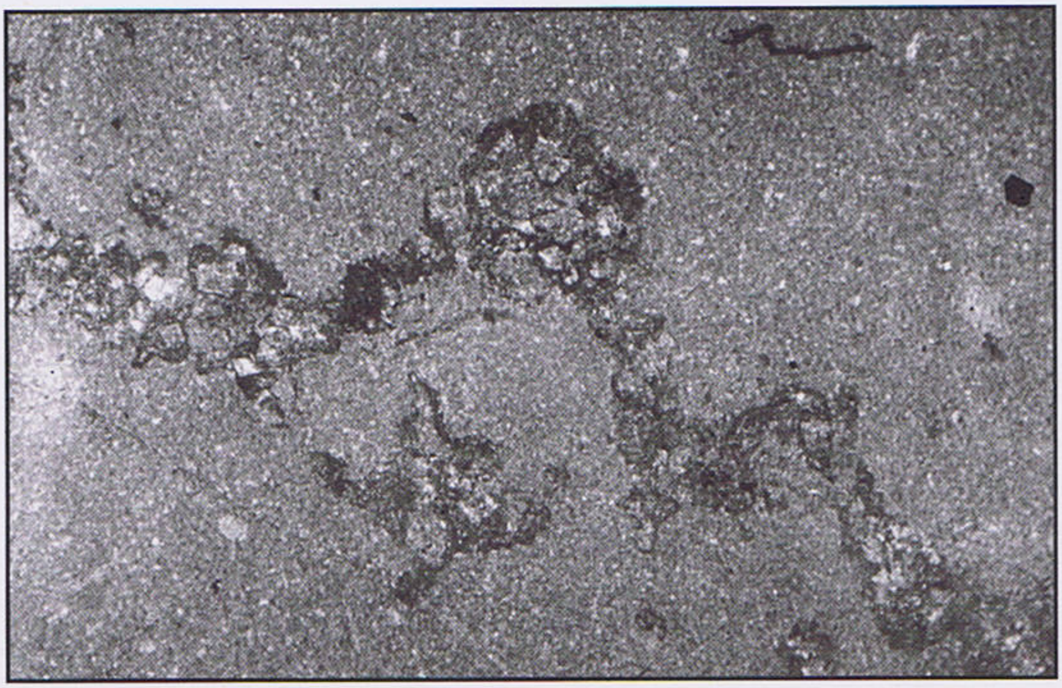

A

B

A: Stylo-cumulate structure is prominent. Dolomite crystals are aligned along stylolite surface. These are commonly present in unlaminated pure lime mudstones of the Chak Jabbi Limestone, Kala Chitta Range. (PPL). Scale bar 550μm.

B: Stylolite and stylolite porosity in the lime mudstone, Chak Jabbi Limestone, Kala Chitta Range. (PPL). Scale bar 550μm.

Plate -4

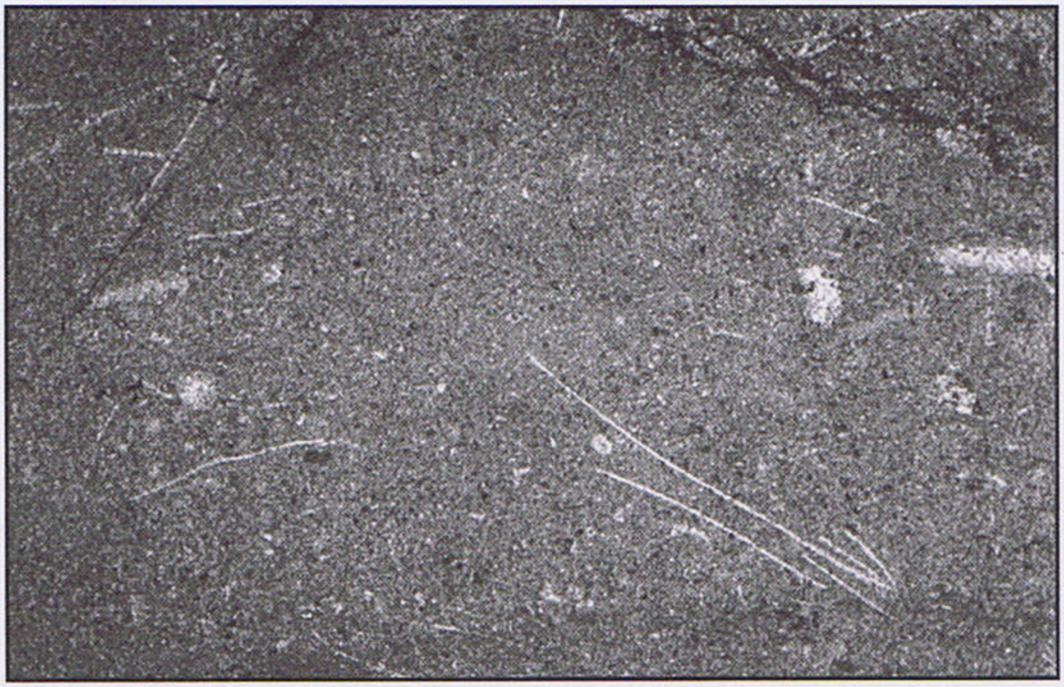

A

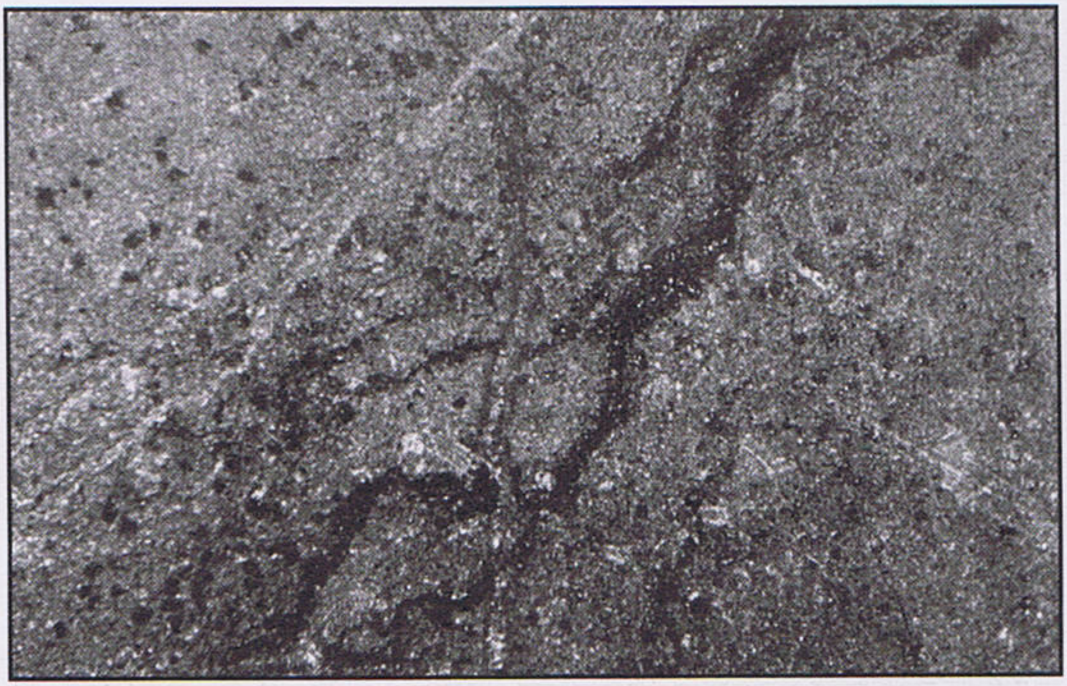

B

A: Filamentous wackestone. Chak Jabbi Rest House section, Kala Chitta Range. (PPL). Scale bar 550μm.

B: Photomicrograph showing horse-tail stylolite in dolomitized carbonate mudstone, Chak Jabbi Limestone, Kala Chitta Range. (PPL). Scale bar 550μm.

Compaction

The mechanical compaction is not observed in the Chak Jabbi Limestone, which is due to early lithification. The chemical compaction is, however, prominent that is observed in the form of variety of stylolites described as under:

Stylolites and stylocumulates

A variety of stylolites are present within the Chak Jabbi Limestone. The stylolites are also abundantly present through out the carbonate rocks of the Kala Chitta Range. Thus these dissolution structures merit to be discussed in detail in order to evaluate these feature in eh Chak Jabbi and other rocks.

Stylolites are generally formed as the result of pressure dissolutioning, and are thin discontinuity zones in rocks. The dissolutioning involves solution around points of contact between mineral grains or the limestone particles in response to pressure (usually weight of overburden). Since certain minerals are more susceptible to pressure solution than others, various burial depths are necessary in order to produce a strong stylolitization (Flugel, 1982). The pressure solution is an important process in supplying carbonate for the precipitation of carbonates cements.

The stylolite structures vary in size from microscopic sutured contacts up to stylolites several meters in length. According to Logan and Semeniuk (1976) the rate of dissolution of calcium carbonate is similar at stylolite interfaces so that small idens disappear preferentially leaving a residue of corroded larger idens together with other less soluble materials. "An iden is a body of material that behaves as statistically homogeneous unit under a set of physical and chemical conditions. It is a finitely extended body independent of scale, geometry and composition." An iden may be a single crystal, a polycrystalline aggregate such as an ooid or skeletal fragment, etc., or a body of rock constituting idens of first two types. The less soluble materials include quartz grains, mica flakes, clay minerals and carbonaceous materials and are termed as reactate by Logan and Semeniuk (1976). With the passage of aqueous solutions through the rock by way of stylolite surfaces, not only is removed in solution but new materials may be introduced and precipitated within the rock and /or stylolitic surfaces. Such new material may include minerals such as dolomite, calcite, quartz etc. for which Logan and Semeniuk introduced the term stylocumulate. Dolomite in particular may be introduced as reactate but with subsequent pressure dissolution may accumulate as stylocumulate. In the Chak Jabbi Limestone the macroscopic stylolites vary in shape and lateral persistence and the stylolite sets are parallel sub-parallel to bedding

Logan and Semeniuk (1976) have also recognized five intergrading structures depending upon the geometry of stylolite sets and the intensity to which the parent rock has been altered by pressure dissolution and other diagenetic processes. These structures have been observed in the Chak Jabbi Limesotne and are as follows:

Stylo-bedding structures These are persistently seen in the Chak Jabbbi Limestone. These structures are described to comprise of subparallel stylolite sets separating sheet like idens of carbonate rocks. The stylo-bedding is usually subparallel to true bedding but may equally be oblique to it. In fact stylo-bedding is frequently mistaken for the true bedding, which probably provided the locus for the initial generation of stylolites.

Stylolaminar The Stylolaminar structures are also frequently found in the lithographic limestone of the Chak Jabbi Limestone. These structures are the result of continuous dissolution of limestone and condensation of the rock on the stylolites that have led to the formation of stylolaminar structure in which a set of closely spaced stylolites are separated by seams of reactate or the residue carbonate idens. The resultant diagenetic rock is called stylolaminate and represents closely spaced set of subparallel stylolites.

Stylonodular structure: Differential dissolution of stylobeds leads to the development of lenticular to rounded residual idens set in a base of stylolaminate, forming stylonodular structure In a sense, stylonodular rock represents an intermediate stage between stylobedded limestone and stylolaminate.

The other two types though not frequent in the Chak Jabbi Limestone are:

Stylobrecciated structure The development of an evenly three dimensional array of stylolites defining irregular three dimensional limestone idens produces stylobreccioid structure.

Stylomottled structures Uneven dissolution of calcium carbonate at the fragment or crystal level within the parent rock may lead to the accumulation of stylocumulate or precipitation of reactate in patches or mottles.

These pressure solutions occur singly or combined in the Chak Jabbi Limetone. They intergrade and show relationship which point to progressions leading from the unaffected parent rock through a stylobedded stage to the eventual stylolaminate end member.

Dolomitization

The Chak Jabbi Limestone is extensively dolomitized the nature and degree of dolomitization has been discussed.

Chemical analysis

The undolomitized limestone samples were chemically analyzed the results are given in Table 1. The chemical composition is almost constant and only minor variations have been recorded.

The magnesium oxide content of the limestone is less than 2%. It ranges from 0.20 to 1.61. The calcium oxide is invariably more than 51% (Table 1) the percentage of insoluble materials, which include silica and clay minerals, is 1.43 to 3.59.

Table .1

The Chemical analysis of the Chak Jabbi Limestone from Chak Jabbi section.

Sample No	Insoluble matter %	Fe_2O_3 %	Al_2O_3 %	CaO %	MgO %	LoI %
KQ-1167	1.70	0.31	0.64	53.28	0.40	43.11
KQ-1166	3.08	0.31	1.34	51.03	1.01	42.47
KQ-1165	1.43	0.24	0.66	52.43	1.61	43.23
KQ-1164	1.85	0.24	0.46	52.99	1.21	43.04
KQ-1163	1.48	0.68	0.88	52.09	1.21	42.90
KQ-1162	3.20	0.40	1.45	52.15	0.20	42.29
KQ-1161	3.22	0.33	1.45	52.15	0.20	42.39
KQ-1160	3.59	0.50	1.25	51.03	0.20	42.52

COMPARISON WITH OTHER AREAS

The Chak Jabbi Limestone is devoid of prominent mega and micro fauna and is correlated with the Tredian Formation of the Salt Range, on the basis of its stratigraphic position lying over the Middle Scythian, ammonoid bearing Mianwali Formation and lying under the Kingriali Formation. In the Balochistan Basin the comparable beds are highly disturbed, and the beds no 6 and 7 of Gowal section are tentatively correlated to be equivalent to the Chak Jabbi Limestone.

Contrary to the Tredian Formation, which is continental in origin, the Chak Jabbi Limestone in a calm marine rock indicating the extension of an arm of the Tethys in the Kala Chitta area when the Salt Range area was exposed.

ENVIRONMENTAL INTERPRETATION

The Chak Jabbi Limestone has been deposited in low energy environment with slow sedimentation in inner shelf environments. However, the lagoonal conditions with hypersaline water also give rise to such depositional pattern. The absence or scarcity of organisms indicates variable salinity conditions creating stress environments for the organisms.

The Chak Jabbi Limestone has been subjected to post depositional diagenesis resulting in the dolomitization. Sheikh (1992) recognized an outer and an inner zone of dolomite crystal through cathodoluminsence petographic study, from samples at Bagh. Fresh water-marine water mixing zone dolomitization model has been interpreted to be the most suitable for the dolomitized beds in the Chak Jabbi Limestone.

CONCLUSIONS

Three microfacies namely, mudstone to wackestone, mudstone and dolomitized mudstone have been identified in the Chak Jabbi Limestone.

The Chak Jabbi Limestone represents a shallow shelf carbonate deposition.

The Chak Jabbi Limestone is essentially medium bedded lithographic limestone deposited in low energy environment of inner shelf zone and barren of fauna. The paucity of fauna reflects the hypersaline conditions responsible for creating unfavorable conditions for the existence of biota.

The Chak Jabbi Limestone has been partly dolomitized and fresh water-marine water mixing zone dolomitization model seems to be the most appropriate interpretation.

REFERENCES

Balme, B.E. 1970 Palynology of Permian and Triassic Strata in the Salt Range and Surghar Range, West Pakistan: In: Stratigraphic Boundary Problem: Permian and Triassic of West Pakistan (ed. B. Kummel and C. Teichert) Univ. Kansas, Geol. Dept. Spec. Publ. 4. 305-454.

Cotter, G. D.P. 1933 The Geology of the part of the Attock Dist., West of L. 72^0 45'E *Geol. Surv. India. Mem.* **55,** 63-161.

Fatmi, A. N. 1973 Lithostratigraphic units of Kohat-Potwar Province, Indus Basin, Pakistan, *Geol. Surv. Pakistan Mem.* **10,** 80 p.

Flugel, E. 1982 Microfacies analysis of carbonate rocks. Springer-Verlage. 1-633.

Folk, R.L. 1959 Practical petrographic classification of limestones. *Amer. Ass. Pet. Geol. Bull.* **43,** 1-38.

Logan, B.W. and Semeniuk, V. 1976 Dynamic metamorphic processes and products in De-Vonian carbonate rocks, Cannig Basin, Western Australia. Spec. Publ. *Geol. Soc.Aus.***16**, 1-138.

Masood, K. R., Qureshi, K.A., Sabri, S. N., Hussain, Z. and Iqbal, M. J. 1992 Stratigraphically significant miospores in the tredian Formation (Triassic) at Nammal Gorge, western Salt Range, *Pakistan, Kashmir Jour. Geol.* **10,** 181-192.

Sheikh, R. 1992 Deposition and diagenesis of Mesozoic Rocks, Kala Chitta Range, Northern Pakistan. Ph.D. thesis. Imperial College, London.

Wilson, J. L. 1975 Carbonate Facies in Geologic History. Springer-Verlage. New York, 472.

Geol. Bull. Punjab Univ. 38, 2003.

TECTONIC STUDY OF LESSER AND SUB-HIMALAYA'S IN MANSEHRA AND ITS ADJOINING AREAS IN NORTHERN PAKISTAN BASED ON GEOPHYSICAL TECHNIQUES

BY

M. RUSTAM KHAN

Institute of Geology, University of Azad Jammu and Kashmir Muzaffarabad, Pakistan.

UMAR FAROOQ

Institute of Geology, University of the Punjab, Lahore-54590, Pakistan.

MUHAMMAD ZAHID AYUB AND ASGHAR ALI

Institute of Geology, University of Azad Jammu and Kashmir Muzaffarabad, Pakistan.

Abstract: *The geophysical study has been carried out in Mansehra and its adjoining areas of northern Pakistan to delineates the thickness of the crust and subsurface active and inactive nature of structural elements. The geological model computed by geophysical experiments demonstrated that in study area the crystalline crust of Indian Plate underthrusted beneath the Lesser and Sub-Himalayas from Mansehra to Muzaffarabad and dips towards northeast at an angle of 6°. The study based on geologic gravity magnetic and seismicity data envisage that Himalayan mountain belt formed by the stacking of different thrust sheets. These thrust sheets consist of crystalline rocks and meta sediments of Precambrian age and sedimentary rocks of Mesozoic to Cenozoic age. The model demonstrated that thrust sheets on the crystalline crust of Indian plate moves southward by the development of thrust faults and strike-slip faults. The continental collision and northward underthrusting of Indian crystalline crust are responsible for the formation of these faults. The model depicted left lateral strike-slip Jhelum fault (JF) near Muzaffarabad which is trending in NW-SE and dips 79° SW. The seismicity slickensides, offset and course sedimentary braccia between Balakot and Muzaffarabad suggested that JF is tectonically active. This study also suggested that Main Boundary Thrust (MBT) does not extend from Rara (Muzaffarabad) to Balakot. In the southwestern part of the study area PT brings the Tanol Formation of Cambrian age over the Hazara slates of Precambrian age. The model depicted the PT near Ghari Habibullah Bridge. The fault plane of PT is steeper near the surface and become gentle in depth and joins the low angle detachment. This study also suggested that Sandogali fault which is depicted in west of Abbotabad is actually the SW ward extension of PT. On the basis of geophysical experiment it is envisaged that PT is tectonically inactive between Sandogali and Balakot. Like MBT and Nathiagali Fault (NT), JF cuts the PT in the north of Balakot. The model computed 52 Km thick Indian plate (crust) under the Mansehara and 55 Km under Muzaffarabad. The thickness of crust increases towards northeast due to the bending of Indian crystalline crust and stacking of different thrust sheets. The seismicity folding faulting and landsliding along the boundary between Lesser and Sub-Himalays indicates that MBT is tectonically active. This study also indicates a thin sedimentary layer in Brarkot area.*

INTRODUCTION

The Himalayan mountain belt is composed of a series of en-echelon mountain ranges. These mountain ranges form sharp syntaxial bends near its eastern and western extremities in Indian plate, Fig.1. The Himalayas have formed along the northern margin of the Indian plate. The collision between Indian and Asian plate is an example of continental to continental collision which followed the closing of the Tathys Ocean and formed the vast mountain range. The spectacular elevation of the Himalayas are the geological expression of the collision, which is responsible for the tectonic activity that is continuing at the present time. Ganssar (1964) subdivided the Himalayas into Sub-Himalayas, Lesser Himalayas and Higher Himalayas. On the other hand in northern Pakistan the Himalayas are tectonically active and complicated as compared to India Himalayas. The structural elements of the study area are still not demarcated on the basis of geophysical experiments. In present geophysical study the attention is focused in Lesser and Sub-Himalayas of northern Pakistan to delineate the active and inactive structural elements of the area.

TECTONIC SETTING

In northern India a belt of ophiolites, the Indus Suture Zone is the apparent boundary between the Indian and Asian plate (Ganssar, 1964). However, in northern Pakistan, the westward extension of the Indus Suture Zone is bifurcated into MMT and MKT and surrounded a sequence of rocks, the Kohistan-arc terrain, Fig. 2 which has been interpreted as a wedge of Island arc. The MMT, southern suture zone, separates the arc terrian from the Indian plate and the MKT the northern suture zone separates the arc terrain from the Asian plate. The Island arc terrian is composed of a sequence of high density rocks, while the rocks of the Indian and Asian plates are typically of lower density (Desio, 1979; Tahirkheli, 1982, 1984). After suturing, the continued convergence of the Indian and Asian plate has been accommodated by crustal shortening along the different thrusts, with an apparent progression of the thrusts from north to south (Le Fort, 1975). These faults are the Main Central Thrust (MCT), PT, Nathiagali thrust (NT) and MBT. The location of the PT in the western limb of HKS and JF are not demarcated on the basis of geophysical data. The PT, MBT and MCT curve around the apex of HKS. In eastern limb of Hazara-Kashmir Syntaxis (HKS), PT runs parallel to MBT whereas in western limb MBT follows an oblique course, Fig. 3. In this area the gap between MBT and PT is wider as compare to its eastern counter part. Greco (1991) suggested that Mansehra Thrust (MT) separates from MBT about 6 Km south of Balakot and continue southward under alluvium upto Ghari Habibiullah. In this area MT is not exposed on the surface. Ghazanfar et al (1991) demarcated the Abbotabad Thrust in the west of Abbottabad between Hazara slats of Precambrian age and Tanol Formation of Cambrian age. The position of JF, PT and MCT in the northwestern Himalayas of Pakistan are not clearly demarcated because the area is highly affected by Nanga Parbat Syntaxis and HKS. Several geological models have been proposed by Wadia (1931), Coward et al (1987) and Treloar and Coward (1991) to explain the tectonic evolution. All these efforts are based on geological data and need to be constrained by geophysical data. The project was formulated to have a geophysical study in the area bounded between latitude 33°30′ to 34°12′ N and longitude 70°30′ to 73°27′ east. The geological and magnetic survey has been carried out in the study area to delineates the PT, JF and their associated structural elements. The gravity data of Rustam (1994) and seismological data of Baluch and Ali (1998) also used to constrain the geological model.

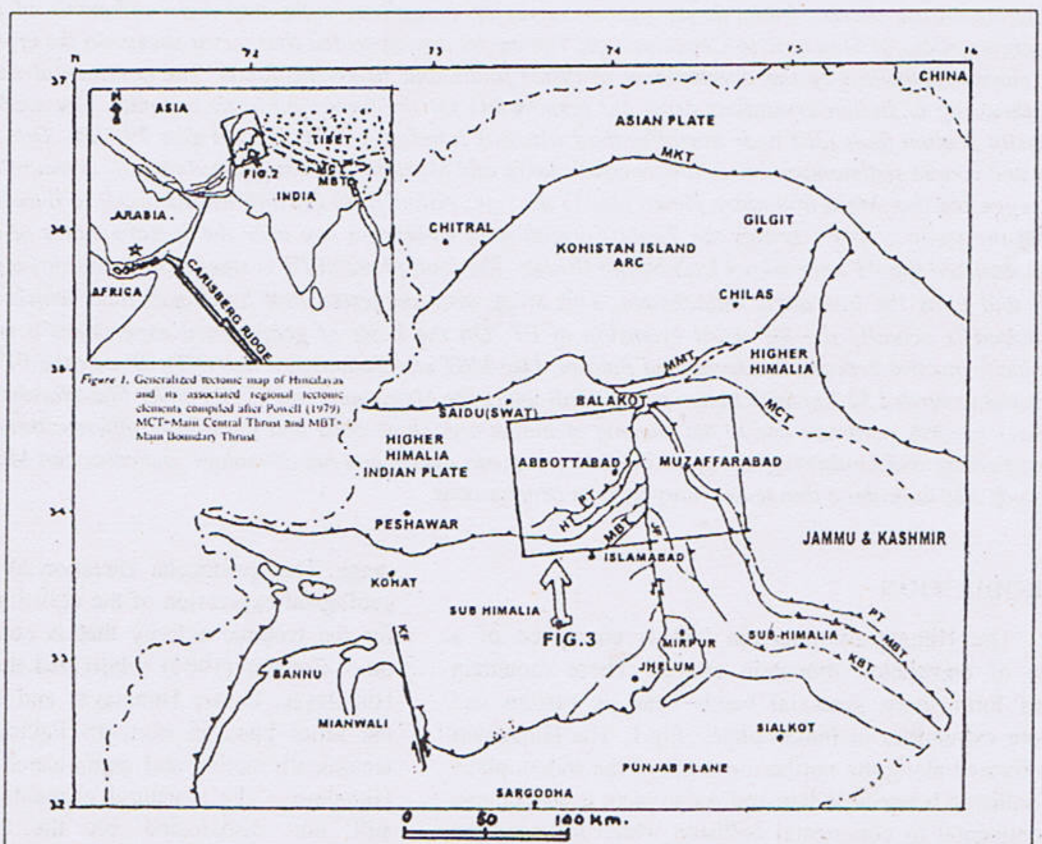

Fig 2. Tectonic map of northern Pakistan. MKT=Main Karakuram Thrust, MMT=Main Mantle Thrust, MCT=Main Central Thrust, PT=Panjal Thrust, MBT=Main Boundary Thrust, NT=Nathiagali Thrust, JF=Jhelum Fault and KF=Kalabagh Fault, compiled after Kazmi and Rana (1982) and Rustam (1994).

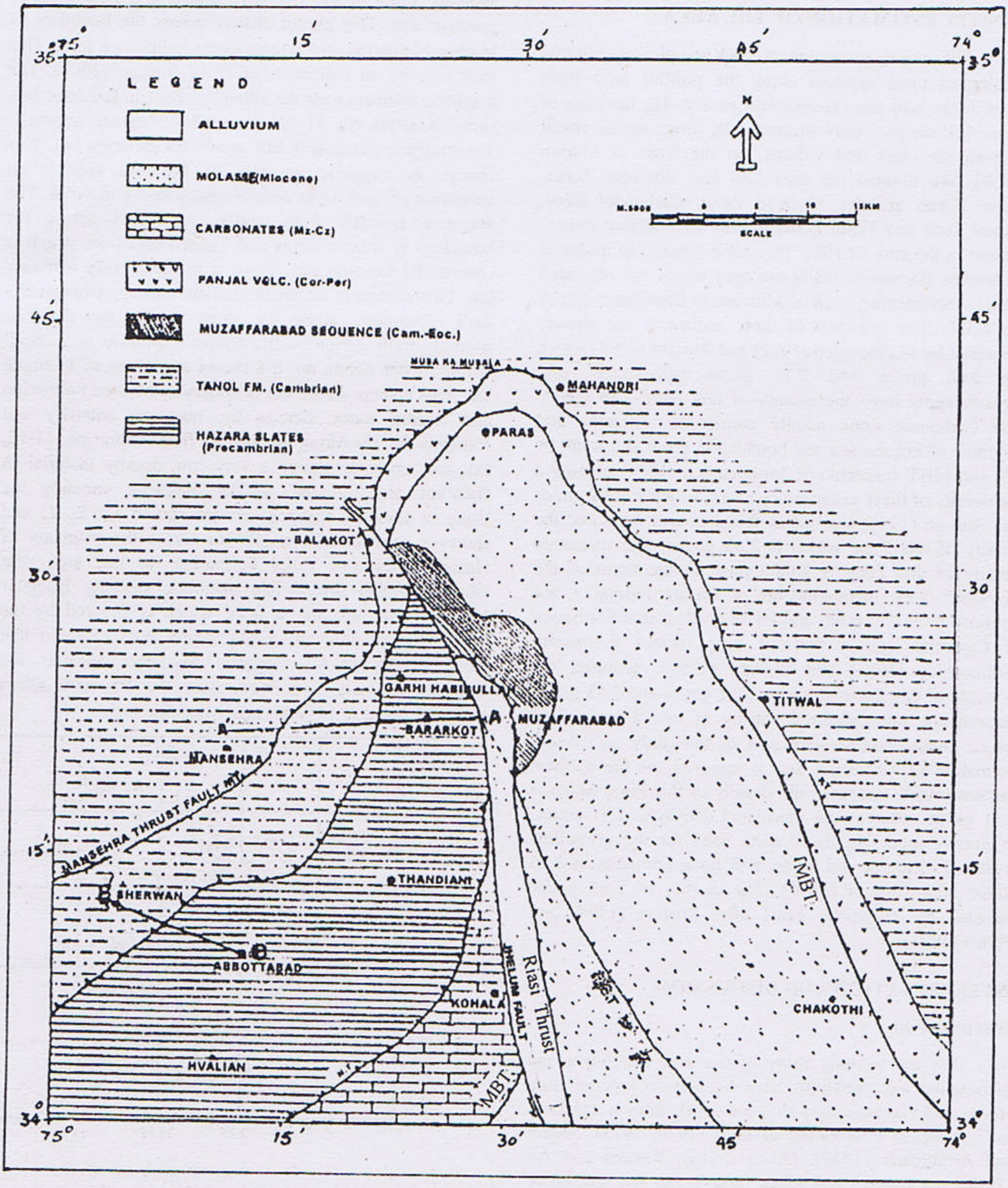

Fig 3. Tectonic map of the Hazara-Kashmir Syntaxis. MCT=Main Central Thrust, PT=Panjal Thrust, MBT=Main Boundary Thrust, KBT=Kashmir Boundary Thrust, NT=Nathiagali Thrust, MT=Mansehra Thrust, JF=Jhelum Fault, compiled after Latif (1970), Calkins et al. (1975), Kazmi and Rana (1982), Rustam and Ali (2001) and Greco (1989).

DENSITY ESTIMATION OF THE AREA

For density measurement, rock samples of different lithological units exposed along the profiles have been taken during and after geophysical survey. The densities of these rock samples were measured by direct measurement of both the mass and volume, on the basis of Marton (1959). We divided the area into four different Zones. These Zones are the Molasse Zone, Carbonate Zone, Hazara Zone and Tanol Zone, Fig. 3. The molasse zone is present in the core of HKS This zone consists of molasses of Murree Formation (Miocene age) which are separated from the sedimentary rock of Miocene to Cretaceous age by the MBT. The densities of these sediments are already measured by Malinconico (1982) and Rustam (1994) which are 2.64 gm/cc and 2.55 gm/cc respectively, our measurements show the density of this Zone 2.56 gm/cc. The Carbonate Zone mainly consist of limestone and dolomite of Eocene age and bounded in north and south by NT and MBT respectively. Molincunico (1982) measured the density of these sedimentary rocks, which is 2.69 gm/cc and Rustam (1994) worked in this area and measured the density of this Zone which is 2.68 gm/cc. Our measured density of this Zone is 2.68 gm/cc. In the north of the Carbonate zone metasediments of Hazara Formation are bounded by NT in south and PT in north. Tanol Formation of Cambrian age is thrusted over Hazara Formation. Molinconico (1982) and Rustam (1994) measured the densities of this Zone which are 2.53 gm/cc and 2.53 gm/cc respectively, our measured density of this Zone is 2.54 gm/cc. In the northwestern part of the study area Tanol Formation of Cambrian age is exposed on the surface. Rustam (1994) measured the density of this Zone which is 2.41 gm/cc, whereas our calculated density is 2.51 gm/cc. In gravity modeling the density used for the crystalline crust is 3.25 gm/cc and for the Salt Rang Formation is 2.25 gm/cc after Rustam (1994). The density of 2.95 gm/cc assigned for crystalline crust after Rustam (1994) and Verma (1991).

INTERPRETATION AND DISCUSSION

Interpretation

For the tectonic study of the area qualitative and quantitative interpretations have been done incorporating gravity and magnetic data with previously known structural and geological information of Latif (1970, 1973), Seeber and Armbruster (1979), Greco (1989), Rustam and Ali (1994) and Rustam and Khan (2001). For the qualitative study of the area total magnetic anomaly and Bougour anomaly profile (A-A′) selected from Muzaffarabad to Mansehra acrosses the different geological units, Fig. 5. Along this profile the magnetic anomaly across station no. 0-5 shows a gradient of 1 gamma/ km but the magnetic anomaly from station no. 6-10 shows a gradient of 30 gammas/ km. This abrupt change across the boundary of Murree Formation and Hazara slates indicates a fault. This fault may be an indication of JF of Rustam (2001). The magnetic anomaly over the alluvium cover in Bararkot area between station No. 11-12 shows a low magnetic anomaly. The magnetic gradient in this area is 20 gammas/ km. This change in magnetic anomaly in Bararkot area is an indication of thick layer of low susceptibility material. The magnetic anomaly from station no. 18-21 across the boundary of Hazara slates and Tanol Formation, which is covered by the alluvium, shows a gradient of 29 gammas/ km. This change in magnetic gradient clearly demarcated a fault. Therefore, along the same profile the Bougour anomaly from station no-0-5 shows a gradient of 2 mgal/ km and from station no. 6-8 shows a gradient of 15 mgal/ km. This change across the boundary of Murree Formation and Hazara slates dictates the magnetic anomaly and confirms the JF. Along this profile from station no. 11-12, Bougour anomaly shows a very low density material in Bararkot area. Similar to the magnetic anomaly the Bougour anomaly changed between station No. 20-21 and shows a gradient of 3 mgal/ km across the boundary of Hazara slates and Tanol Formation. In this area near Gharihabibullah bridge like magnetic anomaly Bougour anomaly also indicates a fault, which is covered by the thick layer of alluvium. Conclusively it is gathered that along profile (A-A′) magnetic anomaly conforms the Bouguer anomaly and demarcated the PT near Ghari Habibullah and JF in Gojra near Muzaffarabad.

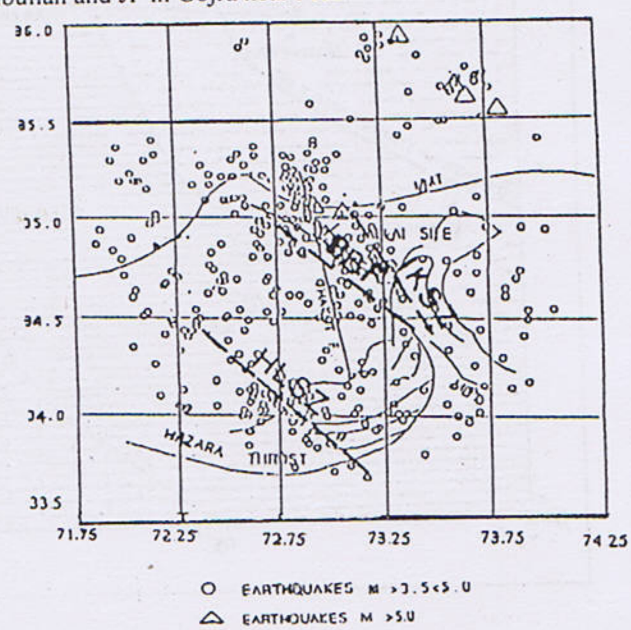

Fig 4. Seismo-tectonic map of northern Pakistan. IKSZ=Indus Kohistan Seismic Zone, BBF=Bagh Basement Fault, HLSZ=Hazara Lower Seismic Zone after Baluch and Ali (1998).

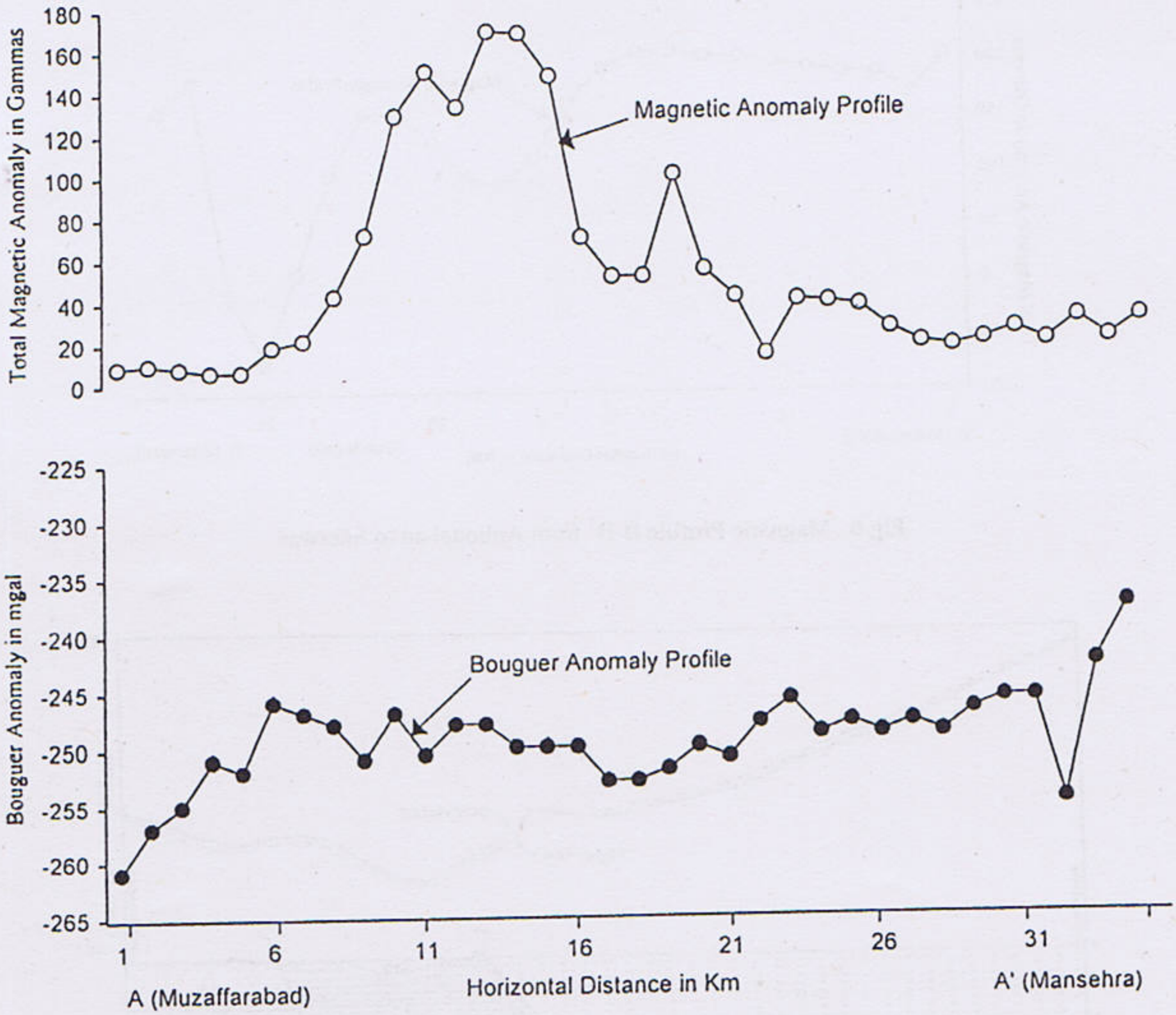

Fig 5. Gravity and Magnatic Profule A-A′ form Muzaffarabad to Mansehra.

The total magnetic anomaly profile B-B′ selected from Abbottabad to Sherwan across the different geological structures, Fig. 6. The magnetic anomaly from station no. 1-11 shows a gentle gradient across the Hazara slates. The magnetic anomaly from station No. 18-21 shows a gradient of 22.6 gammas/ km. This abrupt change in magnetic anomaly in Sundogali across the boundary of different lathological units which are Hazara Slates and Tanol Formation demarcated a fault. This fault may be an extension of PT of Wadia (1931). In Sundogali on surface PT dips 20° W and trends in NE-SW. In the west of Sundogali along the fault plane the carbonaceous material is also exposed on the surface.

For the quantitative study the gravity modelling have been carried out by applying the techniques of Talwani et al. (1959) using the gravity data of Rustam (1994) and software of Malinconico (1986). The profile A′-A is selected which crosses the major tectonic elements i.e. the PT and JF as shown in, Fig. 7. This model is the outcome of several attempts, which are made to have a best compromise among geology, observed gravity and the calculated gravity. This model shows that along the PT comparatively low density metasediments of Tanol Formation (Cambrian age) are thrusted over high density, Hazara Slates (Precambrian age). This fault lies just north of Garhi Habibullah and shows a dip of 65° NW. The density contrast across the PT is 0.04 gm/cc. The JF in Gojra near Muzaffarabad shows a dip of 79° SW and brings in contact the metasedimentary rocks (Hazara Slates) of low density with the post collisional molasses sediment of high density. The estimated density contrast across the JF is 0.03 gm/cc. This model also shows that sedimentary/metasedimentary wedge in the southwestern part near Mansehra is 14 km thick whereas in the northeastern part near Muzaffarabad the thickness is 17 km. The estimated thickness of crystalline crust of Indian plate is 38 km and extended throughout the study area. The geological model derived from the combination of sediments, transitional crust and juxtaposition of Moho is

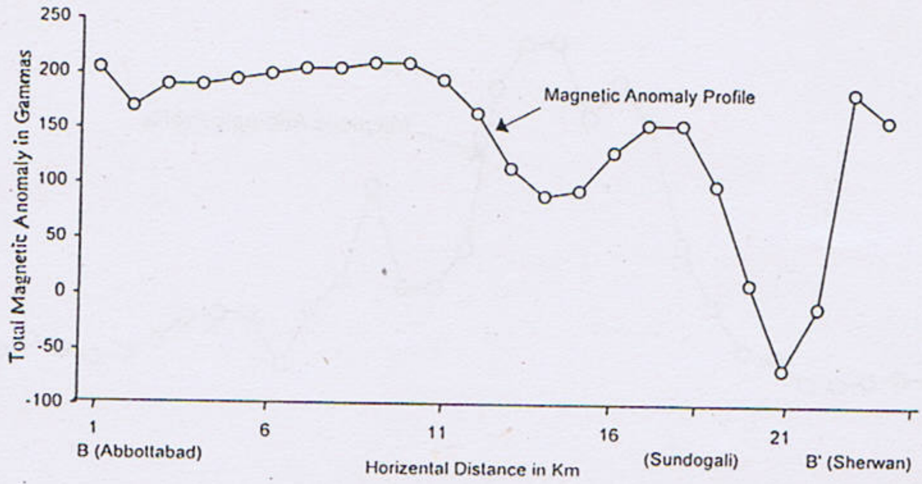

Fig 6. Magnatic Profule B-B´ form Abbottabad to Sherwan.

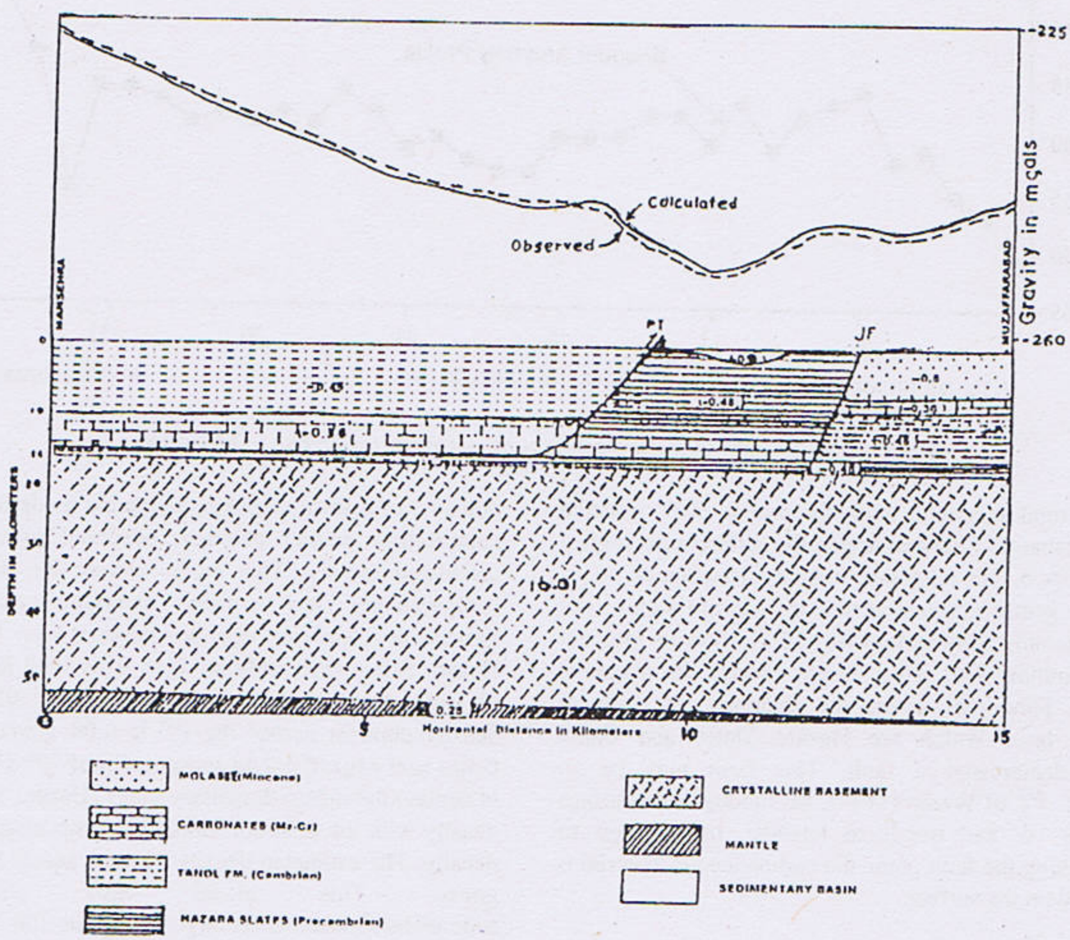

Fig 7. Gravity model shows the combined sediments and Moho effects along the profile A-A´ from Muzaffarabad to Mansehra.

shown in, Fig. 7. The calculated gravity of this model dictates reasonably the observed gravity effect. A sequence of gravity low and high near new Ghari Habibullah Bridge, Bararkot and Gojra Muzaffarabad are the indication of PT, thin layer of sediments (0.5 Km) and JF respectively. This modeling demarcated the PT of Wadia (1931) near Ghari Habibullah Bridge, where Tanol Formation of Cambrian age are thrusted over the Hazara Slates of Precambrian age. The PT dips 65° NW and penetrated upto the depth of 14 Km. In Gojra near Muzaffarabad the JF dips 79° SW and brought the Hazara Slates in contact with Murree Formation of Miocene age. This fault penetrated upto the depth of 16 Km. This model also indicates 52 Km thick crust under the Mansehra and 55 Km under the Muzaffarabad area due to the presence of thick sedimentary/ metasedimentary wedge. The model also suggested that Moho dips at an angle of 6° NE between Mansehra and Muzaffarabad under the crust and these estimates agree reasonably with gravity modelling of Rustam and Ali (1994). Conclusively this study indicates that PT and JF are thin-skined faults. The fault plane of PT appear to dip steeply near the surface and becomes gentle in depth. This study also shows that PT is a low angle fault in the southwestern part in Sundogali and angle of this fault is increasing towards (northeast) Ghari Habibullah. The model also computed 0.5 Km thick sedimentary layer in Brarkot area. The seismotectonic map of the area, Fig. 4 after Baluch and Ali (1989) indicates that PT is tectonically inactive. The Hazara Lower Seismic Zone (HLSZ) and Indus Kohistan Seismic Zone (IKSZ) of Seeber and Armbruster (1979) and Rustam (1994), are seismically active. The Bagh Basement Fault (BBF) of Rustam (1994), MBT and JF are also tectonically active.

DISCUSSION

Rustam (1994) interpreted gravity data and suggested that in HKS between Fatejang and Kundal Shahi gravity gradient changes from –1.0 mgal/ km in the southwest (Fatehjang) to –0.04 mgal/ km in the central part between Taxila and Abbottabad and –2.0 mgal/ km further northeast upto Kundal Shahi. He suggested that Moho dips 4.75° NE between Fatehjang and Kundal Shahi. The present geological model based on gravity data suggests that between Mansehra and Muzaffarabad the gravity gradient is -2.0 mgal/ km and Moho dips 6° NE. Greco (1991) marked the PT in western limb of HKS. Trealor et al. (1989) used the name Mansehra Thrust for another fault which is running near Mansehra with in the Tanol Formation. This fault is trending in the NE-SW and dips in the NW direction. Ghazanfar et al. (1987) marked the Abbottabad Thrust between Hazara Slates of Precambrian age and Tanol Formation of Cambrian age. The present study based on gravity and magnetic data disagree with Greco (1991), Chaudhry and Ghanzanfar (1992) suggested that PT is different from Mansehra Thrust. The present study indicates that Abbotabad Thrust is actually the southward extension of the PT. The PT is depicted near Ghari Habibullah bridge between Tanol Formation and Hazara Slates. This fault is thin skinned fault which is steeper near the surface and become gentle in depth and dips nearly 65° NW and trends in the NE-SW direction between Ghari Habibullah and Sundogali. The magnetic profile (B-B′) from Abbottabad to Sundogali delineated the PT near Sundogali between Tanol Formation of Cambrian age and Hazara Slates of Precambrian age. This study suggested that Abbottabad thrust of Ghazanfar is actually the southward extension of PT of Wadia (1931) which is depicted by gravity and magnetic data near Ghari Habibullah bridge. In the south of study area this fault trends NE-SW and may be join the Khairabad Fault of Yeats and Hussain (1987). The present study also suggested that nearly 0.5 Km thick sedimentary layer is present in Bararkot area. In the northeastern part of study area near Muzaffarabad the qualitative and quantitative study indicates a thin-skined JF between Hazara Slates and Murree Formation trending in the NE-SW and dips 79°NW. In the southwest of Muzaffarabad the MBT separates the Lesser Himalayan pre-collisional sediments from the post collisional molasses sediments in the south throughout along the belt, Fig. 3. In eastern limb of HKS, MBT and PT are less deformed as compared to western limb. The PT and MBT curve around the apex of HKS and then bend southward, Fig. 3. Lawrence and Baig (1987) suggested that a separate left-lateral strike-slip fault truncates the MBT in north of Balakot. Rustam (1994) suggested that JF is a strike slip fault which cuts the MBT and NT near the apex of HKS and the western limb of HKS moves southward along this fault. He also demarcated JF fault 3 Km south of Muzaffarabad which is dipping 80° NW. In present study, the fault depicted in Gojra near Muzaffarabad between Hazara slates and Murree Formation is the northward extension of JF of Rustam (1994). Along this fault the seismicity, folding, faulting, slikenside, offset, course sedimetary braccia and faulted contact of Hazara slates of Precambrian age with Muree Formation of Miocene age conform that JF is an active left lateral strikes-slip fault The thickness of the sedimentary/ metasedimentary wedge is increasing towards north-northeast by the stacking of different thrust sheets. After collision in Oligocene, the Indian shield has been overridden by the slices of its northern margin. These slices have been stacked by a series of south verging thrusts. Which are generally increased in age and grade towards north- northeast. The seismicity indicates that MBT, JF, HLSZ, IKSZ and BBF are tectonically active whereas PT is tectonically inactive, Fig. 3.

CONCLUSION

The Panjal Thrust (PT) depicted between Hazara Slates of Precambrian age and Tanol Formation of

Cambrian age near Ghari Habibullah bridge. In this are PT trends in the N-S direction and dips at an angle of 65°NW. This fault is now tectonically inactive. In west of Ghari Habibullah PT trends in the NE-SW and depicted in Sundogali between Hazara Slates of Precambrian age and Tanol Formation of Cambrian age. In this area PT dips at an angle of 20° W. The angle of this fault increases towards northeast. The fault depicted in Gojra near Muzaffarabad between Murree Formation of Miocene age and Hazara Slates of Precambrian age is southward extension of left lateral strike-ship Jhelum fault (JF). The crystalline crust of Indian Plate between Mansehra and Muzaffarabad dips at an angle of 6°NE. The HLSZ, IKSZ, BBF, JF and MBT are seismically active whereas the PT is seismically inactive.

REFERENCES

Baluch, S.Q. and Ali, M.I., 1998. Seismic risk assessment of Hydropower projects with reference to the tectonic structure of northern Pakistan. *13th Himalaya-Karakoram-Tibet Int. Workshop, Geol. Bull. Uni. Peshawar, Pakistan,* **31,** 29-32.

Calkins, J.A., Offield, T.W., Abdullah, S.K.M., and Ali, S.T. 1975. Geology of the southern Himalayan in Hazara Pakistan and adjacent area. *U. S. Geol. Surv.*, **716-C,** 29p.

Chaudhry, M. N., and Ghazanfar, M., 1992. Some tectono stratigraphic observations on NW Himalaya, Pakistan. *Pakistan J. Geol.*, **2, 1,** 1-14.

Coward, M. P., Butler, R. W. H., Khan, M. A. and Knipe, R. J., 1987. The Tectonic History of Khoistan and its Implication for Himalayan Structure J. *Geol. Soc. Lond.*, **144,** 377-391.

Desio, A., 1979. Geologic evolution of the Karakorum. *In Geodynamics of Pakistan edited by Farah, A., and Dejong, K. A., G. S. P.*, 131-142.

Gansser, A., 1964. The division of Himalayas and Karakoram. *Geol. Bull. Univ.* Peshawar, **13,** 9-22.

Ghazanfar, M., Chaudhry, M.N. and Latif, M.A. 1987. Three stratigraphic provinces of Hazara-Kashmir Syntaxis, Pakistan, *Kashmir, J. Geol.* 5, 65-74.

Greco, A., 1991. Stratigraphy, metamorphism and tectonic of the Hazara Kashmir Syntaxis area, *Kashmir J. Geol.*, **8 & 9,** 39-65.

Kazmi, A. H., and Rana, R.A. 1982. Tectonic map of Pakistan. *Geol. Surv. Pakistan Quetta.*

Latif, M. A., 1970. Explanatory notes on the geology of south-eastern Hazara to accompany the revised geological map. *J. Geol. B.A. Sonderbon*, **15,** 5-20.

Latif, M.A., 1973. Partial extension of the evaporite facies of the Salt Range to Hazara Pakistan. Nature, 244, 14-125.

Lawrence, R. D., and Baig, M. S. 1987. Precambrian Early Paleozoic Orogenesisiz in Himalaya. *Kashmir J. Geol.*, **5,** 1-22.

Le Fort, P., 1975. The collided range present knowledge of the continental arc. *Am. J. Sci.*, 275, 1-44.

Malinconico L. L. Jr., 1986. The structure of Kohistan-Arc terrain in northern Pakistan as inferred from gravity data. *Tectonophysics*, **124,** 297-300.

Malinconico, L. L. Jr., 1986. An interactive modelling programme. Environmental simulations laboratory southern Illinois University, Corbondale, IL 62901.

Powell, C. McA., 1979. A speculative tectonic history of Pakistan and surroundings. In Geodynamics of Pakistan. Farah, A., DeJong, K. A., Ed., *Geol. Surv. Pakistan.*

Rustam, M. K. and Khan M. S., 2001. Study of Shallow Geological Structures in the Core of HKS based on residual gravity data, *4th Pakisan Geol. Conf., Islamabad*, 4.

Rustam, M. K. and Ali, M., 1994. Preliminary Gravity Model of western Himalayas in northern Pakistan. *Kashmir J. Geol.*, **11 & 12,** 59-65.

Seeber, L., and Armbruster, J., 1979. Seismicity of the Hazara Arc in northern Pakistan decollement vs. basement faulting. In: Geodynamics of Pakistan. Farah, A., and DeJong, K.A. eds., *Geol. Surv. Pakistan*, 131-142.

Talwani, M. Worzel, J. L. and Landisman, M., 1959. Rapid gravity computations of two dimensional bodies with application to the Mendocino submarine fracture zone; *J., Geophy. Res.*, **64,** 49-59.

Tahirkheli, R. A. K., 1982. Geology of the Himalaya, Karakoram and Hindukush in Pakistan. *Geol. Bull. Uni. Peshawar*, **15,** 1-50.

Tahirkheli, R. A. K., 1984. Recent Addition of Geotectonic net of Northern Pakistan Keynote, Address In: *First Geol. Cong. Lahore*.

Treloar, P. J., Broughlon, R. D., Williams, M. P., Coward, M.P. and Windley, B.F., 1989. Deformation metamorphism and imbrication of the Indian plates south of the Main Mental Thrust, north Pakistan. *J. Met. Geol.*, **7,** 111-125.

Treloar, P. J., and Coward, M. P., 1991. Indian plate motion and shape constraints on the geometry of the Himalayan orogen *tectonophysics*, 191, 189-90.

Verma, R. K., 1991. Gravity field and nature of continent-continent collision along the Himalaya. In: Geology and geodynamic evolution of the Himalayan collision zone. Part 2, Sharma, K.K., Ed: *Phys. Chem. Earth*, **18,** 385-403.

Wadia, D. N., 1931. The syntaxis of the northwest Himalaya its rocks, tectonics and orogeny Rec. *Geol. Surv. India*, 65, 189-220.

Yeats, R. S., and Hussain, A., 1987. Timing of structural events in Himalayan foothills of Northwestern Pakistan, *Geol. Soc. Am. Bul.*, **99,** 161-176.

Geol. Bull. Punjab Univ. 38, 2003.

AGE DIAGNOSTIC MICROFAUNA FROM DUNGAN FORMATION, ZINDA PIR AREA, EASTERN SULAIMAN RANGE, PAKISTAN.

BY

NAZIR AHMAD AND SHAHID JAMIL SAMEENI
Institute of Geology, University of the Punjab, Lahore-54590, Pakistan.

Abstract:-*Dungan formation is 98 meter thick at Zinda Pir area, unconformably overlying on Pab Sandstone and conformably underlying by Ghazij shale. Dungan formation mainly consists of grey to brownish grey, dark grey to blackish limestone along with a few grey to green coloured sandy/silty/shaly calcareous layers. The Formation contains Late Paleocene fauna in it's lower half like Miscellanea miscella, Lockhartia haemei and in it's upper half lower Eocene fauna like Alveolinids, Nummulites mammilatus, Nummulites atacicus, Discocyclina dispensa, Assilina laminose & Assilina spinosa. So Paleocene–Eocene boundary on the basis of these age diagnostic fauna lies with in the Dungan formation at the thickness of 51 meters from its base.*

INTRODUCTION

The Sulaiman Range is located on the northwestern margin of Indian plate. It forms the middle part of the Indus basin, rocks exposed are from Triassic to Tertiary in age, this part of the Indus basin is known as Sulaiman sub-basin. The Kirthar Range lies in the south, Salt Range in the north and Punjab Plains in the east. On west the marginal zone of the Indian Plate against the Himalayan orogeny bound it.

Zinda Pir area under study is easily accessible from Dera Ghazi Khan, located in eastern Sulaiman Range (Fig-1), lies between lat. 30° 45′ N and long. 70° 50′ E. Paleogene carbonate rocks are the most significant hydrocarbon reservoirs in Pakistan, Dungan Formation is one of the important Paleogene carbonate rock amongst them, widely exposed in eastern Sulaiman Range.

In 1952 the discovery of giant gas fields at Sui in Sulaiman Range attracting the most commercial organizations. The earliest reference regarding the geology of the Sulaiman province are by Steward (1860), Verchere (1867), and Griesbach (1884), Blandford (1883),Oldham (1890) and La Touche (1893) did early reconnaissance work in the Sulaiman Range (as cited by Eames, 1952). Paleogeographic and stratigraphic studies were done on Cretaceous to Paleocene rocks of Sulaiman province by Davies (1939), Eames (1952) worked out the basic stratigrphy in Fort Munro and Zinda Pir area in the eastern Sulaiman Range. The Hunting Survey Corporation carried out major reconnaissance mapping using aerial photographs supplemented with field checks (Jones 1961). Shah (1977) renamed the stratigraphic units of the area according to the new stratigraphic nomenclature (accepted by the stratigraphic committee of Pakistan). Waheed, Wells and Ahmad (1988) carried out sedimentological and paleocurrent studies in northern part of Sulaiman Range. Ahmad (1987) and Malik et. al. (1988) discussed the petroleum potential and prospects of the Sulaiman fore deep.

Geological Survey of Pakistan, Hydrocarbon Development Institute of Pakistan, Oil & Gas Dev. Corporation of Pakistan, has done a great deal of work regarding the stratigraphy, paleontology and economic geology on Sulaiman Range. Although Davies (1941), Khan & Haque (in Lexique, 1956), Latif (1964) and Iqbal (1969) have done lot of work in the area but first time the detailed investigations about Dungan Formation, it's fauna and exact marking of Paleocene-Eocene boundary within the formation has been taken in detail.

The name "Dungan Limestone" was introduced by Oldham (1890) to replace the "Alveolina Limestone" of Griesbach (1881). It includes the "Lower Rakhi Gaj Shale", "Zinda Pir Shale" and "Zinda Pir Limestone (lower part)" of Eames (1952) and "Dungan Group" (excluding Moro Formation), "Dab Formation" and "Karkh Group" of Hunting Survey Corporation (1961). William (1959) refined the term as "Dungan Formation" and the name was approved by the stratigraphic committee of Pakistan (Shah,1977).

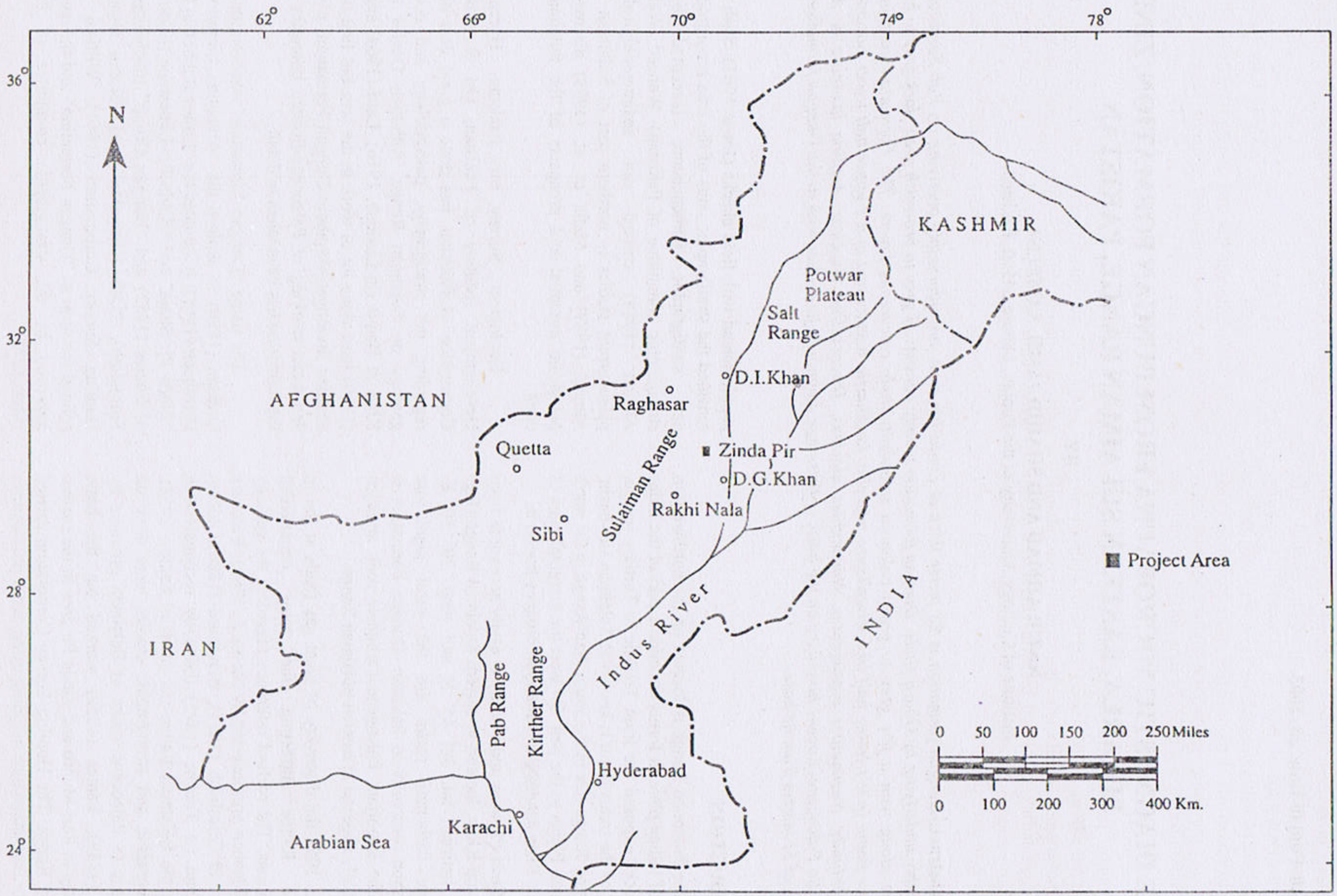

Fig. 1. Location map of the Project Area.

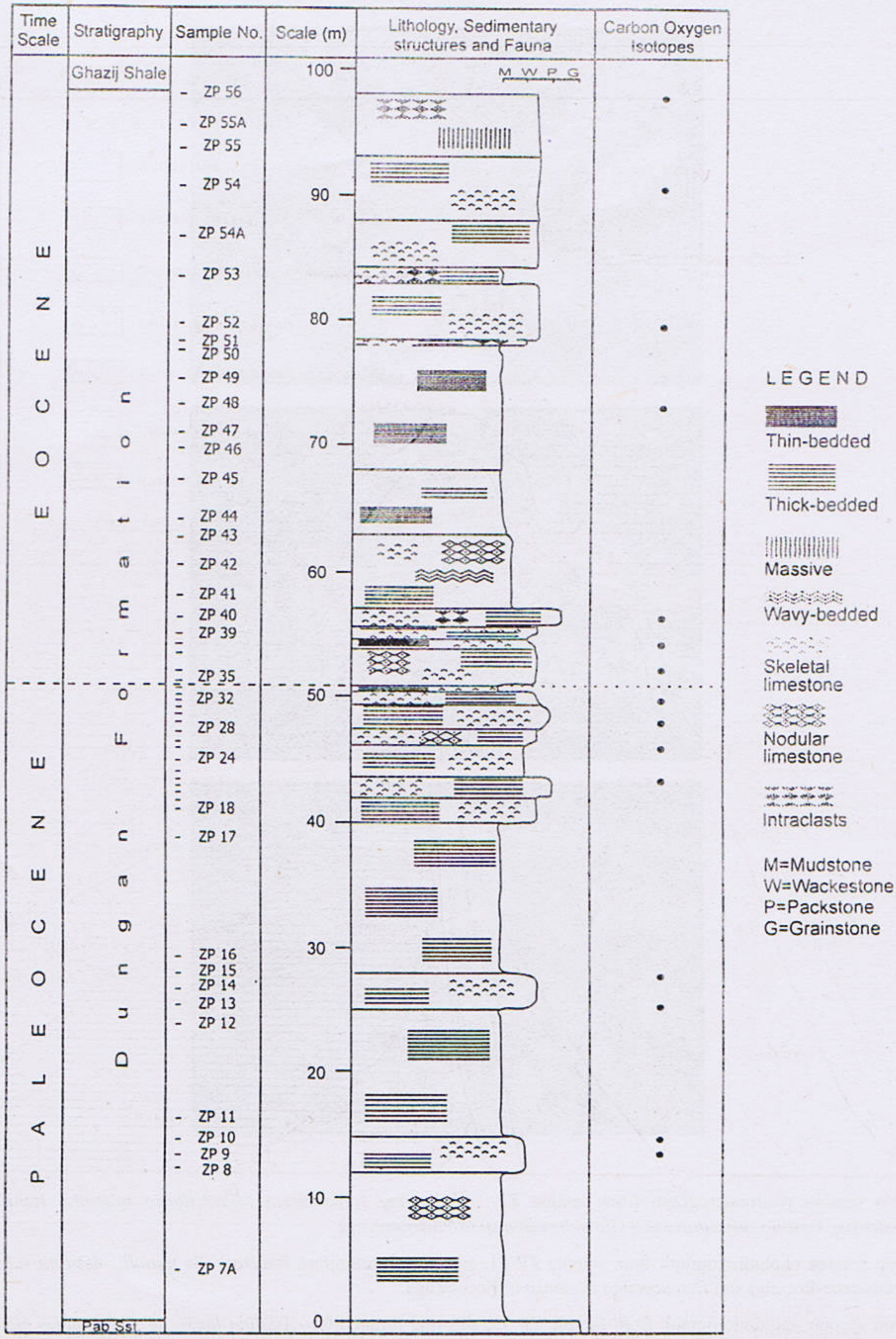

Fig. 2. Lithologic log of Zinda Pir section.

Plate -1

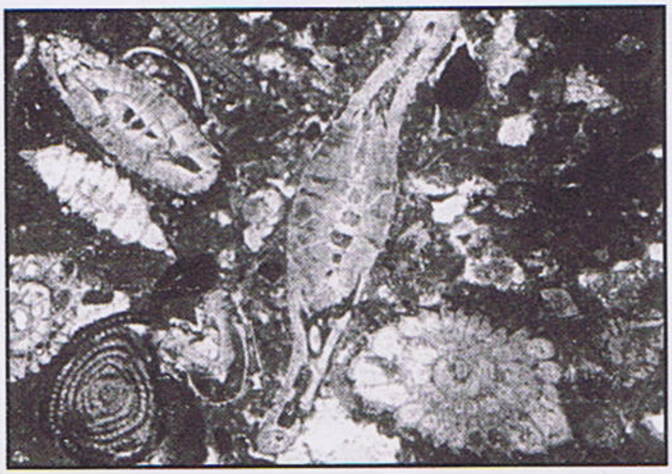

A

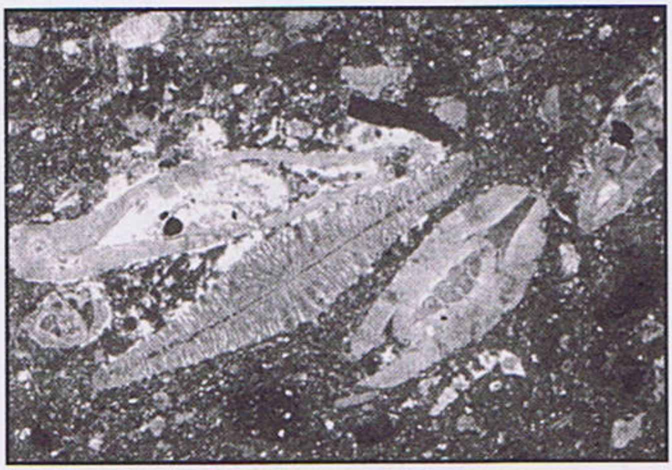

B

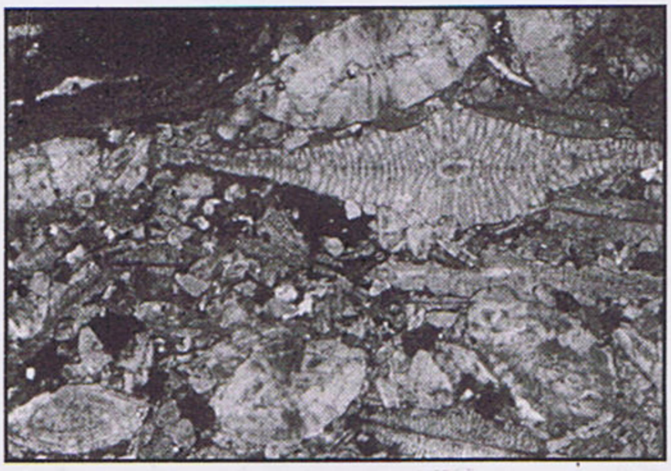

C

A: Thin section photomicrograph from sample ZP 15, showing foraminifera *Miascellanea miscella, Ranikothalia sindensis, Assilina subspinosa* and *Glomalveolina sp.* of Paleocene age.

B: Thin section photomicrograph from sample ZP 51, showing foraminifera *Ranikothalia nuttalli, Assilina subspinosa* (Paleocene-Eocene) and *Discocyclina dispensa* of Eocene age.

C: Thin section photomicrograph from sample ZP 35, showing foraminifera *Assilina laminose, Nummulites mamillatus* and *Discocyclina dispensa* of Eocene age.

Plate -2

A

B

C

A: Thin section photomicrograph from sample ZP 53, showing foraminifera *Ranikothalia sindensis* (Paleocene-Eocene) and *Nummulites mamillatus* of Eocene age.

B: Thin section photomicrograph from sample ZP 40, showing Eocene foraminifera *Nummulites atacicus.*

C: Thin section photomicrograph from sample ZP 38, showing Eocene foraminifera *Nummulites mamillatus*.

Plate -3

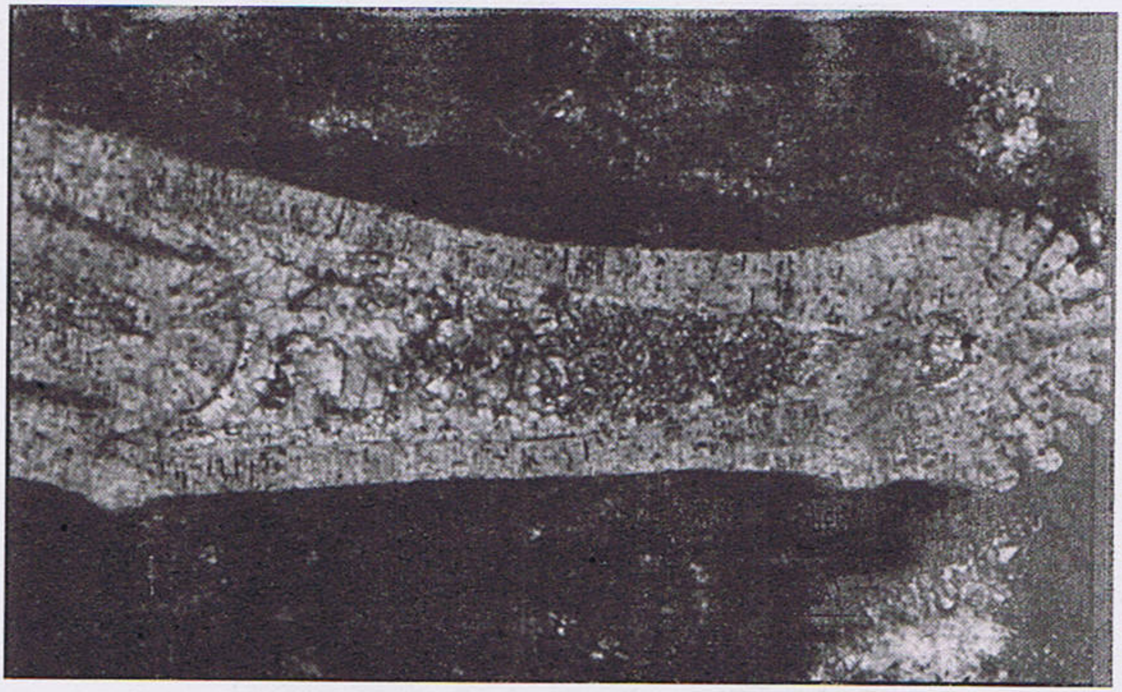
A

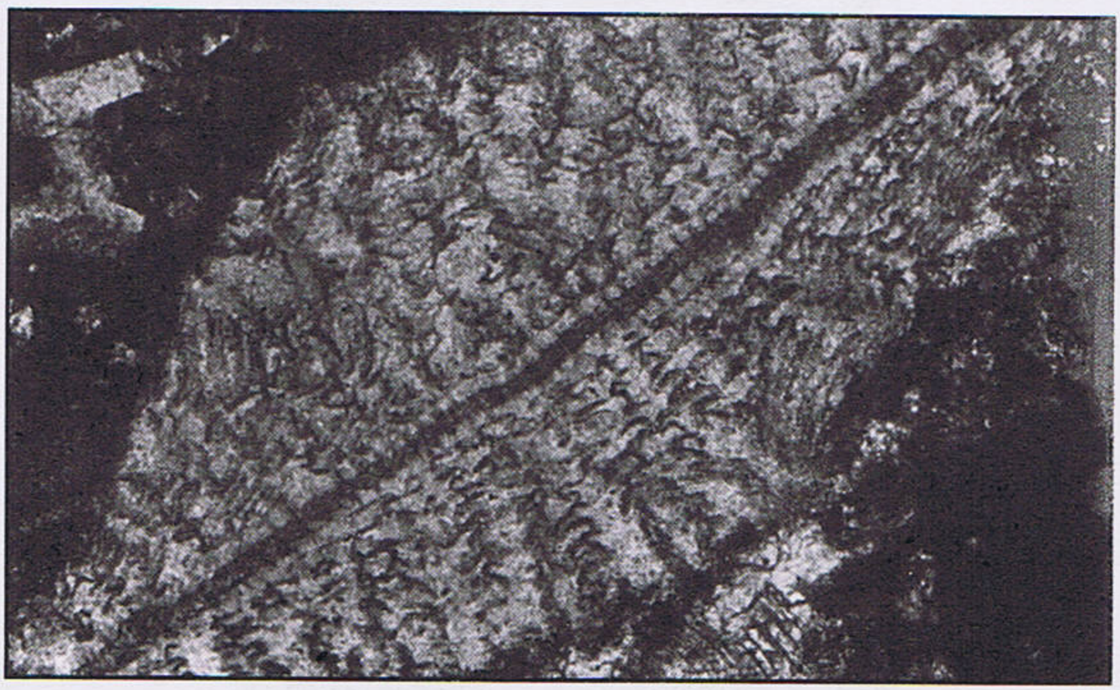
B

A: Thin section photomicrograph from sample ZP 25, showing Paleocene foraminifera *Ranikothalia sindensis* (fan-shape marginal cord).

B: Thin section photomicrograph from sample ZP 38, showing Eocene foraminifera *Discocyclina dispensa.*

MATERIAL AND METHOD

Dungan Formation at Zinda Pir area is 98 m thick, more than 56 samples were collected from bottom to top from every bed/strata/lamina.(Fig-2).The formation is mainly limestone with intercalation of shale. More than 40 thin sections were prepared for microfaunal studies from the hard limestone part of the formation where as lose specimens were also studied from the shaly part of the formation for the identification of foraminiferal species.

OBSERVATIONS

Dungan Formation mainly comprises of thick bedded, at some places thin bedded, nodular to massive limestone, dark to brown & creamy in colour with intercalations of shale, marl and sandstone. Limestone conglomerates are also present. The formation in its lower part consists of thick bedded. A little nodular thick bedded limestone with sufficient foraminifera with intercalations of shale and marl in its middle part. In it's upper half the limestone is again thick bedded to massive with intercalations of shale, sandstone and marl. At certain places the conglomerates of limestones are also present.

Detailed study of the thin sections showed the abundant presence of the following forams in its lower half up to 50 meters.

-Miscellanea miscella (d'ARCHAIC & HAIME)

-Lockhartia haimei (DAVIES)

-Lockhartia tipperi (DAVIES)

-Assilina subspinosa (DAVIES & PINFOLD)

-Discocyclina ranikotensis (DAVIES)

-Ranikothalia sindensis (DAVIES)

-Ranikothalia nuttalli (DAVIES)

-Glomalveolinids

In the upper half of the formation after the thickness of 51 meters from the base the following forams were observed.

-Alveolinids

-Nummulites mamillatus (FICHTEL & MOLL)

-Nummulites atacicus (LEYMERIE)

-Assilina laminose (GILL)

-Assilina spinosa (DAVIES & PINFOLD)

-Discocyclina dispensa (SOWERBY)

-Ranikothlia sindensis (DAVIES)

-Ranikothalia nuttali (DAVIES)

-Lockhartia tipperi (DAVIES)

-Assilina subspinosa (DAVIES & PINFOLD)

The fauna mentioned above is basically from upper Paleocene to early Eocene in age so Dungan Formation belongs to Paleocene to Eocene in age.

CONCLUSION

The foraminiferas observed in Dungan Formation are typical Paleocene to Eocene in age. Amongst the fauna recorded in it's lower half, *Miscellanea miscella* & *Lockhartia haimei* are restricted to upper Paleocene while *Assilina subspinosa, Discocyclina ranikotensis, Lokhartia tipperi, Ranikothalia sindensis, Ranikothalia nuttalli* were of both upper Paleocene & early Eocene in age. Two species of Alveolinids (very close to *Alveolina vredenburgi DAVIES & PINFOLD, 1937* and *Alveolina pasticillata SCHWAGER C. 1883*) belongs to early Ilerdian i.e. early Eocene (SB 5-6) were observed in the upper half the formation. *Nummulites mamillatus ,Nummulites atacicus, Assilina laminosa* & *Assilina spinosa* are typical early Eocene in age.

On the basis of the above observations the lower half of the formation belongs to upper Paleocene age and the upper half of the formation belongs to early Ilerdian i.e. early Eocene age (Shallow Benthic Biozones SB 5-6), and we can draw the line between the Paleocene and Eocene age with in the formation at the level of 51 meters thickness of the formation from its base at Zinda Pir section (Fig-2).

REFERENCES

Ahmad, R. A. 1987. Geologic framework and hydrocarbon potential of Sulaiman sub-basin, Pakistan. Hydrocarbon Dev. *Inst. of Pakistan, Project Report,* 45 p.

Blandford, W. T. 1883. Geological notes on the hills in the neighborhood of the Sind and Punjab frontier between Quetta and Dera Ghazi Khan. *Mem. Geol. Surv. India,* 20, 229-237.

Davies, L. M. 1939. Geographical changes in northwestern India during Late Cretaceous and Early Tertiary times. Proc. Pac. *Sci. Conf. 6th,* **6(2)**, 483-501.

Davies, L. M. 1941. Correlation of Laki beds. *Geological Magazine,* 78, 151-152.

Davies, L. M. 1941. The "Dungan" limestone and the Ranikot beds in Baluchistan. *India Geological Survey,* **78**, 316-317.

Davies, L. M. & Pinfold, E. S. 1937. The Eocene Beds of the Punjab Salt Range. *Pal. Indica,* **24,** 1, 1-79.

Eames, F. E. 1952. A contribution to the study of the Eocene in western Pakistan, The geology of standard sections in western Punjab and in Kohat district. Q. J. *Geol. Soc. London,* **107**, 173-200.

Griesbach, C. L. 1884. Report on the geology of the Takht-i-Suleman. India *Geol. Survey Recs.*, **17**, 175-190.

Hunting Survey Corporation (H. S. C.) 1961. Reconnaissance geology of part of West Pakistan. (Colombo Plan Cooperative Project) Canada Government, Toronto, 550 p.

Iqbal, M. W. A. 1969. The Tertiary pelecypod and gastropod fauna from Drug, Zinda Pir, Vidor (Distt. D. G. Khan), Jhalar and Chharat (Distt. Campbellpur), West Pakistan. *Ibid., Memoir Palaeontologica Pakistanica*, **6,** 77 p.

Jones, A. G. (ed) 1961. Reconnaissance geology of part of West Pakistan. A Colombo Plan Cooperative Project, Hunting Survey Corporation, Maracle Press Toronto, 550 p.

La Touche, T. D. 1893, Geology of the Sherani Hills. *India Geological Survey Recs.,* **26**, 77-96.

Latif, M. A. 1964. Variation in abundance and morphology of Pelagic foraminifera in the Paleocene-Eocene of the Rakhi Nala, West Pakistan. *Punjab Univ. Geol. Bull.,* **4**, 29-109.

Lexique stratigraphique international. 1956. 3, Asie, fasc. 8, (a) India, Pakistan, Nepal, and Bhutan. Centre *Natl. recherche Start., Paris,* 404 p.

Malik, Z., Kemal, A., Malik, A., and Bodenhausen, J. W. 1988. Petroleum potential and prospects in Pakistan. International Symposium on Petroleum for the Future, Ministry of Petroleum and Natural Resources, Islamabad, Pakistan, Jan. 28-30.

Oldham, R. D. 1890. Report on geology and economic resources of the country adjoining the Sind-Pishin railway between Sharing and Spintangi. *Rec. Geol. Surv. India,* **23**, 93-110.

Shah, S. M. I. (ed) 1977. Stratigraphy of Pakistan. *Geological survey of Pakistan, Memoir* **12**, 138 pp.

Stewart, J. L. 1860. Proceedings of the Asiatic Society of Bengal for July, 1860. *Asiatic Soc. Bengal Jour.,* **29**, 314-318.

Verchere, A. M. 1867. Kashmir, the western Himalaya and the Afgan mountains, with a note on the fossils by M. Edouard de Vernueil. *Asiatic Soc. Bengal Jour.,* **36**, 9-50, 83-114, 201-229.

Waheed, A, Wells, N. A. and Ahmad, N. 1988. Paleocurrents beside an obliquely convergent plate boundary, Sulaiman foldbelt, SW Himalayas, west central Pakistan. *Bull. A. A. P. G.,* **72**, 255-256

Williams, M. D. 1959. Stratigraphy of the Lower Indus Basin, West Pakistan. *World Petroleum Cong.,* 5th, New York, Proc., sec. 1, Paper 19, 377-390.

Geol. Bull. Punjab Univ. 38, 2003.

PETROLOGY AND GEOCHEMISTRY OF THE BASIC DYKES AND SILLS ASSOCIATED WITH THE PANJAL VOLCANICS IN AZAD KASHMIR, PAKISTAN.

BY

MOHAMMAD SABIR KHAN
Institute of Geology, University of Azad Jammu and Kashmir, Muzaffarabad.

MOHAMMAD ASHRAF
179-B, PCSIR Housing Society, Canal Road, Lahore-54590.

AND

MOHAMMAD AMJAD AWAN
Institute of Geology, University of Azad Jammu and Kashmir, Muzaffarabad.

Abstract:- *The basic dykes and sills in Lesser Himalayas have variable chemical composition (SiO_2 ranges from 39 to 54 wt.%, P_2O_5 0.19 to 0.56 wt.%, TiO_2 1.63 to 4.15 wt.%, Zr 120 to 432 ppm). Geochemical studies show that these rocks are transitional to mainly alkalic basalts. The rocks are enriched in incompatible trace elements and are characterized with Zr/Nb 2 to 9, Nb/Y 0.74 to 2.65, Zr/Y from 4 ~10 and Ti/Y ratios from 217 to 1025. The dykes and sills are also enriched in light rare earth elements (LREE) relative to heavy rare earth elements (HREE). They show an enrichment of La_N = 55 to 239.5 x chondrite, Ce_N = 195 x chondrite and Yb_N = 8 to 19.55 x chondrite.*

The variation of incompatible elements and LREE enrichment within these rocks is due to lower degrees of partial melting of source region. The rocks show fractional crystallization, which was dominated by the removal of olivine and pyroxene. Low Mg number (0.31 to 0.51) and Ni (32 to 302 ppm) values indicate that magma for the rocks was evolved. Trace elements and REE data like La/Yb_N (7.38 to 12.25), Ce/Yb_N (2.47 to 11.01) and La/Sm_N (3.02 to 4.16) for the dykes and sills samples suggest that their melt has been derived from an 'enriched mantle plume' P type MORB source region.

Comparison of immobile trace elements and REE data of the dykes and sills with that of the predominant tholeiitic basalts of the Panjal volcanics suggest that the magma for the two rocks has been derived from the same source composition.

The Geochemical data of immobile elements of rocks, MORB normalized trace element patterns and chondrite normalized LREE enriched patterns exhibit within-plate setting. Studies based on geochemistry suggest that the transitional to alkalic magma was generated during Upper Palaeozoic extensional environment accompanied by rifting of the northern margin of Gondwana continent.

INTRODUCTION

In northwest Himalayas from Main Boundary Thrust (MBT) to Indus Suture Zone, Main Mantle Thrust (MMT), the northern edge of the Indian plate in this region (Azad Kashmir and Kaghan areas) is intruded by basic dykes and sills. In Higher Himalayas these rocks have been metamorphosed to amphibolite facies metamorphism (Papritz and Rey, 1989; Greco, 1989 and Honegger et. al., 1982).

In the Lesser Himalayas these rocks have also been altered and metamorphosed and are considered equivalent to the Panjal volcanics. Some of them may be contemporaneous or feeders to the lava flows of the Panjal volcanics which are mainly tholeiitic basalts (Khan, 1994). Basic dykes have also been reported from Srinager region and eastern Kashmir (Honegger et al., 1982). On the western side dolerite dykes have been investigated from Hazara (Calckin et al., 1975), Manshera (Shams et al., 1968), Malakand (Chaudhry et al., 1976), Ambela (Rafiq and Jan, 1990), and Swat areas (Majid et al., 1991).

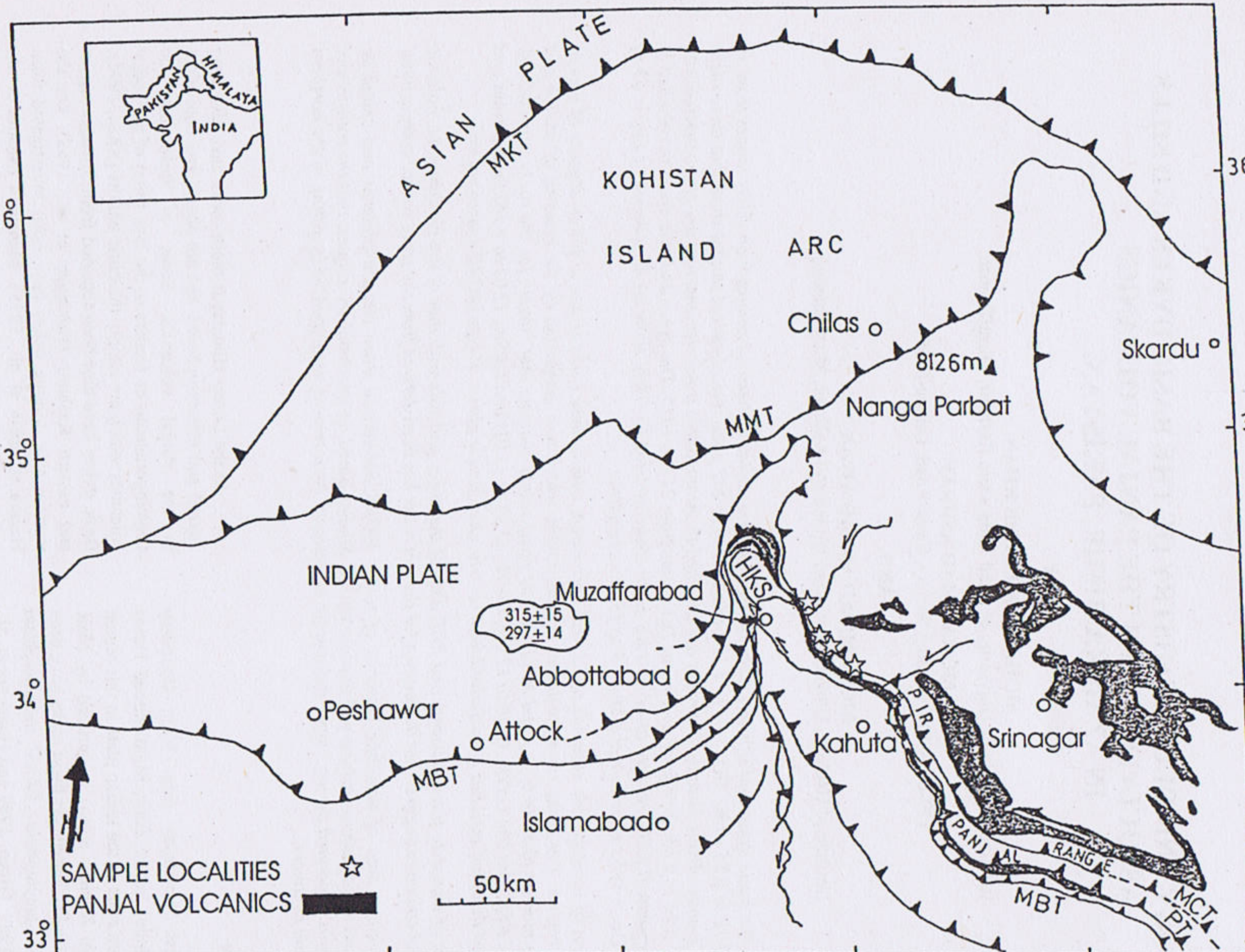

Fig.1. Sketch map of the NW Himalayas showing location of samples for dykes & sills and occurrence of the Panjal volcanics, Modified after Jan & Karim (1990) and Khan et al. (2000). MMT; Main Mantle Thrust, MKT: Main Karakoram Thrust, MCT: Main Central Thrust, PT: Panjal Thrust, MBT: Main Boundary Thrust, HKS: Hazara Kashmir Syntaxis.

The geology of the area was studied by Lydekker (1883), Wadia (1934), Ghazanfar and Chaudhry (1984), Ghazanfar and Chaudhry (1985) and Greco (1989). Geology and geochemical studies of the Panjal volcanics in the Lesser Himalayas have been carried out by Ashraf and Khan (1991), Khan et al. (2000), Khan et al. (1997), Khan (1994), Khan et al. (1991) and Khan and Ashraf (1989).

The present study of the basic intrusive rocks is confined along the Panjal volcanics in the Lesser Himalaya. New geological and geochemical data of major and trace elements is presented. The aim of the study is to describe the compositional features of the basic dykes and sills, their tectonic setting and magmatic relations with the Panjal volcanics.

GEOLOGICAL SETTING

A linear belt of volcanic and associated sedimentary rocks is exposed in the Lesser Himalayas and extend from south east of Muzaffarabad to Kaghan (Fig. 1). These rocks are bound between the MBT and the Panjal Thrust (PT). Along the PT the older metasediments have thrust over these rocks during Himalayan orogeny.

In the area between the PT and MBT from base towards top a sequence of the pryroclastic rocks, agglomeratic slates, and basaltic lava flows with interbedded limestone are exposed on the eastern and western flanks of the Hazara-Kashmir Syntaxis. The Agglomeratic slates are intermediate to acidic in composition overlain by the Panjal volcanics. The Panjal volcanics are massive basaltic lava flows with relict pillow structures and mainly tholeiites in composition (Khan, 1994). The rocks are altered and metamorphosed to greenschist facies metamorphism.. These rocks have thrust over the molasse sediments (Murree Formation) along the MBT in the area.

Dykes and sills have intruded the Agglomeratic slates, older metasediments and Nauseri granite gneiss in the area. They are aligned NW-SE with a dip NE and show a trend parallel to the regional foliation in this area. They are of variable width and length.

On the basis of lithostratigraphic correlation in Srinager region and other parts of Kashmir the Panjal volcanics are considered of Upper Palaeozoic to Early Triassic (Wadia, 1934). Stratigraphic ages have been established between the Artinskian (Kapoor, 1977) and the Sakmarian- Artinskian to Kungurian (Nakazawa et al., 1975). Radiometric dating of a basic dyke (Baig, 1991) in Hazara area using Ar^{40}/Ar^{39} method yielded ages from 284 $\pm$4 Ma to 262$\pm$1 Ma. Based on Ar^{40}/Ar^{39} isochron tentatively the same age has been assigned to the dykes and sills associated with the Panjal volcanics in the Lesser Himalayas Azad Kashmir.

PETROGRAPHY

The basic dykes and sills are altered and metamorphosed to greenschist and amphibolite facies metamorphism during Himalayan orogeny. Metamorphism has affected their original mineralogy. These rocks are massive and show greenish colour on fresh surface while brown to grayish brown on weathered surface. They are composed of plagioclase, brown hornblende, green hornblende and pyroxene. Plagioclase in some rocks has been albitized and altered to calcite, epidote and sericite. Epidote and calcite occur as alteration product within plagioclase. Alteration product of minerals also occur as fine grained groundmass. Pyroxene alters to chlorite and actinolite. Thin sections studies show the minerals albite, epidote, chlorite, sphene, calcite and quartz in addition to minerals mentioned earlier. In general all basic dykes and sills are petrographically similar. They are medium grained to coarse grained. They are composed of various proportions of albite, hornblende, calcite, actinolite, sphene, biotite and opaque minerals.

ANALYSES AND RESULTS

Sampling and analytical techniques

Efforts have been made to collect rock samples with little effects of alteration. Fresh and representative samples of the rocks were selected for inductively coupled plasma (ICP) analysis, for major and trace elements. Rare earth elements (REE) were determined by mass spectrometry inductively coupled plasma (ICP/MS) techniques. For analysis by the ICP method, a 0.2 gram sample was fused with 0.60 gram of $LiBO_2$ and was dissolved in 100 mls 5% HNO_3.

Rock samples were analysed for major elements SiO_2, TiO_2, Al_2O_3, $Fe_2O_3^t$ (Fe_2O_3 was analysed as total iron), MnO, MgO, CaO, Na_2O, K_2O, P_2O_5 and trace elements like Ba, Sr, Nb, Zr, Y, Ni, Cr, and Sc. In addition representative rocks were analysed for REE. Major oxides are presented in wt.% while trace elements and REE are in ppm.

EFFECTS OF ALTERATIONS

Alteration in these rocks is shown by high 'loss on ignition' values (Table-2). Alteration is also reflected by petrographic study of these rocks. The Na_2O and K_2O values in rock samples Nus-1, K-1 and RL-4 accompanied with low MgO contents exhibit the effects of alteration. Alteration is also shown by scatter of the major element data on Harker diagrams (Fig. 2).

MAJOR ELEMENT GEOCHEMISTRY

Major element composition (wt. %) and mg-numbers of dykes and sills are presented from Muzaffarabad area in Table 1.

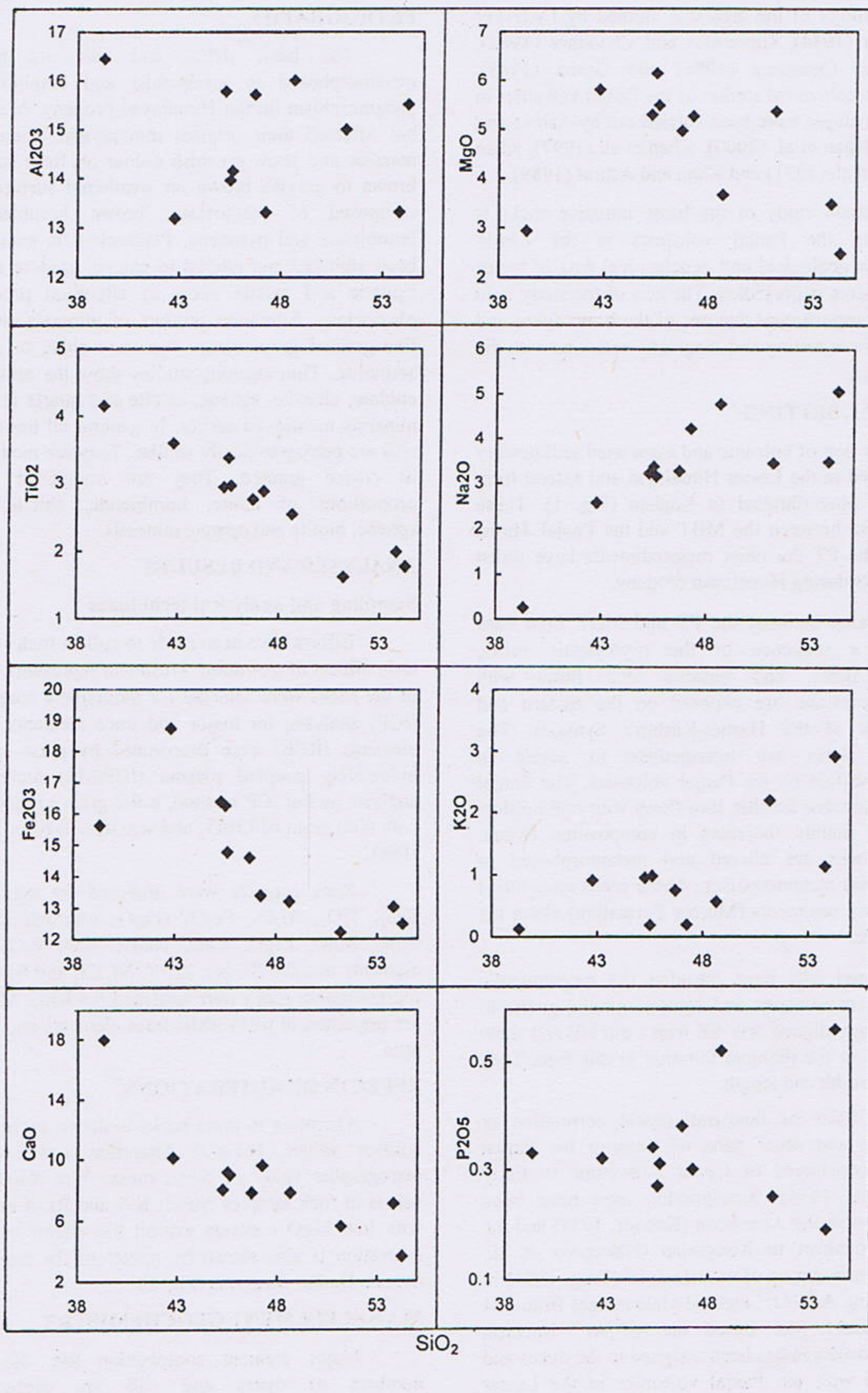

Fig.2. Variation of major elements vs SiO_2 for the dykes and sills.

Table 1.

Geochemical analyses of the basic dykes and sills associated with the Panjal volcanics.

	K-11	**K-1**	**Nus-11**	**Nus-1**	**Nus-6**	**RL-3**	**RL-4**	**RL-6**	**LBC-1**	**LB-4**	**LB-3**
	alk	thol	alk	thol	alk	alk	alk	alk	thol/alk	alk	alk
SiO_2	45.62	51.19	47.25	54.26	45.51	42.78	48.66	45.28	53.82	39.31	46.72
TiO_2	2.96	1.63	2.88	1.78	3.37	3.59	2.54	2.94	1.99	4.15	2.76
Al_2O_3	14.15	15.00	13.31	15.51	13.96	13.19	16.01	15.78	13.32	16.45	15.71
$Fe_2O_3^t$	14.78	12.22	13.39	12.49	16.25	18.73	13.21	16.38	13.04	15.62	14.60
MnO	0.23	0.18	0.24	0.19	0.21	0.22	0.17	0.22	0.19	0.24	0.23
MgO	5.49	5.37	5.27	2.49	6.15	5.81	3.67	5.30	3.48	2.94	4.97
CaO	8.96	5.61	9.58	3.62	9.14	10.09	7.82	8.02	7.08	17.98	7.81
Na_2O	3.15	3.45	4.23	5.06	3.37	2.57	4.78	3.22	3.48	0.26	3.27
K_2O	0 .98	2.20	0.20	2.92	0.19	0.91	0.57	0.95	1.13	0.13	0.75
P_2O_5	0.31	0.25	0.30	0.56	0.27	0.32	0.52	0.34	0.19	0.33	0.38
LOI	3.6	2.3	3.7	1.2	1.9	0.9	1.2	1.8	2.00	2.00	2.5
Mg #	0.46	0.51	0.48	0.32	0.47	0.42	0.39	0.43	0.38	0.31	0.44
F/M	2.69	2.28	2.54	5.02	2.64	3.22	3.60	3.10	3.75	5.31	2.94
K/N	0.31	0.64	0.05	0.58	0.06	0.35	0.12	0.26	0.32	0.5	0.23
C/Al	0.63	0.37	0.72	0.23	0.65	0.76	0.49	0.51	0.53	1.1	0.50
Zr/Ti	0.05	0.11	0.04	0.08	0.04	0.05	0.05	0.02	0.09	0.04	0.04
					Trace elements (ppm)						
Ba	364	853	169	928	86	274	253	376	274	17	269
Sr	407	306	345	259	300	432	518	612	217	3034	591
Nb	36	55	31	47	53	51	41	39	29	33	20
Zr	168	279	132	432	120	153	246	167	178	145	151
Ni	302	119	167	81	127	134	81	71	32	97	59
Cr	83	123	95	21	111	27	21	12	20	12	12
Sc	24	18	24	10	29	23	15	15	-	-	-
Co	37	27	32	15	40	45	27	42	67	111	99
Y	30.3	45	22	54	20.2	21	39.7	20	43	33	27
Cu	151	49	120	32	89	371	177	277	29	207	205
Zn	158	106	114	185	113	117	89	119	193	114	150
Zr/Nb	4.7	5.07	4.26	9.19	2.26	3	6	4.3	6.13	4.39	7.6
Ti/Y	739	217	785	243	1010	1025	525	881	411	754	613
Zr/Y	7	6.2	6	10	6	7.3	8.5	8.4	4	4	8
Nb/Y	1.5	1.22	1.41	1.10	2.65	2.43	1.41	1.95	2.60	1	0.74
Y/Nb	0.67	0.82	0.71	0.94	0.34	0.41	0.57	0.51	1.48	1.0	1.35
Ti/Zr	105.6	35	131	25	168	141	62	106	67	172	110
Zr/TiO_2	0.095	0.029	0.008	0.04	0.006	0.007	0.02	0.009	0.02	0.006	0.009
Zr/P2O5	0.05	0.11	0.04	0.08	0.04	0.05	0.05	0.02	0.09	0.04	0.04

(abbreviations: alk. alkaline, thol. Tholeiite, F/M= FeO^t/MgO, K/N=K_2O/Na_2O, C/Al =CaO/Al_2O_3, Zr/Ti= $Zr/TiO_2 x 10^4$)

The basic dykes and sills reveal a wide range in major element composition. SiO_2 contents range between 39.31 to 54.26 wt.%. Al_2O_3 varies from 13.19 to 16.45 wt.% in these rocks. $Fe_2O_3^t$ has values from 12.22 to 18.73 wt.%, MgO ranges from 2.49 to 6.15 wt.%, CaO shows variation from 3.62 to 17.98 wt.%, Na_2O ranges from 0.26 to 5.06 wt.%, K_2O varies from 0.13 to 2.92 wt.%. TiO_2 ranges from 1.63 to 4.15 wt.%, P_2O_5 shows variation from 0.19 to 0.56 wt.%. MnO exhibits values from 0.17 to 0.24 wt.% in these rocks. Most of the rocks are basaltic in composition. One rock sample Nus-1 is basaltic andesite in composition. One sample (LB-4) has SiO_2 39 wt.% with low mg number (0.31). TiO_2, FeO^t, MgO, and CaO exhibit a negative correlation with SiO_2. Na_2O and K_2O show an increase with increase in content of SiO_2. Al_2O_3 shows a scattered positive correlation with SiO_2 (Fig. 2). With increase in SiO_2 content a decrease in Mg number and Ni content is noticed. The ratios CaO/Al_2O_3 also show a decrease with increase in SiO_2 (Table-1).

The petrological character of the rocks was determined by using TiO_2–$Zr/(P_2O_5 \times 10^4)$ Nb/Y, Ti/Y and Y/Nb ratios (Table-1) (Fig. not shown). The rocks are tholeiites (K-1 & Nus-1) transitional (LBC-1) to alkalic basalts (Table-1). Major element data presented above and in Table 1 show that the rocks have been evolved with respect to their mg number (0.31-0.51), low MgO (2.49 to 6.15 wt%) and Ni contents (32 to 302 ppm). These rocks have K_2O/Na_2O ratios varying from 0.05 and 0.64 (Table-1). The lower values are generally due to high content of Na_2O in rocks.

TRACE ELEMENT GEOCHEMISTRY

The trace element composition of the dykes and sills are presented in Table 1. The Ni contents of the rocks vary between 32 to 302 ppm. Cr abundances vary between 12 to 123 ppm in these rocks and. decrease with decrease in MgO wt.% in the rocks. Co values range from 15 to 111 ppm. Ni, Cr and Co values accompanied by lower mg number indicate evolved nature of the rocks. These rocks are also enriched in incompatible elements like K, Ba, Sr and Nb (Table-1).

A total of five rock samples have been analysed for REE and data are presented in Table 2. The rocks are LREE- enriched (La_N = (55-239.5) x chondrite, (Yb_N = (8-19.55) x chondrite) relative to HREE.

TECTONIC SETTING

In order to evaluate the tectonic setting the geochemical data of basic dykes and sills were plotted on different discrimination diagrams.

Tectonic setting of the altered basalts can be determined by using elements, P, Zr, Nb, Y, Ni, Cr, and Ti, which are considered immobile during processes of alteration and metamorphism (Pearce and Cann, 1971, 1973; Floyd and Winchester, 1975; Pearce and Norry, 1979; Pearce, 1982; Humphris, 1984; Wilson, 1989). The immobile geochemical data of these rocks were plotted on different discrimination diagrams used to find out the tectonic setting of altered and metamorphosed basalts.

Pearce (1980) used Ti-Zr diagram to discriminate between arc basalts, within plate basalts (WPB) and mid ocean ridge basalts (MORB). When the geochemical data of the rock samples are plotted on the Ti-Zr diagram, they fall in the field of WPB (Fig. 3).

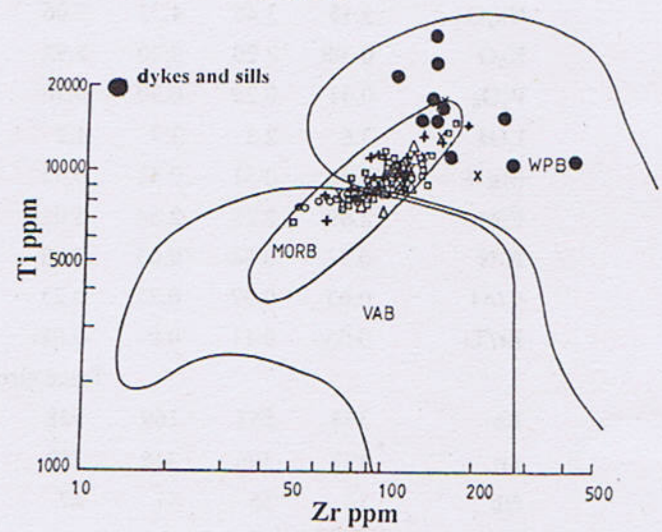

Fig.3. Plot of the dykes and sills in the Ti versus Zr tectonic discriminant diagram. Fields distinguishing mid ocean ridge basalts (MORB), within plate basalts (WPB), and volcanic arc basalts (VAB) are after Pearce (1980). Stippled area shows Panjal volcanics.

The geochemical data of dykes and sills have been plotted on the Zr/Y versus Zr diagram (Fig. 4) of Pearce and Norry (1979). This diagram explains geochemical differences between MORB, oceanic arcs and WPB. The dykes and sills geochemical data fall in WPB.

La/Sm and Sm/Yb ratios are used to know the source region for the basaltic rocks. Jones et al. (1993) discriminated between (OIT) (tholeiitic shield basalts of Hawaiian chain) and P-type MORB basalts by using La/Sm and Sm/Yb ratios. The ratios of Sm/Yb_N (2.34 - 3.25) and La/Sm_N (3.02 - 4.16) in these rocks show P-type MORB source for these rocks (Fig. 5).

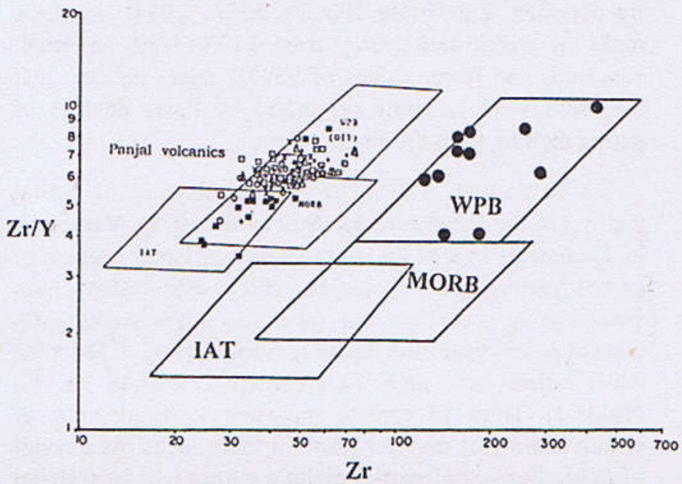

Fig.4. Geochemical data of the dykes and sills in Zr/Y versus Zr diagram. Field boundaries separating mid ocean ridge basalts (MORB), island arc tholeiites (IAT), and within plate basalts (WPB) are after Pearce and Norry (1979). Symbols as in Fig. 3.

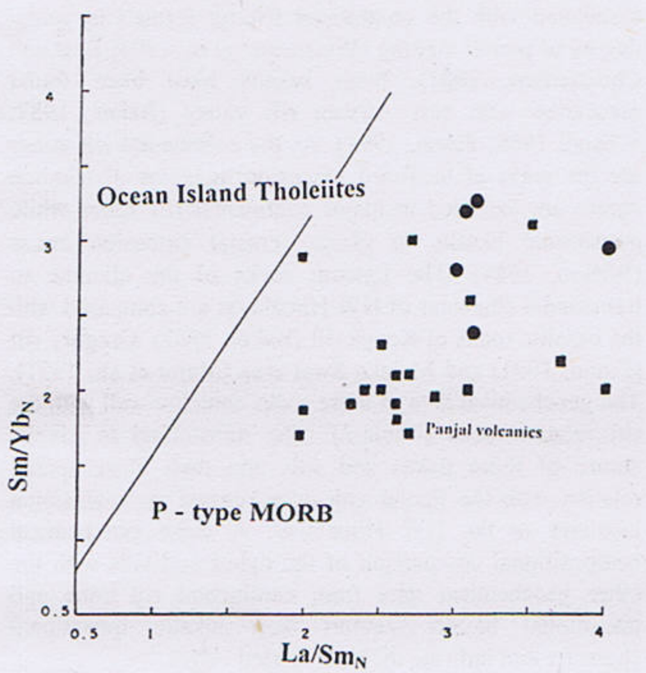

Fig. 5. Discrimination diagram of Sm/Yb versus La/Sm for the dykes and sills. Field for OIT and P-type MORB are after Jones et al. (1993). Symbols as in Fig. 3.

TRACE ELEMENT PATTERNS

Trace element patterns of the rocks normalized to MORB values after Pearce (1982) are shown in Fig. 6. Elements like Sr, K, Ba, P, Zr, Ti, Y, Sc, Cr, and Ni normalized to MORB values, are plotted for these rocks. The large ion lithophile (LIL) elements (Sr, K and Ba), which are mobile during alteration and metamorphic processes are plotted on the left side of the diagram. The immobile, high field strength (HFS) elements are plotted to the right side in these patterns. In these rocks LIL elements are enriched relative to HFS elements (Fig. 6). MORB normalized trace element patterns of the dykes and sills samples resemble WPB and represent a WPB setting. The elements like K, Ba, P, Zr, and Ti are enriched in the dykes and sills. However, in these rocks Sc, Cr and Ni are depleted relative to MORB values. These patterns are identical to those observed in WPB of alkaline affinity (Pearce 1982).

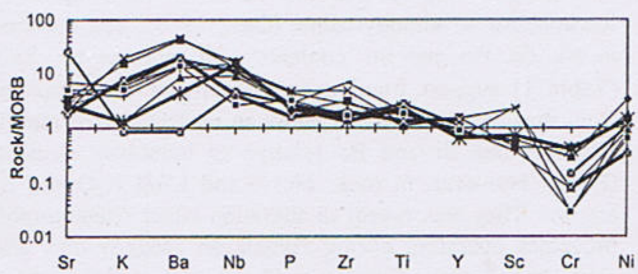

Fig. 6 MORB normalized trace element patterns of the dykes and sills. Normalizing values are after Pearce, 1982.

The chondrite normalized REE plots for the dykes and sills are shown in Fig. 7. The shape of the REE patterns indicate that LREE are enriched relative to HREE. LREE enrichment in these rocks are also shown by La/Yb$_N$ ratios ranging from 7.38 to 12.25 whereas Ce/Yb$_N$ ratios from 2.47 to 11.01. La/Sm$_N$ ratios in the rocks range from 3.02 to 4.16 (Table-2).

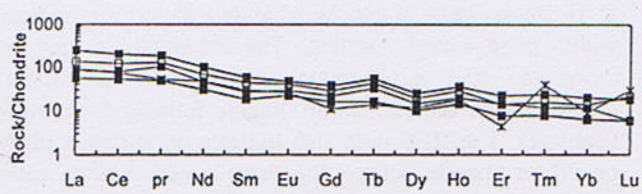

Fig. 7 Chondrite normalized REE diagram for the dykes and sills. Normalizing values are after Nakamura (1974).

DISCUSSION

On the basis of major element chemistry Panjal volcanic rocks are classified as basalts and basaltic andesites. As shown by Harker's diagrams FeO^t, MgO and CaO abundance generally decrease with increase in SiO_2 (Fig. 2). The mg number and ratios of CaO /Al_2O_3 also decrease with increase in SiO_2 (Table-1). All this can be explained that magma has under gone some degrees of fractionation.

Geochemical variations in the rocks exhibit that they have been affected by fractional crystallization which was accompanied by olivine and clinopyroxene fractionation. Crystal fractionation is indicated by the trace element patterns (Fig. 6) of the rocks and Ni, Cr and Co variable values (Table-1). Ni is partitioned in olivine while Cr and Co are strongly partitioned into clinopyroxene. Cr and Co are rapidly depleted in a residual liquid by fractionation of clinopyroxene (Gast, 1968). The decrease in Ni, Cr, Co and Sc, contents with increase in SiO_2 (Table 1) suggest fractionation of olivine and pyroxene from magma. These rocks show an enrichment of mobile elements like Sr and Ba relative to immobile elements (Fig.6). However, in rocks Nus-6 and LB-4 K_2O and Ba are low. They may reveal an alteration effect. Metamorphic processes operating during Himalayan orogeny may also cause enrichment of elements like Sr, Ba and K in these rocks. The ratios of incompatible elements like Zr/Nb= 2.26 - 9.11, Zr/Y= 4 - 10, Ti/Y= 217 - 1025, Y/Nb= 0.34 - 1.48, Ti/Zr= 25-172 and Nb/Y= 0.74 - 2.65 (Table-1). They indicate that fractional crystallization was in operation. The variation in the trace element content of these rocks might also have resulted by addition of crustal component to the mantle derived basic magma. Crustal contamination of basic magma results an increase in incompatible elements (Thompson, 1982). Crustal contamination is indicated by high values of K_2O and Nb/Y ratios in some of the rocks (Table–1). Trace element patterns (Fig. 6) also suggest that crustal contamination to some degrees for these rocks can not be ruled out.

Geochemical data of immobile elements of the dykes and sills is used to infer their tectonic setting (Figs. 3 & 4). On the basis of geochemical data these rocks indicate within plate tectonic setting. The incompatible elements ratios and other geochemical data support for enriched mantle source region for the magma forming these rocks (Table-1). The REE data also indicate an enriched plume or P-type mantle source for these rocks. Sm/Yb ratios indicate depth of melting of basaltic rocks (White et al., 1993). For these rocks Sm/Yb_N ratios vary from 2.34 to 3.25 (Table-2). These ratios represent melting of source rocks in the garnet stability field. The variations in Sm/Nd ratios represent different degrees of partial melting, crystal fractionation and rifting (Furnes et al., 1994). In these rocks the Sm/Nd ratios range from 0.19 to 0.20. The small variations and lower values of Sm/Nd ratios indicate that the rocks were probably originated by lower degrees of partial melting from the single source

Ti content is used to estimate degrees of partial melting in the basaltic rocks (Sun et al., 1979). Variations in Ti contents in igneous rocks exhibit different degrees of partial melting of the source which could also cause variations in trace element ratios. In these rocks TiO_2 content is less than 2 wt. % for two rocks (1.63-1.78 wt.%) while others have high TiO_2 content (2 - 4.15 wt. %) (Table-1). High Ti content represent lower degrees of partial melting of source region for these rocks. As a result of lower degrees of partial melting garnet will be residual phase in the source to deplete HREE. Thus the lower degrees of partial melting of the source region for the dykes and sills has caused variations in trace element contents and enriched LREE.

There is a general consensus that transitional to alkalic basalts exhibit an extensional environment and are associated with the continental rifting, formed by small degree of partial melting (Winchester et al. 1995; Best and Christiansen, 2001). Such basalts have been found associated with east African rift valley (Baker, 1987; Wilson, 1989; Fitton, 1991). As the continental rift zones are the areas of localized extension, magmas of alkaline nature are extruded in major continental rift zones while transitional basalts in greater crustal extension zones (Wilson, 1989). The igneous rocks of the alkaline to transitional character of NW Himalayas are compared with the basaltic rocks of Kenya rift (Baker, 1987), Gregory rift (Fitton, 1991) and Malaka Swat area (Majid et al., 1991). The geochemical data of these rocks compare well with the rift related rocks (Table-3). The transitional to alkalic nature of these dykes and sills and their close spatial relation with the Panjal volcanics suggest an extensional tectonics in the NW Himalayas. A close geochemical compositional comparison of the dykes and sills with the other geochemical data from continental rift zone and transitional basalts support their alkalic transitional character and indicate their rift related origin.

Alkaline rocks have not been found in spatial relation with the Panjal volcanics and dykes and sills in Azad Kashmir and Kaghan areas. However, these rocks occur in Peshawar alkaline Igneous Province and were dated Middle to Upper Carboniferous. The Rb/Sr whole rock isochron for Koga nepheline syenite is 297±4 to 315± 15 Ma (Le Bas et al., 1987) and Carboniferous U-Pb zircon age for syenites (Zeitler, 1988). These rocks and doleritic dykes in Peshawar Plain Alkaline Igneous Province are considered to represent a rifting phase in the area (Jan et al,

Table 2.

Rare earth elements (ppm) of basic dykes and sills associated with the Panjal volcanics.

	K-11	Nus-1	Nus-6	RL-4	LB-3
La	27.6	78.8	18.1	44.1	30
Ce	67.5	168.6	45.1	103.3	72.83
Pr	9.7	17.4	4.7	12.1	5
Nd	28.4	62.0	19.0	42.7	30
Sm	5.4	11.7	3.7	8.9	6
Eu	2.2	3.6	1.7	3.1	2
Gd	6.0	10.4	4.4	7.9	3
Tb	1.2	2.00	0.6	1.6	1
Dy	5.0	8.5	3.4	6.6	4
Ho	1.1	2.0	0.8	1.6	1
Er	3.2	4.9	1.7	3.1	1
Tm	0.3	0.6	0.2	0.4	0.5
Yb	2.5	4.3	1.4	3.0	2
Lu	0.2	0.6	0.2	0.7	0.4
La/Ce_N	1.08	1.23	1.06	1.12	1.25
La/Yb_N	7.38	12.25	8.65	9.86	10.03
Ce/Yb_N	6.87	11.01	8.84	5.80	2.47
Sm/Nd_N	0.59	0.59	0.60	0.65	0.62
Sm/Yb_N	2.34	2.95	2.87	3.22	3.25
La/Sm_N	3.15	4.16	3.02	3.06	3.09

Table 3.

Geochemical comparison of basic (1) dykes and sills with the (2) average Panjal volcanics (Khan, 1994, (3 & 4) alkali basalts Kenya rift (Baker, 1987) (5) average Ocean Island Basalts (Wilson, 1989). and (6)Gregory (Kenya) Rift (Fitton, 1991); (7) average dolerites from Malaka lower Swat (Majid et al., 1991).

	1	2	3	4	5	6	7
SiO_2	47.31	49.77	47.6	47.5	44.84	47.93	48.25
TiO_2	2.78	1.55	2.0	2.6	3.09	2.11	2.95
Al_2O_3	14.76	15.23	14.8	14.7	13.42	15.01	13.25
$Fe_2O_3^t$	14.61	15.23	12.7	13.9	13.07	2.99	3.60
FeO	-	-	-	-	8.96	7.50	
MnO	0.21	0.18	0.2	0.2	0.18	0.20	0.20
MgO	4.63	6.29	6.4	5.9	8.94	6.94	7.9
CaO	8.70	7.47	11.5	11.6	10.35	12.05	11.10
Na_2O	3.35	3.27	2.7	2.9	-	-	2.96
K_2O	0.92	1.15	0.8	1.0	1.24	0.80	0.67
P_2O_5	0.34	0.17	0.3	0.5	0.67	0.32	0.10
				Trace elements (ppm)			
Ba	351	255	390	472	479	300	-
Sr	638	265	453	447	764	428	-
Nb	39	14	-	-	52.9	35	-
Zr	197	108	116	140	276	112	-
Ni	115	99	86	69	188	76	-
Cr	52	252	-	-	321	83	-
Y	32	27	-	32	30.4	24	-

1990; Rafiq and Jan, 1990). In Kaghan and Azad Kashmir dykes and sills closely associated with the Panjal volcanics are transitional tholeiites to alkalic of Upper Palaeozoic (Ar^{40}/Ar^{39} 284±4 to 262±1 Ma). The Panjal volcanics (lava flows) are also considered of the same age. This data show that in Peshawar Alkaline Igneous Province alkaline magmatism occurred during Upper Carboniferous (297±4 to 315±15 Ma) while on eastern side alkalic -transitional to tholeiite magmatism took place during Upper Palaeozoic (284±4 to 262±1 Ma). The igneous activity in the area may indicate rifting phase of the northern margin of the Gondwana continent. The Late Palaeozoic is a time of rifting in the north Gondwana margin for the opening of Neo Tethys. For example Zagros rift in Late Permian (Husseini, 1992) and Gulf of Oman and the Zagros suture (Sengor, 1979). Occurrence of alkaline igneous rocks, geochemistry of basic dykes and sills of transitional to alkali nature and tholeiitic to mildely alkalic Panjal volcanics suggest that similar processes were in operation on eastern side of the north margin of Gondwana continent in Upper Palaeozoic. The occurrence of these rocks also support the view that the Upper Palaeozoic was time of intense crustal extension, rifting and emplacement of magma in the region.

GEOCHEMICAL COMPARISON OF THE BASIC DYKES AND SILLS WITH THE PANJAL VOLCANICS AND OTHER ROCKS

Table 3 shows the composition of major elements of these rocks, averages of Panjal volcanics, OIB, Gregory Rift (Kenya) and Dolerites from Malaka area lower Swat.

Major and trace elements data of the dykes and sills have been shown for comparison with major and trace elements data of the Panjal volcanics (Table-3). The mid ocean ridge normalized trace element patterns (Fig. 6) of dykes and sills and chondrite normalized REE patterns (Fig. 7) are similar to the trace elements (Fig. 8) and REE patterns (Fig. 9) of the Panjal volcanics normalized with MORB and chondrite values respectively. Trace element patterns are enriched in incompatible elements whereas REE are enriched in LREE in the dykes and sills.

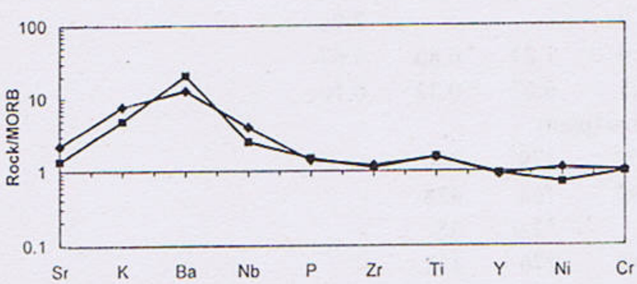

Fig. 8 MORB normalized trace element patterns of the Panjal volcanics for comparison with dykes and sills patterns (after Khan, 1994).

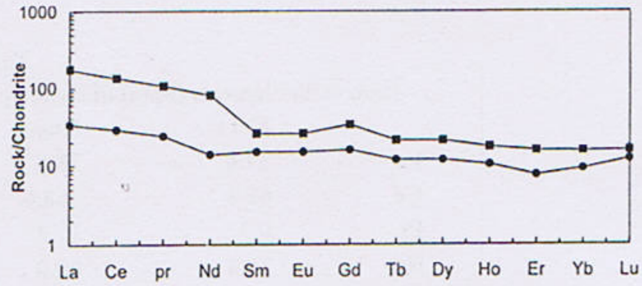

Fig. 9 Chondrite normalized composite REE diagram for the Panjal volcanics (after Khan, 1994).

Comparison of the geochemical data of dykes and sills with the Panjal volcanics is shown in Table-3. The dykes and sills are slightly low in SiO_2, MgO, and K_2O. They are high in CaO, Na_2O and MnO. The Al_2O_3 and Fe_2O_3 contents in these rocks are approximately equal to the Panjal volcanics.

Incompatible elements like Ba, Sr, Nb and Zr are high in these rocks. Elements like P and Ti are enriched in the dykes and sills as compared to the Panjal volcanics (Table-3). Dykes and sills also exhibit an enrichment in incompatible elements (Fig. 6) than the Panjal volcanics (Fig. 8). REE data of the dykes and sills like La/Yb_N ratios are from 7.38 to 12.25, Ce/Yb_N from 2.47 to 11.01 and La/Sm_N ratios range from 3.02 to 4.16 (Table-2). The Panjal volcanics also exhibit LREE enrichment relative to HREE. Normalized REE ratios in the Panjal volcanics are La/Yb_N from 3.29 to 11.16 whereas Ce/Yb_N ratios from 2.83 to 8.62. La/Sm_N ratios in the Panjal volcanics range from 1.96 to 4.09 (Khan et al., 2000). The comparison of REE data show that the dykes and sills (Fig. 7) are slightly more enriched in LREE than the Panjal volcanics (Fig. 9). La/Ce_N ratios exhibit small range and suggest that transitional to alkalic magma of the dykes and sills was also derived from the same source as the magma for the Panjal volcanics (Table-2). The rocks reveal 4-6% partial melting as compared to the Panjal volcanics which indicate more than 15% partial melting of source rocks (Khan 1994). The difference in chemical character of incompatible elements in the dykes and sills and the Panjal volcanics may be due to different degrees of partial melting of the same source in the upper mantle.

A comparison of chemical composition of these rocks is made with the chemical compositions of the ocean island basalts (OIB). OIB are mainly alkalic in nature (Wilson, 1989). There is a general consensus that the OIB magma has been derived by convecting upper mantle and represent a primitive mantle composition. When compared with an average OIB composition the dykes and sills are somewhat lower in MgO, CaO, TiO_2, K_2O and P_2O_5 and higher in SiO_2 , Al_2O_3, Fe_2O_3 (Table-3). These rocks have lower values of Ba, Sr, Nb and Zr.

Therefore, it is suggested that transitional to alkalic character of the dykes and sills as compared to the Panjal volcanics is due to crystal fractionation of magma accompanied by small degrees of partial melting of the source rocks. The mantle heterogeneity and crustal contamination may have also affected the chemical composition of these rocks.

CONCLUSIONS

The dykes and sills in Lesser Himalayas erupted during late Palaeozoic. They are mainly transitional to alkalic in nature, metamorphosed to greenschist and amphibolite facies metamorphism during Himalayan orogeny.

Geochemically the dykes and sills can be divided into transitional to alkalic between alkalic and tholeiitic basalts.

These rocks indicate a within-plate tectonic setting.

These rocks have been fractionated. The high-pressure fractionation was dominated by the removal of olivine and pyroxene. Most of the rocks are evolved in terms of Mg number and low Ni and Cr values.

Considering highly incompatible elements 4 to 6% partial melting of the source material (garnet peridotite) occurred for these rocks.

The Zr/Nb Zr/Y ratios and REE data of the dykes and sills indicate that their melt was derived from enriched or P-type mantle source. The basic dykes and sills and the Panjal volcanics were derived from the same source by different degrees of partial melting.

The chemical characteristics of these rocks invoke a rifting in northern part of Gondwana continent for the opening of Neo-Tethys.

ACKNOWLEDGEMENTS

The data used in this paper was obtained during Ph.D research by M. Sabir Khan. Financial support for this programme was sponsored by the University of Azad Jammu and Kashmir, Muzaffarabad.

REFERENCES

Ashraf, M., and Khan, M. S., 1991. Geology of Panjal volcanics in Azad Jammu and Kashmir, Pakistan. *Min. Assoc. Canada. SEG. Abst. Programs,* **16,** A5, P9.

Baig, M. S., 1991. Geochronology of Pre-Himalayan and Himalayan tectonic events, northwest Himalayas, Pakistan. *Kashmir Jour. Geol.,* **8,** & 9, 197.

Baker, B. H., 1987. Outline of the petrography of the Kenya rift alkaline province: in alkaline igneous rocks. *Geol. Society Special Pub.* No. 30 editors, Fiton, J.G. and Upton, B.G.J. 293-311.

Best, M. G., and Christiansen, E. H., 2001. Igneous Petrology. Blackwell Science Inc., Publ. USA. 458p

Calckin, J. A., Offield, T.W., Abdullah, S. K. M. and Ali, S.T, 1975. Geology of the Southern Himalayas in Hazara, Pakistan and adjacent areas. U.S. Geol. Surv. Prof. Paper 716-c, 1-29.

Chaudhry, M. N., Ashraf, M., Hussain, S. S, and Iqbal, M, 1976. Geology and petrology of Malakand and a part of Dir. Geol. Bull. Punjab Univ. **12,** 17-39.

Fitton, J. G. , James, D., and Leewan, W. S., 1991. Basic magmatism associated with Late Cenozoic extension in the western united States: Compositional variations in space and time. *Jour. Geophys. Res.* **.96 (B38)** 13698-13711.

Floyd, P. A., and Winchester, J. A., 1975. Magma type and tectonic setting discrimination using immobile elements. *Earth Planet. Sci. Lett.,* **27,** 211-218.

Furnes, H., Kryza, R., Muszynski, A., Pin, C. and Garmann, L.B. 1994. Geochemical evidence for progressive, rift related early Palaeozoic volcanism in the western Sudentes. *Jour., Geol. Soc., London,* **151,** . 91-109.

Gast, P. W., 1968. Trace element fractionation and the origin of tholeiitic and alkaline magma types. *Geochim. Cosmochim. Acta,* **32,** 1057-1086.

Ghazanfar, M., and Chaudhry, M. N., 1985. A third suture in northwest Himalaya. *Kashmir Jour. Geol.,* **3,** . 103-108.

Ghazanfar, M., and Chaudhry, M. N., 1984. A Paleozoic ophiolite and island arc sequence of Hazara - Kashmir Syntaxis, District Mansehra. *Kashmir Jour. Geol.*, **2, (1)**, 37-38.

Greco, A. M., 1989. Tectonics and metamorphism in the Western Himalayan syntaxis area (Azad Kashmir, NE-Pakistan). Ph.D Dissertation ETH - Zurich , Nr. 8779, Zurich, 193p.

Honegger, K., Dietrich, V., Frank, W., Gansser, A., Thoni, M., and Trommsdorff, V., 1982. Magmatism and metamorphism in the Ladakh Himalayas (the Indus-Tsangpo suture zone). *Earth Planet. Sci. Lett.*, **60**, . 253-292.

Humphris, S. E., 1984. The mobility of the rare earth elements in the crust. In: Henderson, P. (ed.), Rare earth element geochemistry. Elsevr, Amstrdam, 317-342.

Hussein, M. I., 1992. Upper palaeozoic tectono-sedimentary evolution of the Arabian and adjoining plates. *Jour.Geol. Society London,* **149**, .419-429.

Jan, M. Q. and Karim, A., 1990. Continental magmatism related to Late Palaeozoic-Early Mesozoic rifting in northern Pakistan and Kashmir. *Geol. Bull. Univ. Peshawar,* **23**, 1-25.

Jones, G, Sano, H. and Valsami-Jones, E., 1993. Nature and tectonic setting of accreted basalts from the Mino terrane, central Japan. *Jour. Geol. Soc. London,* **150**,. 1167-1181.

Kapoor, M., 1977. Lower Gondwana of Nishat Bagh, Kashmir and its significance. *Geophytology,* **7**, .188-196.

Khan, M. S., Ashraf, M., and Chaudhry, M. N., 2000. Tectonomagmatic environment of the Panjal volcanics in Azad Kashmir and Kaghan areas, Pakistan. *Geol. Bull. Univ. Punjab* **35**, 73-87.

Khan, M. S., Ashraf, M., and Chaudhry, M. N., 1997. Geochemical evidence for the tectonic setting of the Panjal volcanics in Azad Kashmir and Kaghan area. *Geol. Bull. Univ. Punjab* **31 & 32**, pp. 73-87.

Khan, M. S., 1994. Petrlogy and geochemistry of the Panjal volcanics in the Azad Kashmir and Kaghan areas, the NW Himalaya, Pakistan. Unpublished Ph.D. thesis, Punjab University, Lahore, Pakistan, 233p.

Khan, M. S., Ashraf, M., and Chaudhry, M. N., 1991. Geochemical evidence for an oceanic affinity of the Panjal volcanics in Kaghan valley, Pakistan. *Kashmir Jour. Geol.*, **8 & 9**, 1-18.

Khan, M. S., and Ashraf, M., 1989. Panjal volcanics: geochemistry and tectonic setting in Azad Jammu and Kashmir and Kaghan valley. *Kashmir Jour. Geol.,* **6 & 7**, 61-81.

Le Bas, M. J., Mian, I. and Rex, D.C., 1987. Age and nature of carbonitite emplacement in north Pakistan. *Geol. Runnd.* **76(2)**, 317-323.

Lydekker, R., 1883. The geology of Kashmir and Chamba territories and the British Districts of Kaghan. *Mem. Geol. Surv. India,* **22**, 31-34.

Majid, M., Danishwar, S. and Hamidullah, S., 1991. Petrographic and chemical variations in the rift-related basic dykes of the Malka area (lower Swat), N.W.F.P., Pakistan. *Geol. Bull.Univ. Peshawar,* **24**, 1-23.

Nakamura, N., 1974. Determination of REE, Ba, Mg, Na and K in carbonaceous and ordinary chondrites. Geochim. Cosmochim. Acta, **38**, 757-775.

Nakazawa, K., H. M., Ishii, K., Bando, Y., Okimura, Y. and Tukuoka, T., 1975.The Upper Permian and Lower Triassic in Kashmir, India. *Mem. Fac. Sci. Kyoto University, Ser. Geol. Mineral.*, **42**, 1-106.

Papritz, K., and Rey, R., 1989. Evidence for the occurrence of Permian Panjal Trap basalts in lesser and higher Himalayas of the western syntaxis area, NE Pakistan. *Eclogae Geol. Helv.*, **82**, part-2, 603-627.

Pearce, J. A., and Cann, J. R., 1971. Ophiolite origin investigated by discriminant analyses using Ti, Zr and Y. Earth Planet. Sci. Lett., Vol. 12, pp. 339-349.

Pearce, J. A., and Cann, J. R., 1973. Tectonic setting of basic volcanic rocks determined using trace element analyses. *Earth Planet. Sci. Lett.*, **19**, 290-300.

Pearce, J. A., and Norry, M. J., 1979. Petrogenetic implications of Ti, Zr, Y and Nb variations in volcanic rocks. *Contrib. Mineral. Petrol.*, **69**, 33-47.

Pearce, J. A., 1980. Geochemical evidence for the genesis and eruptive setting of lavas from Tethyan ophiolites. In: Panoyiotou, A., (ed.), proceedings of the seminar on ophiolites. *Geol. Surv. Depart., Nicosia, Cyprus,* 261-272.

Pearce, J. A., 1982. Trace element characteristics of lavas from destructive plate boundaries. In Thorpe, R. S., (ed.), Andesites: Orogenic andesites and related rocks. John Wiley and Sons, New York, 525-548.

Rafiq, M. and Jan, M. Q., 1990. Petrogenesis of basic dykes from the Ambela granitic complex, NW Pakistan. *Abs. Sec. Pak. Geol. Cong.* 45.

Sengor, A. M. C., 1979. Mid Mesozoic closure of Permian-Triassic Tethys and its implications. *Nature,* **279,** 590-593.

Shams, F. A. and Ahmed, Z., 1968. Petrology of the basic minor intrusives of the Manshera-Amb state area, NW Pakistan, part 1, the dolerite. *Geol. Bull. Punjab Univ.* **7,** 45-57.

Sun, S. S., and Nesbitt, R. W., and Sharaskin, A. Ya., 1979 Geochemical characteristics of mid-ocean-ridge basalts. *Earth Planet. Sci. Lett.,* **44,** 119-138.

Thompson, R. N., 1982. Magmatism of the British Tertiary Province. *Scottish Jour. Geol.,* **18,** 49-107.

Wadia, D. N., 1934. The Cambrian-Trias Sequence of North-Western Kashmir (parts of Muzaffarabad and Bramula Districts). Rec. *Geol. Surv. India,* **68,** part-2, 121-176.

Winchester, J. A., Floyd, P.A., Chocyk, M., Horbowy, K., and Kozdroj, W., 1995. Geochemistry and tectonic environment of Ordovician meta-igneous rocks in the Rudawy Janowickie Complex, SW poland. *Jour. Geol. Society,* **152,** 105-115.

White, W. M., McBirney, A. R. and Duncan, R. A., 1993. Petrology and geochemistry of the Galapagos Islands: Portrait of a pathological mantle plume. *Jour. Geophy. Res.,* **98, (B11),** 19533-19563.

Wilson, M., 1989. Igneous Petrogenesis: a Global Tectonic Approach. Unwin Hyman Inc., Publ. Winchester U.S.A. 466p.

Zeitler, P. K., 1988. Ion microprobe dating of zircon from the Malakand granite, NW Himalaya Pakistan. A constraint on the timing of Tertiary metamorphism in the region. *Geol. Soc. Am. Abs. Programs* **20,** 323.

Geol. Bull. Punjab Univ. 38, 2003.

SEDIMENTARY GEOLOGY AND BIOSTRATIGRAPHY OF THE CRETACEOUS-EARLY TERTIARY ROCKS IN THE MURREE-BREWERY GORGE AND THE HANNA LAKE AREA, QUETTA VALLEY, WESTERN SULAIMAN RANGE, PAKISTAN

BY

RIAZ AHMAD SHEIKH, AFTAB AHMAD BUTT AND SHAHID GHAZI
Institute of Geology, University of the Punjab, Lahore-54590, Pakistan.

Abstract: *Depositional environments and the biostratigraphic framework of the Cretaceous-Early Tertiary carbonate succession of the Murree-Brewery Gorge and the Hanna Lake around Quetta have been outlined which lie in the western extremity of the Sulaiman Range.*

The Cretaceous begins with the deepening environmental style when the Goru Formation (Aptian-Turonian) and the overlying Parh Limestone (Coniacian-Campanian) develop planktonic foraminiferal lime mudstone to packstone facies. The Parh Limestone, in its uppermost part, shows shallowing trend from tidal flat to ultimate exposure surface indicated by the presence of dolomitic limestone with gypsum to lateritic soil.

Transgression is again envisaged by the thin deposition of the unfossiliferous siliciclastic assemblage regarded to constitute the Mughal Kot Formation at the base of the shallow marine Maastrichtian Murree Brewery Limestone (formerly "Orbitoidal Limestone").

The K-T boundary shows shallow shelf carbonate platform deposition when the Late Cretaceous Murree-Brewery Limestone and the overlying Early Tertiary Dunghan Limestone were deposited. In these formations are found stratigraphically important benthonic larger foraminifera. Wackestone, packestone and grainstone microfacies of shallow shelf environments are observed.

The Murree Brewery limestone is flanked by a widely distributed blanket of the regressive facies of the fossil starved Pab Sandstone of the same age which can be visualized on regional framework.

INTRODUCTION

The Murree-Brewery Gorge Section has been a focus of attention for geological activities over the years because of the logistics being in the vicinity of the main town Quetta and exposure of stratigraphic sequence over a limited distance offer opportunities for a variety of sedimentological and paleontological studies. The Cretaceous and Lower Tertiary succession contain age diagnostic planktonic and benthonic larger foraminifera and thus depict both deeper marine and shallow marine environments.

The Cretaceous Goru Formation (Aptian-Turonian) and the Parh Limestone (Coniacian-Companian) contain planktonic foraminifera indicative of deeper marine environments, while the overlying Late Cretaceous Murree-Brewery Limestone and the Lower Tertiary Dunghan Limestone containing stratigraphically important benthonic larger foraminifera indicate shallow marine environments. These shallow water carbonates are, in fact, carbonate platform deposits and the K-T boundary is interestingly preserved in the carbonate succession.

The Murree-Brewery area lies in the eastern part of the Chiltan-Range, situated southwest of Quetta and the Hanna lake area lies in the east of Quetta from where regional strike takes swing from EW to NS in the Sor Range.

The Cretaceous sedimentation at both Murree-Brewery Gorge and the Hanna Lake section took place mainly as transgressive episode with some sea level changes. This transgressive episode is marked by the presence of age diagnostic planktonic foraminifera. The shallowing of the sea occurred at the Campanian-

Maastrichtian boundary and continued along the K-T boundary. The planktonic foraminiferal biofacies of the Parh limestone was replaced by the age diagnostic benthonic larger foraminifera occurring in the Murree Brewery Limestone. The uppermost part of the Parh Limestone is marked by a tidal flat environment till an exposure surface. A thin deposition of unfossiliferous siliciclastic sediments intervenes between the Parh Limestone and the Murree-Brewery Limestone which is interpreted here as belonging to the Mughal Kot Formation.

Allemann (1979) provided a comprehensive account of the Murree-Brewery Gorge Section and illustrated foraminiferal fauna from the Cretaceous-Lower Tertiary strata. Aubry et al (1991) illustrated Globotruncana species from the Parh Limestone. The present contribution is an attempt towards identifying various microfacies of the Cretaceous-Early Tertiary succession with reference to the foraminiferal content.

STRATIGRAPHIC AND SEDIMENTOLOGIC FRAMEWORK

Goru Formation

The formation is typically developed into chocolate brown flaggy beds sandwiched with off white strata. The variegated beds give a distinctive character to the formation.

There are four bioclastic microfacies which are lime mudstones, lime mudstones to wackestones, wackestones and dolomitic wackestones. The bioclasts are planktonic foraminifera.

PARH LIMESTONE

The Parh Limestone is distinctly off white well bedded limestone with shale partings. The uppermost part is dolomitic limestone with gypsum and lateritic soil.

The formation is dominantly represented by limemudstone with some wackestone. The upper part comprises dolomitic wackestones and dolostones. The bioclasts are planktonic foraminifera.

MUGHAL KOT FORMATION

A thin deposition of unfossiliferous siliciclastic assemblage has been interpreted to belong to the Mughal Kot Formation which underlies the Maastrichtian Murree-Brewery Limestone.

MURREE-BREWERY LIMESTONE (formerly Orbitoidal Limestone of Gigon, 1962)

The formation is typically developed as dark grey thick bedded hard limestone which forms part of the cliff face of the Murree-Brewery Gorge. Three bioclastic microfacies packestones, packestone to grainstone and grainstone have been identified. The bioclasts are bentonic larger foraminifera belonging to the genera *Siderolites Omphalocyclus* and *Orbitoides*.

DUNGHAN LIMESTONE

The Dunghan Limestone represents the upper portion of the cliff face of the Murree-Brewery Gorge. In other words the Murree-Brewery Limestone and the Dunghan Limestone are forming the cliff. The dominant microfacies is the bioclastic grainstone. Other microfacies are bioclastic wackestone, bioclastic packestone and bioclastic packestone to grainstone.

PALEONTOLOGICAL NOTES

Allemann (1979) illustrated planktonic foraminifera from the Goru Formation and the Parh Limestone whereas the benthonic larger foraminifera from the Murree-Brewery Limestone and the Dunghan Limestone.

Allemann (1979, pl.6, fig.1-3) illustrated *Orbitoides apiculata* (Schlumberger), *Orbitoides sp., Siderolites calcitrapoides* (Lamarck) and *Omphalocyclus macroporus* (Lamarck)

Aubry etal (1991, fig.2, 1-8) illustrated *Globotruncana fornicata* Plummer, *Globotruncana ventricosa* White, *Globotruncana arca* (Cushman), *Globotruncana stuartiformis* Dalbiez, *Globotruncana coronata* Bolli, *Globotruncana concavata* (Brotzen), *Globotruncana schneegansi* Sigal and *Globotruncana sigali* Reichel from the Parh Limestone from the Quetta region.

The Murree-Brewery Limestone has been found to contain these age diagnostic foraminifera (Akhtar & Butt, 2000) as already illustrated by Allemann (1979) thus confirming the Upper Cretaceous (Maastrichtian) age. The presence of these benthonic larger foraminifera indicate the shallow marine inner shelf (inner neritic) environments.

Allemann (1979, pl 6, figs.4-6) illustrated *Somalina sp., Glomalveolina cf., lepidula (Schwager), Miscellanea miscella* (d' Archiaec & Haime) indicating an Upper Paleocene (Lower Ilerdian age).

However Akhtar & Butt, (2000) recorded the association of *Miscellanea miscella* (d' Archiac & Haime) with *Ranikothalia sindensis* (Davies). *Ranikothalia nuttalli* (Davies), *Nummulites mamillatus* (Fichtel & Moll), *Somalina stefaninii*, Silvestri, *Discocyclina dispansa* (Sowerby), *Operculina subsalsa*, (Davies & Pinfold), *Assilina dandotica* (Davies & Pinfold) and alveolinids. Their observations gave further support to the results of Davies (1927) regarding the stratigraphic range of *Miscellanea miscella* from Paleocene to Eocene.

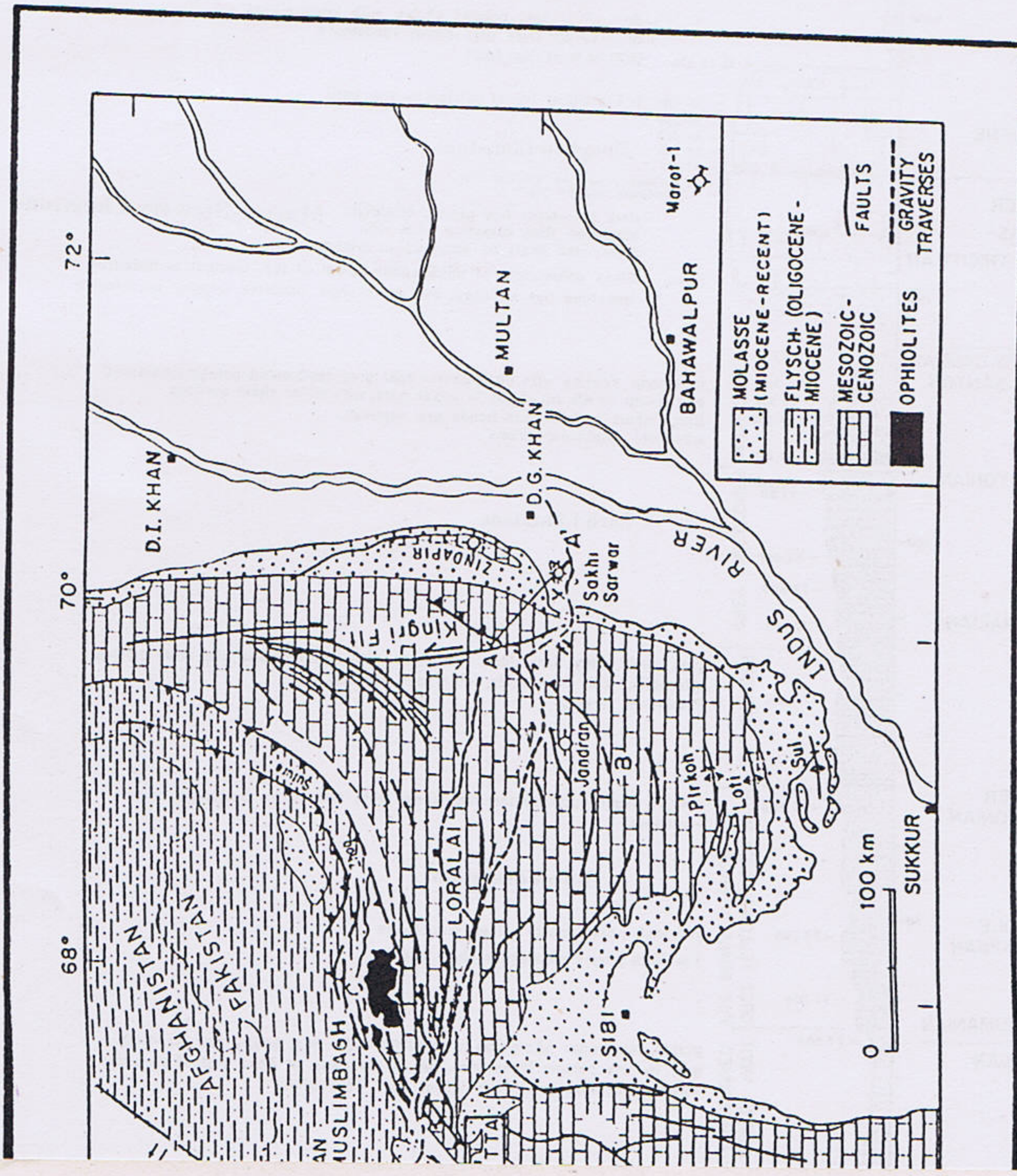

Fig.1. Location map of the Murree-Brewery Gorge and Hanna Lake, Quetta Valley, Southern Pakistan.

Plate -1

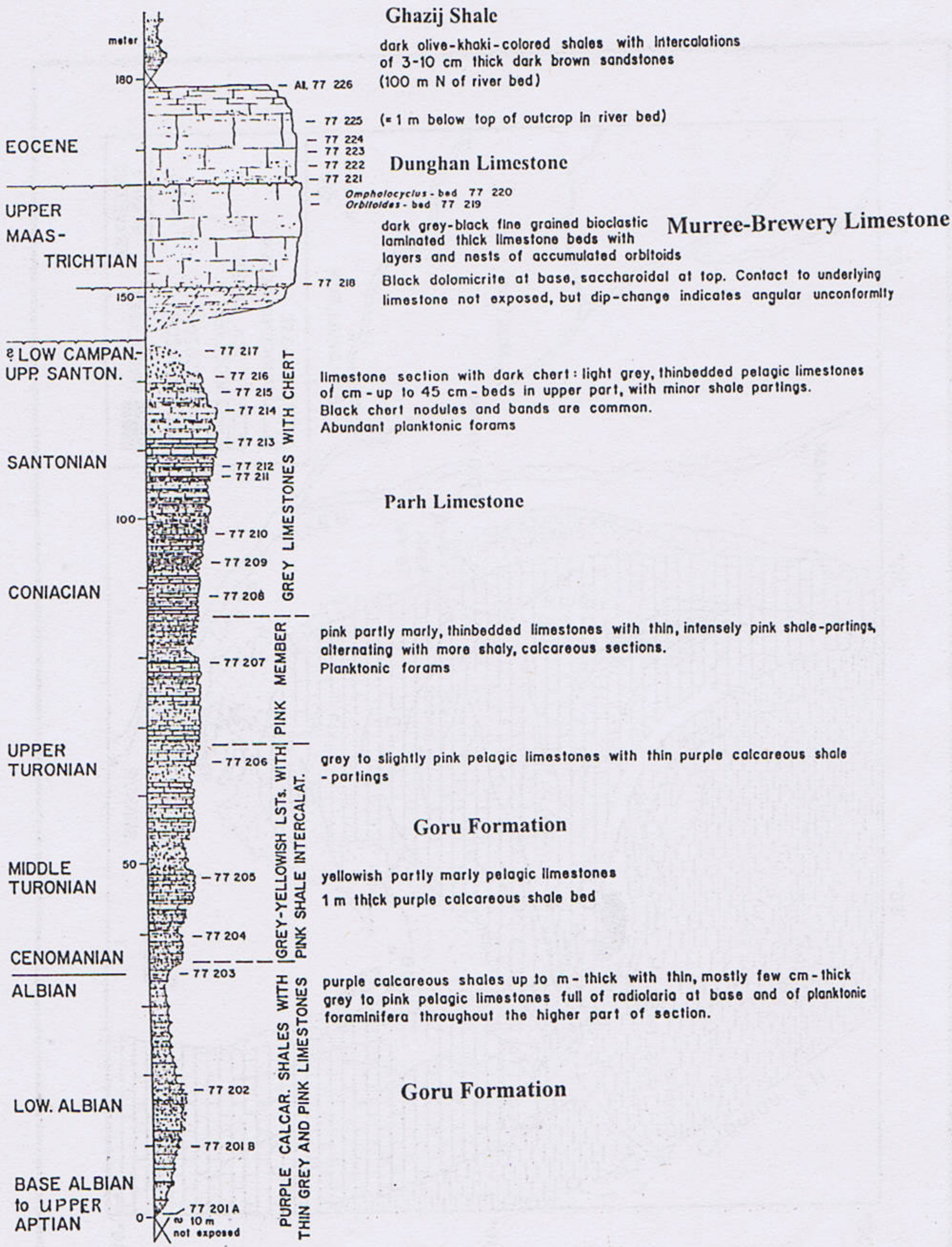

Fig.2. Murree-Brewery Gorge Section (after Alleman, 1979) Nomenclature after Stratigraphic Committee of Pakistan.

Plate -1

a

b

a: Murree-Brewery Gorge Section showing the Late Cretaceous Strata. The flaggy beds of the Goru Formation at the bottom right (near wall) are overlain by the Parh Limestone in the middle (white looking) and finally overlain by the Murree-Brewery Limestone ("Orbiotiodal Limestone") at the top left darker looking. Mughal Kot Formation is not visible.

b: Murree-Brewery Gorge Section, exposing the K-T boundary between the Late Cretaceous Murree-Brewery Limestone ("Orbiotiodal Limestone") and Limestone of the Early Teriary Dunghan Formation. This K-T boundary is marked by lateritic encrustation below cliff making limestone of the Early Tertiary Dunghan Formation.

Plate -2

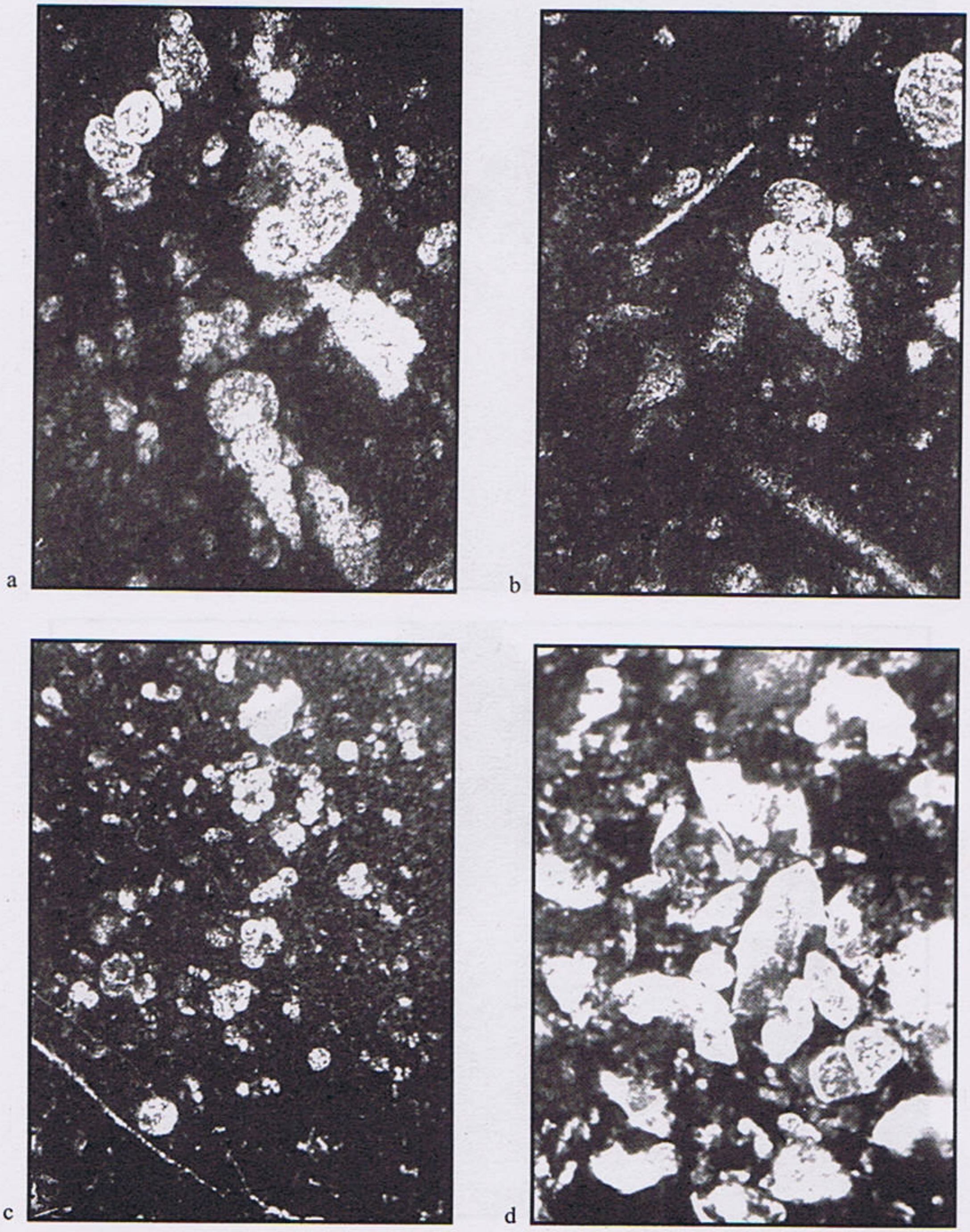

a-d: Lime mudstone (micrite) microfacies of the Late Cretaceous Goru Formation and the Parh limestone. Bioclasts are the planktonic foraminifera. Fig.1 & Fig. 2 Heterohelix globulosa (Ehrenberg), (Parh Limestone, upto Campanian). Fig.3 Rotalipora Spp. and Fig. 4 Hedbergella Spp. (Goru Formation, Cenomanian-Turonian).

Plate -3

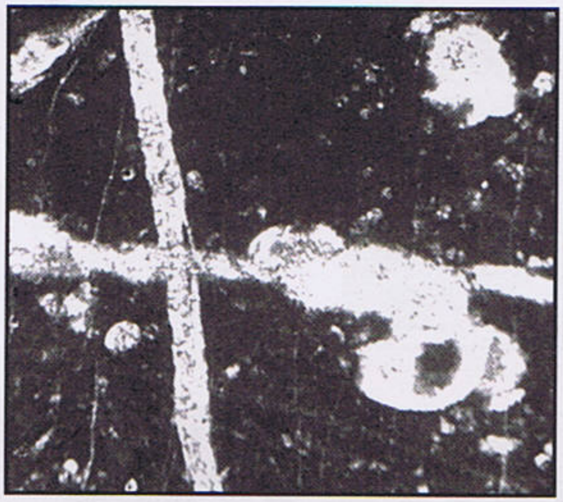
a

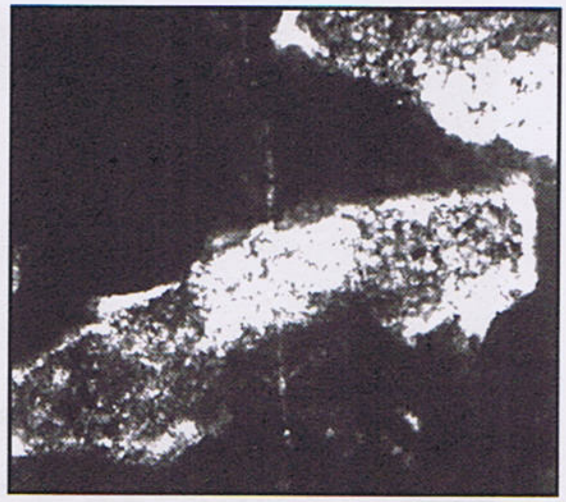
b

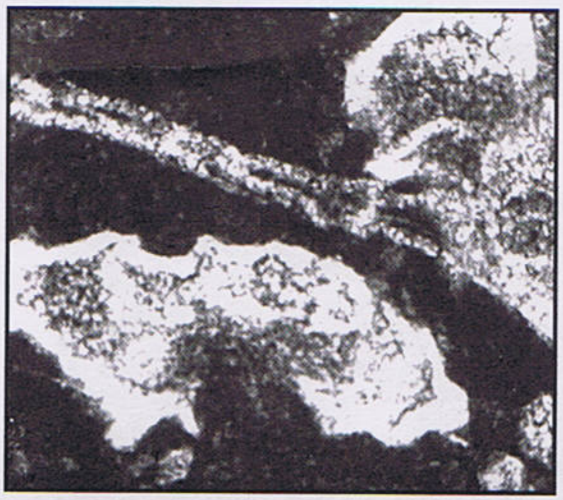
c

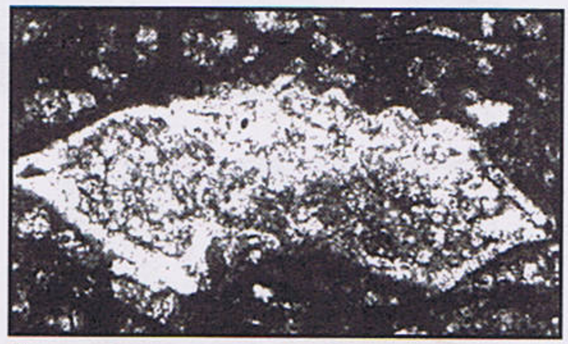
d

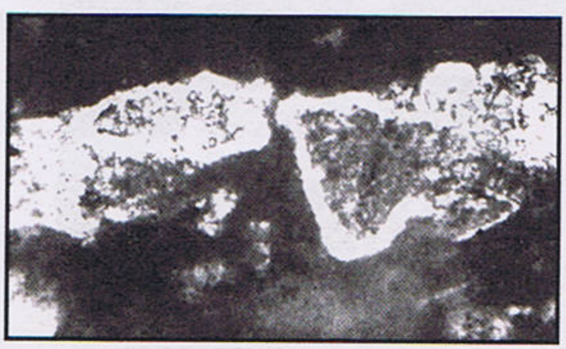
e

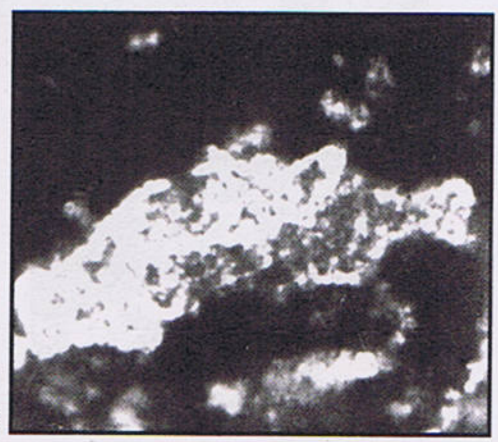
f

a: Lime mudstone (micrite) microfacies of the Late Cretaceous Goru Formation. Bioclast is <u>Globotruncana helvetica</u> Bolli.

b: Lime mudstone (micrite) microfacies of the Late Cretaceous Parh Limestone. Bioclast is <u>Globutruncana linneiana</u> (D' Orbigny)

c: Lime mudstone (micrite) microfacies of the Late Cretaceous Parh Limestone. Bioclasts are Globotruncana ventricosa. While at bottom and Globotruncana elevata (Brotzen) top right corner.

d: Lime mudstone (micrite) Microfacies of the Late Cretaceous Parh Limestone. Bioclast is Globotruncana sigali Reichel.

e: Lime mudstone (micrite) Microfacies of the Late Cretaceous Parh Limestone.Bioclasts are Globotruncana linneiana (D'orbigry) left side and Globotruncana elevata (Brotzen) right side.

f: Lime mudstone (micrite) microfacies of the Late Cretaceous Parh Limestone Bioclast is Globotruncana coronata. (Bolli).

Plate -4

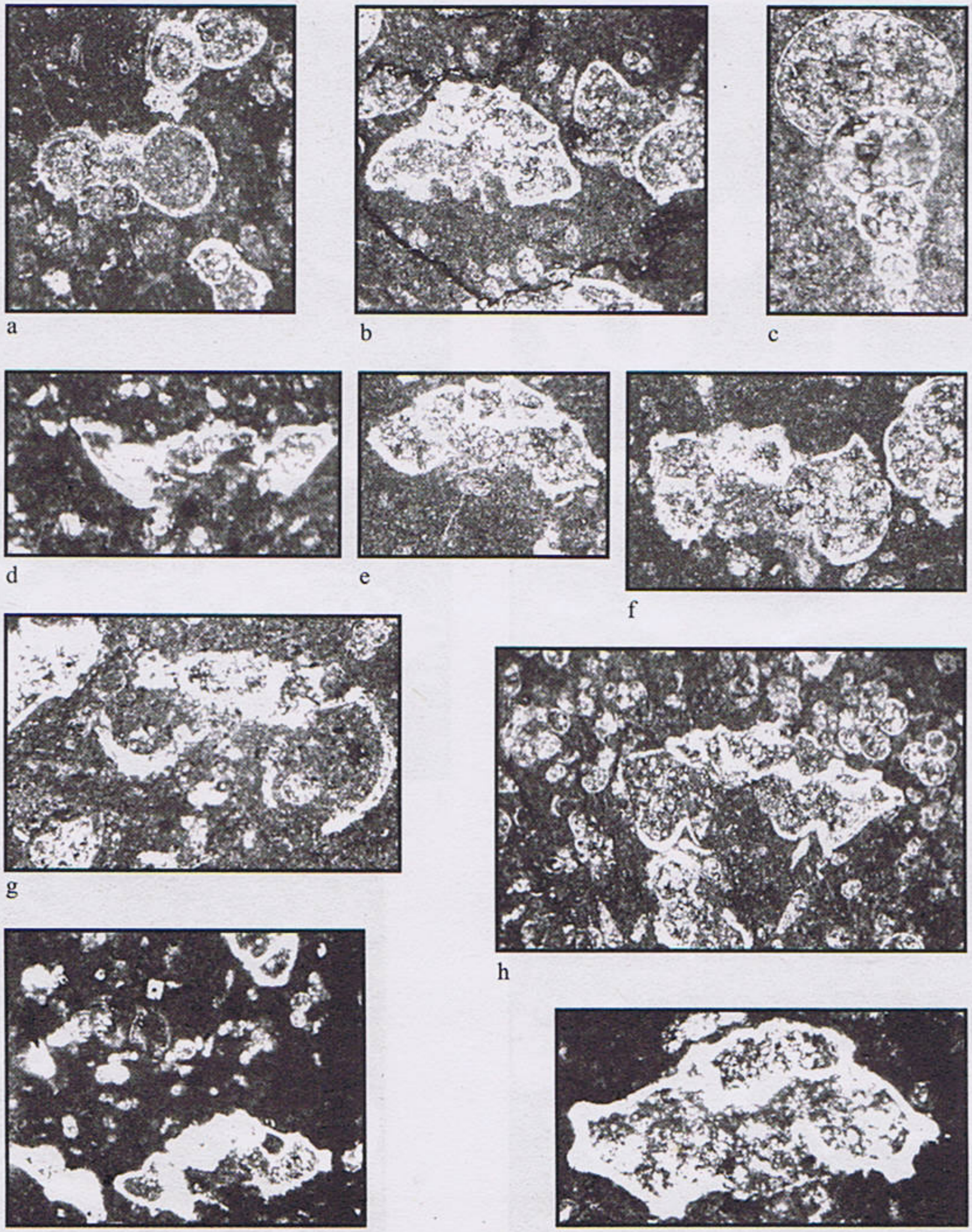

a: Lime mudstone (micrite) facies, Goru Formation. Bioclast is Globigerinelloides breggiensis (Gandolfi).
b: Lime mudstone (micrite) facies, Goru Formation. Bioclast is Praeglobotruncana turbinate (Reichel).
c: Lime mudstone (micrite) facies, Parh Limestone. Bioclast is Heterohelix globulosa (Ehrenberg)
d: Lime mudstone (micrite) facies, Goru Formation. Bioclast is Globotruncana sp.
e: Lime mudstone (micrite) facies, Goru Formation. Bioclast is Dicarinella primitiva (Dalbiez).
f,g: Bioclasts are Helveto globotruncana Helvetica (Bolli).
h,i: Bioclasts is Globotruncana sp
j: Bioclasts is Globotruncana area. (Cushman)

Plate -5

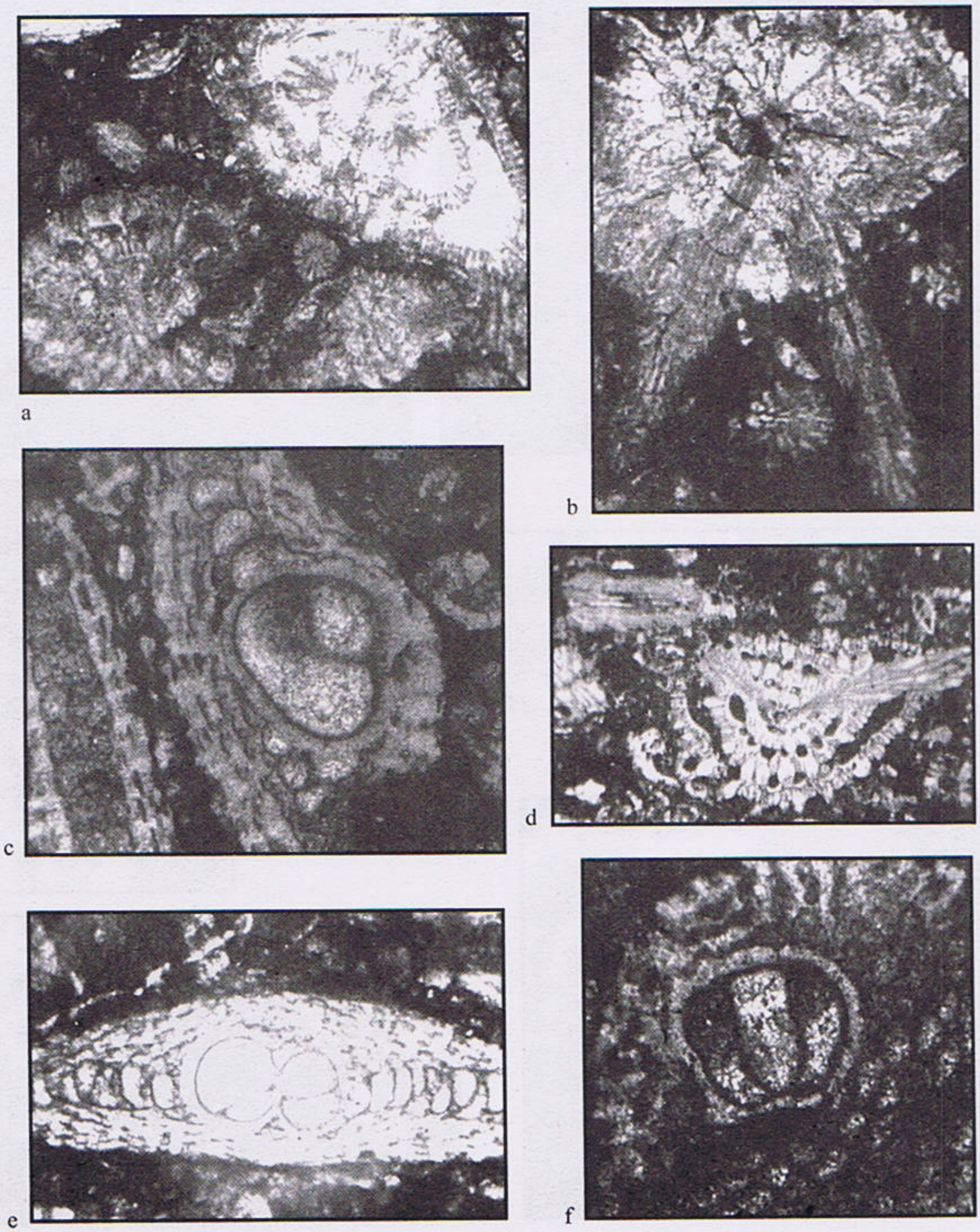

a-e Murree-Brewery Gorge Section showing benthonic larger foraminifera of the Late Cretaceous (Maastrichtian) Murree-Brewery Limestone (" Orbitoidal Limestone"). 1. Vertical radial, 2. Horizontal spine.

a,b and d Siderolites calcitrapoides (Lamarck)

c,e and f Orbitoides apiculatus (Schlumberger)

Plate -6

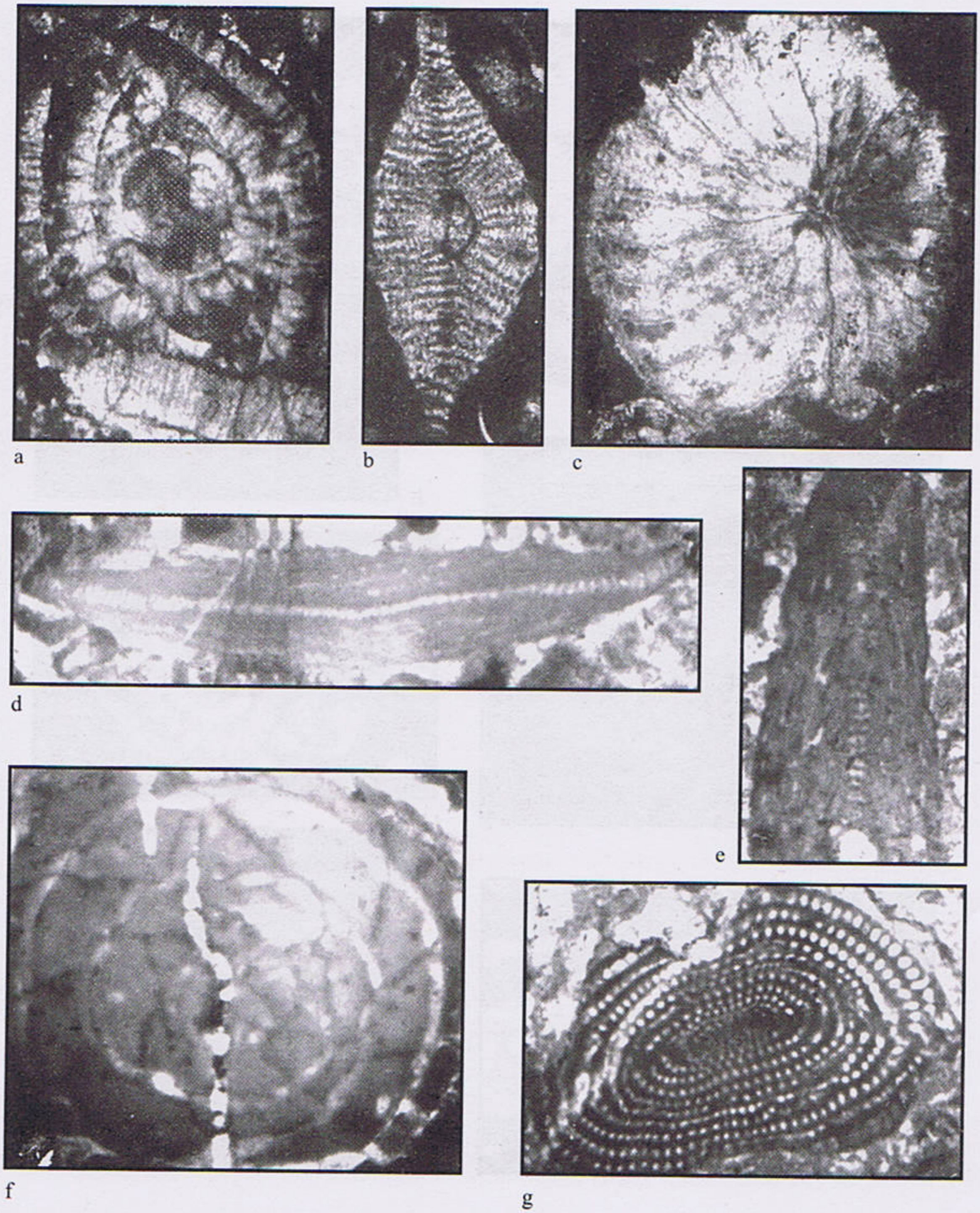

a-g Murree-Brewery Gorge Section showing benthonic larger foraminifera of the Early Tertiary Dunghan Limestone.

a. Miscellanea miscella (D' Archiae & Haime) is associated with the Lower Eocene benthonic larger foraminefera (Figs. 2-7)

b. Discocyclina dispansa (Sowerby).

c. Nummulites mamillatus (Fichtel & Moll) slightly oblique view showing the umbonal plug (dark area) and the brancling septal filaments.

d,e Somalina stefaninii (Silvestri)

a. Alveolina pasticillata (Schwager)

b. Alveolina Sp.

Plate -7


a


b


c

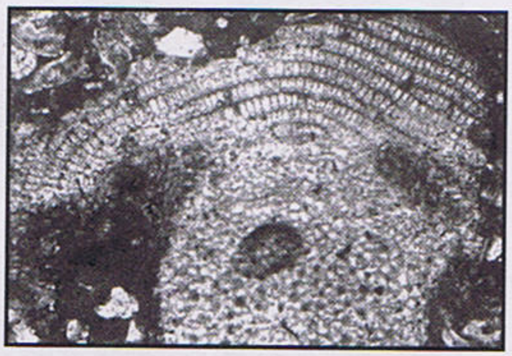
d

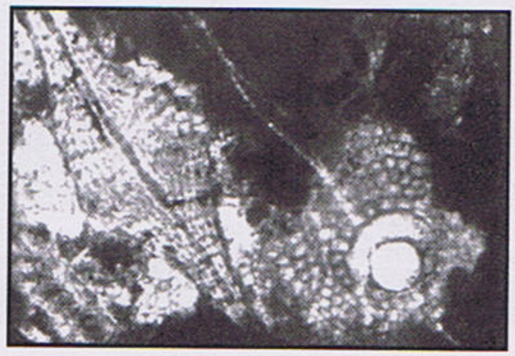
e


f

a-f: Discocyclina dispansa (Sowerby). Fig.6 also showing Nummulites.

Plate -8

a

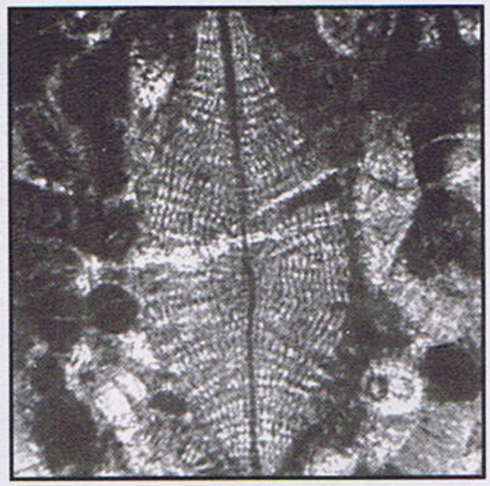

b

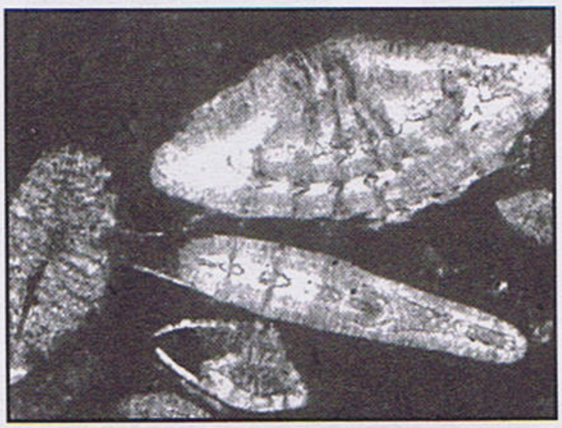

c

d

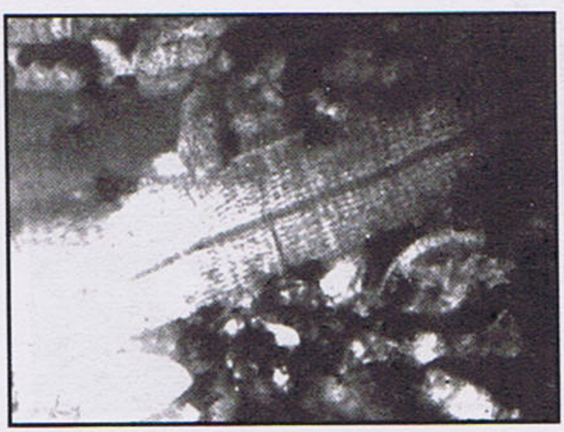

e

a-e: Discocyclina dispansa (Sowerby). Fig c also shows Nummulites and Operculina.

CONCLUDING REMARKS

The K-T boundary exists in carbonate platform deposition between the Murree-Brewery Limestone and the Dunghan Limestone containing age diagnostic benthonic larger foraminifera. This succession is characteristic of shallow shelf environments.

The Goru Formation and the Parh Limestone exhibit planktonic foraminiferal assemblage demonstrating deeper water environments.

Bioclastic lime mudstone, wackestone, packestone and grainstone microfacies of both shallow shelf and deeper environments are present. Bioclasts are planktonic foraminifera in the Goru and Parh Formations, whereas benthonic larger foraminifera occur in the Murree-Brewery Limestone and the Dunghan Limestone.

REFERENCES

Akhtar, M. and Butt, A.A 2000. Significance of Miscellanea miscella (d'archiac and Haime) in the Early Paleogene Stratigraphy of Pakistan. *Revue Paleobiologie* **19(1),** 123-135.

Alleman F., 1979 Time of emplacement of the Zhob Velley Ophiolites and Bela Ophiolites, Balochistan (preliminary report) in : (eds. Farah A. And De jong K.A. "Geodynamics of Pakistan", Geological Survey of Pakistan, Quetta .245-285.

Aubry T., Durrani K.H., and Baloch M.K., 1991 Biostratigraphy of the Upper Cretaceous Parh Limestone from Quetta region, *Pakistan Acta Mineralogica Pakistanica* **5,** 121-128.

Butt A.A., 1992 "The Upper Cretaceous bio-stratigraphy of Pakistan": A synthesis. *Geologie Mediterraneenne* XIX, **4,**265-272.

Davies, L.M. 1927. The Ranikot beds at Thal. *Quart. Jour. Geol. Soc. London.* **83,** 260-290.

Gigon, W.O. (1962) Upper Cretaceous stratigraphy of te well Giandari-1 and its correlation with the Sulaiman and Kirthar Ranges, West Pakistan 2nd ECAFE Petrol. Symp. Tehran.

Geol. Bull. Punjab Univ. 38, 2003.

TEACHING STAFF LIST OF THE INSTITUTE OF GEOLOGY, UNIVERSITY OF THE PUNJAB ON 31ST DECEMBER, 2003

No.	Name and Qualifications	Designation	Field of Specialization
1.	**Mr. Umar Farooq** M.Sc. (Pb), M.Sc., D.I.C. (London), GTC (Japan)	Director	Exploration Geophysics
2.	**Mr. Zahid Karim Khan** M.Sc. (Pb) PGD Delft (N.Lands)	Associate Professor	Engineering. Geology, Geohydrology, Aggregate Materials
3.	**Dr. Iftikhar Hussain Baloch** M.Sc. (Pb), M.Sc. (Leicester), Ph.D. (Leicester) UK	Associate Professor	Industrial Mineralogy
4.	**Dr. Akhtar Ali Saleemi** M.Sc. (Pb), M.Sc. (Leicester), Ph.D. (Leicester) UK	Associate Professor	Mineralogy, Petrology, Industrial Mineralogy
5.	**Dr. Nasir Ahmed** M.Sc. (Pb), Ph.D (Leeds)	Associate Professor	Environmental Science
6.	**Dr. Riaz Ahmad Sheikh** B.Sc. (Hons), M.Sc. (Pb), D.I.C., Ph.D (London)	Associate Professor	Structure & Petroleum Geology, Sedimentology, Regional Tectonics
7.	**Dr. Nazir Ahmad** M.Sc. (Pb), Ph.D. (Leicester) UK	Associate Professor	Structural & Petroleum Geology, Mapping, Sedimentology, Regional Tectonics
8.	**Dr. Muhammad Saeed Farooq** M.Sc. (Pb), Ph.D. (Pb)	Associate Professor	Engineering Geology, Geohydrology
9.	**Dr. Syed Alim Ahmad** M.Sc. (Pb), Ph.D (Pb)	Assistant Professor	Mineralogy, Petrology
10.	**Dr. Muhammad Hafeez** M.Sc. (Pb), Ph.D. (U.K.) (on leave)	Assistant Professor	Environmental Science
11.	**Dr. Muhammad Ashraf Siddiqui** M.Sc. (Pb), PGD (Leicester) UK, Ph.D (Pb)	Assistant Professor	Mineralogy, Petrology, Industrial Mineralogy
12.	**Syed Mahmood Ali Shah** M.Sc. (Pb)	Assistant Professor	Mineralogy, Petrology

13.	**Dr. Shahid Jameel Sameeni** M.Sc. (Pb), Ph.D. (Pb), PGD (Swiss)	Assistant Professor	Paleontology
14.	**Mr. Sajid Rashid** M.Sc. (Pb) (on leave)	Assistant Professor	Engineering Geology, Geohydrology
15.	**Mr. Naveed Ahsan** M.Sc. (Pb)	Assistant Professor	Structural & Petroleum Geology, Tectonics
16.	**Mr. Shahid Ghazi** M.Sc. (Pb)	Assistant Professor	Petroleum Exploration Stratigraphy & Sedimentology
17.	**Mr. Mustansar Naeem** M.Sc. (Pb)	Assistant Professor	Engineering Geology
18.	**Mr. Iftikhar Ahmad** M.Sc. (Pb), M.Phil (UET)	Assistant Professor	Engineering Geology & Hydrology
19.	**Mr. Abdus Sattar** M.Sc. (Pb)	Assistant Professor	Geochemistry, Mineralogy
20.	**Mr. Abdur Rauf Nizami** M.Sc. (Pb)	Assistant Professor	Petroleum Geology, Remote Sensing, Sedimentology
21.	**Mr. Kamran Mirza** M.Sc. (Pb)	Lecturer	Micropaleontology, Stratigraphy, Sedimentology
22.	**Miss Farzana Aslam** M.Sc. (QAU), M.Phil (QAU) (on study leave)	Lecturer	Physics

Geol. Bull. Punjab Univ. 38, 2003.

NON TEACHING STAFF MEMBERS LIST OF THE INSTITUTE OF GEOLOGY, UNIVERSITY OF THE PUNJAB ON 31ST DECEMBER, 2003

Sr. No.	Name of Employee	Designation
1.	Mr. Masood Ahmad Khan	Admin. Officer
2.	Mr. Waqar Ahmad Siddiqui	Private Secretary
3.	Mr. Sharafat Ali Khan	Librarian
4.	Mr. Masud Minhas	Senior Artist
5.	Mr. Nadeem Younas	Senior Stenographer
6.	Mr. Bashar-ul-Islam	Assistant
7.	Mr. Muhammad Yaseen	Store Supervisor
8.	Mr. Safdar Ali	Senior Clerk
9.	Mr. Muhammad Farrukh Javed	-do-
10.	Mr. Ali Akbar Sandhu	Junior Clerk
11.	Mr. Qaim Ali Shah	-do-
12.	Mr. Tasneem Ahmed	Draftsman
13.	Mr. Zafar Ullah Butt	Senior Technician
14.	Mr. Muhammad Younas	Museum Assistant
15.	Mr. Muhammad Ilyas	Head Lab. Assistant
16.	Mr. Sami Ullah Khan	Junior Technician
17.	Mr. Liaqat Ali S/o Ilam Din	-do-
18.	Mr. Riaz Qadeer	Lab. Assistant
19.	Mr. Muhammad Jehanzeb	Driver
20.	Mr. Muhammad Riaz	-do-
21.	Mr. Asif Ali	Machine Assistant
22.	Mr. Ghulam Mustafa	Lab. Attendant
23.	Mr. Haq Nawaz	-do-
24.	Mr. Liaqat Ali S/o Barkat Ali	-do-
25.	Mr. Nazir Ahmed	-do-
26.	Mr. Muhammad Rafi	-do-
27.	Malik Muhammad Nazir	Library Attendant
28.	Mr. Arshad Ali	Naib Qasid
29.	Mr. Muhammad Ramzan	-do-
30.	Syed Sajid Hussain Shah	Coolie

OBITUARY NOTE ON LATE PROF. MARTIN

Late Professor Dr. Norman Roy Martin was a person who contributed more to the geological achievements of Pakistan than any other person, especially on his development of the very first fountainhead in Pakistan for the production of geological manpower.

At the time of its creation on August 14, 1947, Pakistan inherited no geological institution from (British) India. Although, the Jammu College had a Department of Geology, and was affiliated to the Punjab University, Lahore, but it was located in the Indian-occupied part of Kashmir. The Pakistan Government was well aware of this fact; particularly as more than 70% of the New State was geologically terra non-recognita. On the other hand, there was severe shortage of geological manpower. (Only six geologists of the Geological Survey of (British) India opted for Pakistan). The initiative to start teaching of Geology was taken by the Punjab University. In 1952, a protocol signed with UNESCO brought in an expert from Norway, who could built a small nucleus, but the entry of Professor Martin in 1955, as Head of Technical Assistance Mission at the Punjab University, opened way for rapid flow of foreign experts and finances. With this success, Professor Martin could build a durable foundation of the Department of Geology, introduced world-level courses of studies and initiated a dynamic programme of field research to provide basis for advanced training of students and production of data for geological publications.

Once again, there was no professional outlet for geological publications, while the research data were accumulating rapidly. His two-pronged field approach—Hazara district in the east, and Swat district in the west—was a magical move. This covered the classical sedimentary, metamorphic and igneous provinces of northern Pakistan, and thus laid foundation for build-up of trends of future geological research, not only by staff and students of the Punjab University but by researchers on regional scale. His work on Lower Swat was historically the first to discover a ophiolite belt, that later got recognized as the Main Mantle Thrust (MMT) zone, making northern edge of the subducting Indian Plate. It is now well known that all theories about the origin of northern montane Pakistan could never do without this pioneer discovery of Prof. Martin.

Another legacy of Professor Martin refers to his almost army-like maneuvering during summer field seasons. He would move the entire teaching and non-teaching staff to field, leaving one clerk and one peon behind in the Department. He will allocate field project to each staff member, to whom group or groups of M.Sc. Final Year students would be attached; each student would carry out research for Report/Thesis. A comprehensive Field Programme would be printed and distributed, even to all other geological organizations in the country. He will put up his field headquarter at Nathiagali, and will visit every field party to check up the work. Towards end of the field season, all parties would be summoned to Nathiagali, where party leaders were required to make presentation of their work. After returning to Lahore, every teacher was required to write his report.

(Late) Prof. Dr. N. R. Martin & Prof. Dr. F. A. Shams at "Nathia", England, 1989.

As the field work progressed, followed by necessary lab. work, the research data built up to feed research papers of publishable standard. This was the stage when Professor Martin decided to initiate publication of a research journal as there was none in Pakistan. It was called "Geological Bulletin of the Punjab University" and its first Number was published in 1961. Simultaneously, he also encouraged students to bring out a students' journal, which was named Wynneana", after A.B. Wynne who carried out very early researches in the Punjab Salt Range. A prized competition was held to propose title picture of the journal, the successful entry was a painting of the Kirana Hills, Sargodha District.

There are many more to be remembered and written about the Great Martin, who was responsible for establishing a model of geological education in Pakistan, to be followed by all institutions that were established in the country. Thus, he made a wholesome contribution to this country from end to end.

After leaving Pakistan in May, 1962, he settled in his home in the County Kent, England, naming it "Nathia", after Nathiagali, a place that remained his favourite summer resort throughout his stay in Pakistan. He died on 11 October, 2001, at the age of 77 years.

Prof. Dr. F. A. Shams
(Former Director, Institute of Geology, Punjab University, Lahore)